Fluid Mechanics for Astrophysicists

From kinetic theory to fluids and plasmas

MAUCA Fundamental Course 2019 – Course Notes

Instructor:
Oliver HAHN
oliver.hahn@oca.eu

MAUCA
MASTER IN ASTROPHYSICS

UNIVERSITÉ CÔTE D'AZUR

Contents

Further Reading

If you want to cover material in more depth than these lecture notes, I can recommend the following monographs:

The massive 1500 page book “Modern Classical Physics”[5] by Kip Thorne and Roger Blandford provides an excellent overview over *all* classical physics, from mechanics to all the material of this course. It is very exhaustive, heavily illustrated and an excellent resource also for research.

Focusing only on fluid mechanics and plasma physics, I can recommend Arnab Choudhuri’s “The Physics of Fluids and Plasmas” [1], which covers almost exactly what also this course covers, and which was used heavily in the preparation of these notes; Jim Pringle and Andrew King’s “Astrophysical Fluid Flow”[4], which provides also many worked out applications of fluid mechanics to astrophysical problems; Dimitri Mihalas and Barbara Weibel-Mihalas’ “Foundations of Radiation Hydrodynamics" [3], which is excellent for its kinetic theory and fluid mechanics parts, and also covers in detail radiative transfer and the interaction of radiation and fluids, which we do not cover in this course. Finally, also the very classical series on theoretical physics by Lew Landau and Evgeny Lifshitz has truly excellent volumes on “Fluid Mechanics”[2] and kinetic theory – the recent book by Thorne and Blandford might however be more up-to-date and usable for students today.

Chapter 1

Kinetic Theory: From Microscopic Particles to the Fluid Equations

1.1 Describing many particles in physics

The study of the dynamics of fluids (or gases) concerns itself with a macroscopic description of a large number of microscopic particles. It thus has to start with a repetition of what is typically called statistical physics. The laws we shall derive will describe large ensembles of particles. The trajectories of individual particles thus cannot be followed due to their sheer number and the *mechanistic* description will turn into a *statistical* one. At the same time, while the motion of an individual particle does not play a role, in all cases, however, the microscopic properties of the particles will be reflected in the properties of the statistical ensemble. Such properties are e.g. whether the particles carry an electric charge, whether they have internal degrees of freedom (such as excited atomic or molecular states), whether they carry a mass or not (e.g. photons), whether they often scatter off each other and also whether we should treat them as classical particles or as quantum mechanical objects. We will start by formalising these ideas first, before we turn to describing the dynamics of ensembles.

1.1.1 Levels of description

Level 0: the quantum world

As quantum mechanics tells us, fundamentally, all particles are really quantum mechanical objects. This means that they are described by a wave function, which we can e.g. write as $\psi(\mathbf{x}, t)$. The probability of finding the particle at position $\mathbf{x}$ is then given by $p(\mathbf{x}, t) = \psi^*(\mathbf{x}, t)\,\psi(\mathbf{x}, t)$. At the same time, the de Broglie wavelength λ of such a particle of typical momentum p is

$$\lambda = \frac{h}{p} \approx \frac{h}{\sqrt{3mkT}}, \tag{1.1}$$

where k is the Boltzmann constant. In this expression, we have used that the typical velocity v of a point particle of mass m in an ensemble of N particles to which we assign a temperature T is $\frac{N}{2}mv^2 = \frac{3}{2}NkT$. If the number density of particles is given by n, then the mean distance between particles is of order

$\ell \approx n^{-1/3}$. The condition that particles on average have a separation much larger than their de Broglie wavelength (so that the wave functions are non-overlapping) becomes then

$$\frac{hn^{1/3}}{\sqrt{3mkT}} \ll 1. \tag{1.2}$$

When this condition is satisfied, each quantum particle can be treated like a classical particle and we can safely neglect quantum mechanical effects in our macroscopic description. Typical quantum mechanical objects in astrophysics are white dwarfs and neutron stars, which cannot be described in terms of classical mechanics alone.

The classical limit of quantum mechanics is usually stated in terms of Ehrenfest's theorem. It simply states that the expectation values for the position and momentum of a wave function follow the classical equations of motion if the potential energy changes by a negligible amount over the dimensions of the wave packet. In that limit, we can then fully describe the description in terms of an evolution of the expectation values, which are $\langle \mathbf{x} \rangle = \int \psi^* \mathbf{x} \psi \, \mathrm{d}^3x$, and $\langle \mathbf{p} \rangle = \int \psi^* \left(-i\hbar \boldsymbol{\nabla}\right) \psi \, \mathrm{d}^3x$. We thus get

$$\frac{\mathrm{d} \langle \mathbf{x} \rangle}{\mathrm{d}t} = \frac{\langle \mathbf{p} \rangle}{m}, \qquad \frac{\mathrm{d} \langle \mathbf{p} \rangle}{\mathrm{d}t} = - \langle \boldsymbol{\nabla} V \rangle \, . \tag{1.3}$$

Level 1: the classical world – individual particles

In those cases, in which we can neglect quantum mechanical effects, the motion of individual particles is governed by the classical equations of motion (1.3). In the case of an ensemble of N particles $(\mathbf{x}_1, \ldots, \mathbf{x}_N, \mathbf{p}_1, \ldots, \mathbf{p}_N)$, we would have separate equations for all particles, i.e. $2N$ equations in total. If the motion of each particle occurs in d dimensions, the state of the system is fully described by $2 \times d \times N$ numbers. Describing the system in this way is stating that any given state is given by a unique point in a $2dN$-dimensional phase-space Γ, where $\Gamma \subset \mathbb{R}^{2dN}$. The motion of the system is then governed by standard Newtonian dynamics, such that we can use Hamilton's equations to write their motion as gradients of the Hamiltonian of the well known form

$$\dot{\mathbf{p}}_i = -\frac{\partial H}{\partial \mathbf{x}_i} \qquad \dot{\mathbf{x}}_i = \frac{\partial H}{\partial \mathbf{p}_i}. \tag{1.4}$$

The Hamiltonian $H = H(\mathbf{x}_1, \ldots, \mathbf{x}_N, \mathbf{p}_1, \ldots, \mathbf{p}_N, t)$ is usually a function of all the coordinates, momenta and time of the form

$$H = \sum_{i=1}^{N} \mathbf{p}_i^2 / 2m_i + V. \tag{1.5}$$

While this description is appropriate in some cases (reasonably small N, or simple interaction potential V), generally solving for the individual trajectories of particles is neither possible nor practical, since for $N \to \infty$ the dimensionality of the space and the number of equations to be integrated becomes infinite. The motion of such classical particles can be shown in *phase space* (see Fig. 1.1 for the phase space of a single particle) where certain characteristics of the system become more apparent.

Level 2: the distribution function and the collisionless Boltzmann equation

In order to maintain a meaningful limit as the number of particles becomes very large (formally $N \to \infty$), one reduces the number of dimensions to only $2 \times d$ and introduces the notion of a phase-space density or distribution function $f(\mathbf{x}, \mathbf{p}, t)$. Formally, this can be achieved by the notion of a statistical

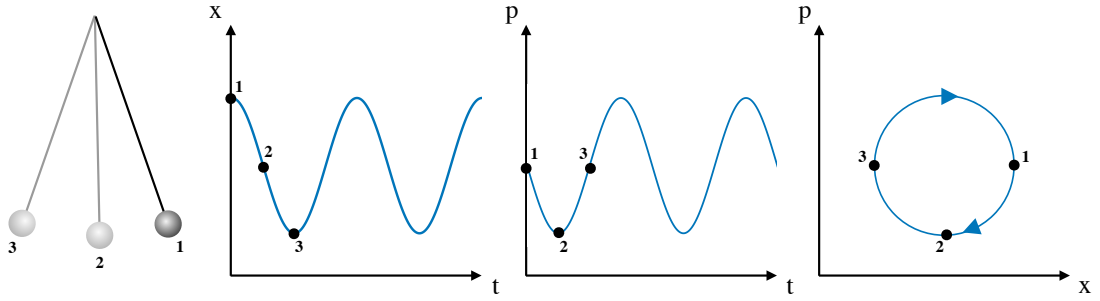

Figure 1.1: The phase space of a harmonic oscillator (a mathematical pendulum here): The motion of the pendulum (a single 'particle') is described either by the graphs of the position $x(t)$ and momentum $p(t)$ over time, or by the combination of the two into *phase space* (right-most panel) where both position and momentum are shown and time corresponds to a certain point on the closed curve. A periodic *orbit* corresponds to a closed curve.

ensemble. The idea is that when N is very large, we can have many possible microscopic realisations, in terms of different points in Γ-space, that are not relevantly different when viewed from a macroscopic point of view. What is important is only how many of the particles of the total system occupy a certain volume in position and velocity space $\mathrm{d}^d x\,\mathrm{d}^d p$ in the sense of an average over ensembles, not how exactly they do that. So instead of talking about the positions and velocities of individual particles, we simply express everything in terms of the density of points $f(\mathbf{x},\mathbf{p},t)$ in a reduced $2d$-dimensional phase-space, or μ-space. Then $f(\mathbf{x},\mathbf{p},t)\,\mathrm{d}^d x\,\mathrm{d}^d p$ is the expected number of particles in a small volume of phase-space at time t centred at point $(\mathbf{x},\mathbf{p})$. This limit

$$f(\mathbf{x},\mathbf{p},t) = \lim_{\delta V\to 0^+} \frac{\delta N}{\delta V} \quad \text{with} \quad \delta V \to d^n x\, d^n p \tag{1.6}$$

is really a physical limit in the sense that we want that δV is a volume that is much smaller than the volume of the system, but still contains a large enough number of ensemble particles.

We will now derive how this density evolves over time. To see this, we will investigate how the phase-space density changes along the trajectory of one of the microscopic particles. Let us pick one of the microscopic particles randomly, say a particle i. Between time t and time $t+\delta t$, it will have moved from $(\mathbf{x}_i,\mathbf{p}_i)$ to $(\mathbf{x}_i+\delta\mathbf{x}_i,\mathbf{p}_i+\delta\mathbf{p}_i)$. Such a derivative along a trajectory, we call substantial derivative or Lagrangian derivative and denote it by the symbol $\mathrm{D}/\mathrm{D}t$. We then have

$$\frac{\mathrm{D}f}{\mathrm{d}t} = \lim_{\delta t\to 0} \frac{f(\mathbf{x}_i+\delta\mathbf{x}_i,\mathbf{p}_i+\delta\mathbf{p}_i,t+\delta t) \;-\; f(\mathbf{x}_i,\mathbf{p}_i,t)}{\delta t}. \tag{1.7}$$

Using Taylor-expansion, we can write up to first order

$$f(\mathbf{x}_i+\delta\mathbf{x}_i,\mathbf{p}_i+\delta\mathbf{p}_i,t+\delta t) = f(\mathbf{x}_i,\mathbf{p}_i,t) + \delta\mathbf{x}_i\cdot\frac{\partial f}{\partial\mathbf{x}}\bigg|_{\mathbf{x}_i} + \delta\mathbf{p}_i\cdot\frac{\partial f}{\partial\mathbf{p}}\bigg|_{\mathbf{p}_i} + \delta t\,\frac{\partial f}{\partial t}, \tag{1.8}$$

where the vertical lines indicate that the derivatives have to be taken at that point. Substituting this into eq. (1.7), we have

$$\frac{\mathrm{D}f}{\mathrm{D}t} = \frac{\partial f}{\partial t} + \dot{\mathbf{x}}_i\cdot\frac{\partial f}{\partial\mathbf{x}}\bigg|_{\mathbf{x}_i} + \dot{\mathbf{p}}_i\cdot\frac{\partial f}{\partial\mathbf{p}}\bigg|_{\mathbf{p}_i}. \tag{1.9}$$

Background: Continuity equation

We now have to introduce the notion of a continuity equation by means of Gauss' theorem. Let us consider the number of particles in some volume V of our $2d$-dimensional phase space and let us use $\boldsymbol{\mu} = (\mathbf{x}, \mathbf{p})$ as a coordinate in this $2d$-dimensional space. Then we have

$$N_V(t) = \int_V f(\boldsymbol{\mu}, t)\, \mathrm{d}V \tag{1.10}$$

as the number of particles occupying the volume V. This number will change as particles enter or leave the volume element. Let us denote by $\boldsymbol{\omega}$ the $2d$-dimensional flow field in phase-space, i.e. $\boldsymbol{\omega} = (\dot{\mathbf{x}}, \dot{\mathbf{p}})$. This might seem complicated, but it is really just the rate at which particles move, i.e. the normal velocity $\mathbf{v} = \mathbf{p}/m$ in the first d coordinates, and the rate at which particles accelerate, e.g. $-\boldsymbol{\nabla} V$ in the case of a long-range potential, in the second d coordinates, as given by the Hamiltonian equations of motion. The rate at which particles enter or leave the volume V is of course proportional to the density of particles at the boundary of the volume times the component of $\boldsymbol{\omega}$ normal to the surface of the boundary (cf. Figure 1.2, left), i.e. we can write

$$\frac{\partial}{\partial t} \int_V f(\boldsymbol{\mu}, t)\, \mathrm{d}V = - \oint_{\partial V} f(\boldsymbol{\mu}, t)\, \boldsymbol{\omega} \cdot \mathrm{d}\boldsymbol{S}, \tag{1.11}$$

where the integral on the right-hand-side is over the closed boundary ∂V of V and where $\mathrm{d}\mathbf{S}$ is the outward-pointing normal vector at each point of the volume surface boundary.

We can now apply Gauss' theorem (also sometimes called Ostrogradsky's theorem, or divergence theorem) to this surface integral in order to turn it into a volume integral. Indeed we find

$$\frac{\partial}{\partial t} \int_V f(\boldsymbol{\mu}, t)\, \mathrm{d}V = - \oint_{\partial V} f(\boldsymbol{\mu}, t)\, \boldsymbol{\omega} \cdot \mathrm{d}\boldsymbol{S} = - \int_V \boldsymbol{\nabla}_{\boldsymbol{\mu}} \cdot \left(f(\boldsymbol{\mu}, t)\, \boldsymbol{\omega} \right) \mathrm{d}V. \tag{1.12}$$

Note that we have added an index $\boldsymbol{\mu}$ to the $\boldsymbol{\nabla}$ operator. This means that it is not the usual 3-dimensional operator but contains $2d$-derivatives with respect to all components of $\mathbf{x}$ and $\mathbf{p}$.

If we fix the volume V in time, we can pull the time derivative into the integral and since we have made no further assumptions about the volume V, the equation has to hold also directly for the integrand, i.e.

$$\frac{\partial}{\partial t} f(\boldsymbol{\mu}, t) \; + \; \boldsymbol{\nabla}_{\boldsymbol{\mu}} \cdot \left(f(\boldsymbol{\mu}, t)\, \boldsymbol{\omega} \right) = 0. \tag{1.13}$$

This equation will always hold as long as the number of particles in the system is conserved, i.e. as long as no particles are created in the system or disappear from it.

We already notice that equations (1.11) and (1.13) bear some resemblance. We note that we can rewrite the second (divergence) term in eq. (1.13) as

$$\boldsymbol{\nabla}_{\boldsymbol{\mu}} \cdot \left(f(\boldsymbol{\mu}, t)\, \boldsymbol{\omega} \right) = f(\boldsymbol{\mu}, t)\, \boldsymbol{\nabla}_{\boldsymbol{\mu}} \cdot \boldsymbol{\omega} + \boldsymbol{\omega} \cdot \boldsymbol{\nabla}_{\boldsymbol{\mu}} f(\boldsymbol{\mu}, t) \tag{1.14}$$

Next we notice that the $2d$-dimensional velocity $\boldsymbol{\omega}$ at the position of the particle that we fixed, i.e. at the location $(\mathbf{x}_i, \mathbf{p}_i)$ in phase-space, must be given by the phase-space velocity of that particle, i.e. $\boldsymbol{\omega}(\mathbf{x}_i, \mathbf{p_i}) = (\dot{\mathbf{x}}_i, \dot{\mathbf{p}}_i)$. Since we assumed that the system is governed by Hamiltonian dynamics, we must be able to express this velocity using the Hamiltonian of the system, i.e. $\boldsymbol{\omega} = (\frac{\partial H}{\partial \mathbf{p}_i}, -\frac{\partial H}{\partial \mathbf{x}_i})$. This implies

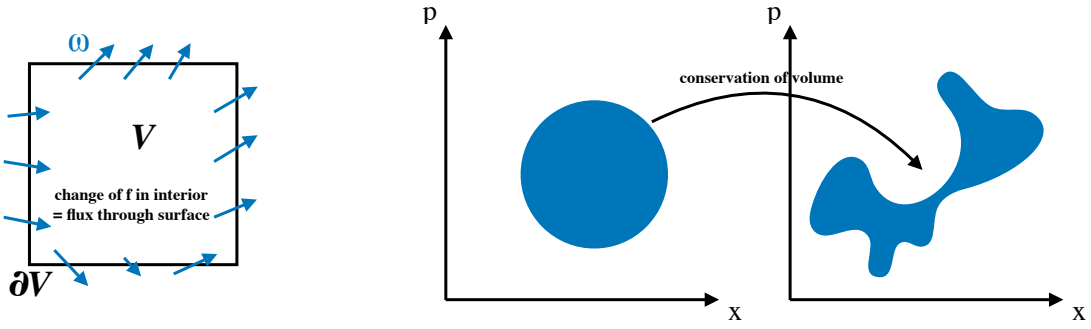

Figure 1.2: *Left:* If no particles are created or destroyed, then the number of particles in a volume V of phase space changes depending on how many particles flow into and out of this volume. *Right:* Illustration of Liouville's theorem: the phase space density is conserved along particle trajectories, which implies that the phase space density behaves like an incompressible flow in phase space, i.e. in the figure, the blue area remains conserved but may become arbitrarily complicated.

that the divergence of the phase space velocity at the location of the particle i must be

$$(\boldsymbol{\nabla}_{\boldsymbol{\mu}} \cdot \boldsymbol{\omega})|_{(\mathbf{x}_i, \mathbf{p}_i)} = \frac{\partial^2 H}{\partial \mathbf{x}_i \partial \mathbf{p}_i} - \frac{\partial^2 H}{\partial \mathbf{p}_i \partial \mathbf{x}_i} = 0. \tag{1.15}$$

This means that the phase-space velocity field $\boldsymbol{\omega}$ is divergence-free! The motion of the distribution function f in phase-space is thus incompressible.

Under this condition, the continuity equation simplifies exactly to eq. (1.7), and we have simply

$$\frac{\mathrm{D}f}{\mathrm{D}t} = \frac{\partial f}{\partial t} + \dot{\mathbf{x}}_i \cdot \left.\frac{\partial f}{\partial \mathbf{x}}\right|_{\mathbf{x}_i} + \dot{\mathbf{p}}_i \cdot \left.\frac{\partial f}{\partial \mathbf{p}}\right|_{\mathbf{p}_i} = 0. \tag{1.16}$$

This is the collisionless Boltzmann equation: the phase-space density f is conserved along the Hamiltonian trajectories. Note that the Hamiltonian nature of the system as well as the conservation of particles in the system are necessary for it to hold. It is usually expressed without recurrence to actual particle trajectories by replacing $\dot{\mathbf{x}} = \mathbf{p}/m$ and $\dot{\mathbf{p}} = \mathbf{F}$, where $\mathbf{F}(\mathbf{x})$ is some external force field given by the gradient of the potential:

$$\frac{\mathrm{D}f}{\mathrm{D}t} = \frac{\partial f}{\partial t} + \frac{\mathbf{p}}{m} \cdot \boldsymbol{\nabla}_{\boldsymbol{x}} f + \mathbf{F} \cdot \boldsymbol{\nabla}_{\boldsymbol{p}} f = 0, \tag{1.17}$$

it is then clear that f is conserved along the trajectories fulfilling the canonical Hamiltonian equations of motion.

But why have we called this equation "collisionless"? The reason is that we lost the possibility to describe the interaction between individual particles when going from Γ-space to μ-space! The binary interaction of two particles at positions $(\mathbf{x}, \mathbf{p})$ and $(\mathbf{x}', \mathbf{p}')$ in Γ-space cannot trivially be expressed in μ-space, since it has no longer a notion of single particles. We have to introduce some additional formalism to treat the case of such binary interactions in a statistical sense in μ-space, which we will do next.

1.2 Collisions between particles

In order to introduce the notion of binary interactions, or collisions, between particles, we will assume that the interactions occur only over a small distance a in space (which we can think of as the particle size). We can then quantify how collisional such a system would be by comparing the mean distance $n^{1/3}$ between particles to this interaction radius. A system for which $na^3 \ll 1$ has on average much fewer than one particle per interaction volume and we shall call it a dilute gas. In general, we can estimate the mean distance between collisions of particles to be given by the mean free path

$$\lambda \approx \frac{1}{\pi n a^2}. \tag{1.18}$$

You will later show yourself why the mean free path takes this form.

1.2.1 Binary Collisions and the Collision Integral

From the collisionless to the full Boltzmann equation

Collisions between individual particles can be incorporated into our μ-space description by realising that the phase space density in this more general case is no longer conserved along particle trajectories. Instead, particles can exchange momentum and energy among each other. This effect can be incorporated by adding a collision term to the right-hand-side of the Boltzmann equation (1.16) so that we get

$$\frac{\mathrm{D}}{\mathrm{D}t} f(\mathbf{x}, \mathbf{p}, t) = \left[\frac{\mathrm{d}f}{\mathrm{d}t}\right]_{\text{coll.}} =: \frac{C_{\text{in}} - C_{\text{out}}}{\mathrm{d}^3x\, \mathrm{d}^3p}, \tag{1.19}$$

where C_{in} and C_{out} are the rates at which particles are scattered into and out of a volume element $\mathrm{d}^3x\, \mathrm{d}^3p$ of μ-space. Note that for now this is just a way of expressing what we intend to do. Let us look at the details of a collision next.

Description of elastic binary collisions

We will concern ourselves here only with the case of elastic binary collisions, i.e. collisions in which

1. only two particles participate at any given time,
2. the particle number remains constant (i.e. no particles disappear or new ones appear),
3. the total momentum and the total energy of the two particles are conserved in the collision.

In a dilute gas, the rate of three-body interactions is significantly lower than that of two-body interactions, so that we can safely ignore it here and the above assumptions are reasonable ones. An example of non-elastic collisions would be if the particles had internal degrees of freedom (such as internal atomic energy levels or rotational degrees of freedom of molecules that can be excited), which would require a more sophisticated treatment than what we are set out to do here.

We thus assume a binary interaction between two particles described by a their respective points in Γ-space as $(\mathbf{x}_1, \mathbf{p}_1)$ and $(\mathbf{x}_2, \mathbf{p}_2)$ which get scattered into new states $(\mathbf{x}_1', \mathbf{p}_1')$ and $(\mathbf{x}_2', \mathbf{p}_2')$. If the collision is elastic, then also momentum and energy are conserved, i.e.

$$\begin{aligned} \mathbf{p}_1 + \mathbf{p}_2 &= \mathbf{p}_1' + \mathbf{p}_2' \\ \frac{|\mathbf{p}_1|^2}{2m} + \frac{|\mathbf{p}_2|^2}{2m} &= \frac{|\mathbf{p}_1'|^2}{2m} + \frac{|\mathbf{p}_2'|^2}{2m}. \end{aligned} \tag{1.20}$$

The two momenta of the final state have together six degrees of freedom. With these two conservation equations, we fix four of them. The fifth one is fixed if the interaction force betweeen the two particles is purely radial. In that case also the angular momentum is conserved and the collision will remain in the plane defined by the two incoming momentum vectors. The sixth and final condition comes from the nature of the interaction between the particles and is related to the angle by which the collision changes the individual momenta, which is thus typically termed the deflection angle.

For our statistical analysis, we are happy with a probability for deflection under various angles. This notion is captured by the idea of a differential scattering cross-section, which can be calculated for any given interaction potential. Since it is a statistical concept, it does not make sense to apply it to single interactions. Let us thus instead consider two beams of particles, the first of particle number density n_1 with a momentum $\mathbf{p}_1$, the second with a density n_2 and momentum $\mathbf{p}_2$. Obviously, a particle in the second beam sees a flux $j_2 = n_1 \left|\mathbf{p}_2 - \mathbf{p}_1\right| / m$ of particles from the first beam. We are interested in the number of collisions δn_c per unit volume and unit time, which scatter particles from the second beam into a solid angle $\mathrm{d}\Omega$. Clearly, this number must be proportional to the number density of particles n_2 in the second beam. It must also be proportional to the incoming flux j to which the particles are exposed and the solid angle $\mathrm{d}\Omega$ into which they scatter:

$$\delta n_c = \sigma(\mathbf{p}_1, \mathbf{p}_2 \,|\mathbf{p}_1', \mathbf{p}_2'\,)\; n_2\; \frac{\left|\mathbf{p}_2 - \mathbf{p}_1\right|}{m}\, n_1 \,\mathrm{d}\Omega. \tag{1.21}$$

The monstrous constant of proportionality is the differential scattering cross-section. Since we are describing elastic collisions, energy is conserved and thus the entire process must be reversible so that

$$\sigma(\mathbf{p}_1', \mathbf{p}_2' \,|\mathbf{p}_1, \mathbf{p}_2\,) = \sigma(\mathbf{p}_1, \mathbf{p}_2 \,|\mathbf{p}_1', \mathbf{p}_2'\,). \tag{1.22}$$

Note that the cross-section has dimensions of an area and directly reflects the area through which another particle has to pass so that scattering occurs.

The collision integral

We now want to evaluate the collision terms in equation (1.19). Let us begin with the out-scattering term C_{out}. Let us assume that the first beam of particles has their momentum vectors within $\mathrm{d}^3 p_1$ around $\mathbf{p}_1$, and the second within $\mathrm{d}^3 p_2$ around $\mathbf{p}_2$. The number density of particles in the first beam is then $n_1 = f(\mathbf{x}_1, \mathbf{p}_1)\,\mathrm{d}^3 p_1$, while that in the second is $n_2 = f(\mathbf{x}_2, \mathbf{p}_2)\,\mathrm{d}^3 p_2$. The term C_{out} can then be obtained by multiplying δn_c by $d^3 x$ (meaning that we localise the collisions in a region of space $\mathrm{d}^3 x$ around $\mathbf{x}$) and then integrating over all Ω and $\mathbf{p}_2$. We thus find

$$C_{\text{out}} = \mathrm{d}^3 x\, \mathrm{d}^3 p_1 \int \mathrm{d}^3 p_2 \int \mathrm{d}\Omega\; \sigma(\mathbf{p}_1, \mathbf{p}_2 \,|\mathbf{p}_1', \mathbf{p}_2'\,)\, \frac{\left|\mathbf{p}_2 - \mathbf{p}_1\right|}{m} f(\mathbf{x}, \mathbf{p}_1, t)\, f(\mathbf{x}, \mathbf{p}_2, t). \tag{1.23}$$

The in-scattering term C_{in} is just given by considering a process in the other direction, where particles start with the primed momenta and end up in the un-primed ones. The rate of collisions is then simply

$$\delta n_c' = \sigma(\mathbf{p}_1', \mathbf{p}_2' \,|\mathbf{p}_1, \mathbf{p}_2\,)\; \frac{\left|\mathbf{p}_2' - \mathbf{p}_1'\right|}{m} f(\mathbf{x}, \mathbf{p}_1', t)\, f(\mathbf{x}, \mathbf{p}_2', t)\, \mathrm{d}\Omega\, \mathrm{d}^3 p_1'\, \mathrm{d}^3 p_2'. \tag{1.24}$$

The conservation equations (1.20) for momentum and energy imply that

$$\left|\mathbf{p}_2 - \mathbf{p}_1\right| = \left|\mathbf{p}_2' - \mathbf{p}_1'\right|. \tag{1.25}$$

We now use that $\mathrm{d}^3p_1\,\mathrm{d}^3p_2 = \mathrm{d}^3p_1'\,\mathrm{d}^3p_2'$ if the interaction can be described by a Hamiltonian (this follows from Liouville's equation). All this lets us rewrite the in-scatter collision term as

$$C_{\text{in}} = \mathrm{d}^3x\,\mathrm{d}^3p_1 \int \mathrm{d}^3p_2 \int \mathrm{d}\Omega\ \sigma(\mathbf{p}_1, \mathbf{p}_2\,|\mathbf{p}_1', \mathbf{p}_2')\ \frac{|\mathbf{p}_2 - \mathbf{p}_1|}{m} f(\mathbf{x}, \mathbf{p}_1', t)\, f(\mathbf{x}, \mathbf{p}_2', t). \tag{1.26}$$

We can now insert all this into equation (1.19), after setting without loss of generality $\mathbf{p} := \mathbf{p}_2$, then the full equation using the collisionless Boltzmann equation for the left-hand side is

$$\frac{\mathrm{D}f}{\mathrm{D}t} = \frac{\partial f}{\partial t} + \frac{\mathbf{p}}{m} \cdot \boldsymbol{\nabla}_{\boldsymbol{x}} f + \mathbf{F} \cdot \boldsymbol{\nabla}_{\boldsymbol{p}} f = \int \mathrm{d}^3p_1 \int \mathrm{d}\Omega\ \frac{|\mathbf{p} - \mathbf{p}_1|}{m} \sigma(\Omega)\,[f'\, f_1' - f\, f_1]\,, \tag{1.27}$$

where we have simplified the notation by using $f := f(\mathbf{x}, \mathbf{p}, t)$, $f_1 := f(\mathbf{x}, \mathbf{p}_1, t)$, $f' := f(\mathbf{x}, \mathbf{p}', t)$, $f_1' := f(\mathbf{x}, \mathbf{p}_1', t)$ and $\sigma(\Omega) := \sigma(\mathbf{p}, \mathbf{p}_1\,|\mathbf{p}', \mathbf{p}_1')$. While the first four are really just abbreviations, the last definition for $\sigma(\Omega)$ makes use of the fact that σ is in the end only a function of the scattering angle Ω between the incoming momenta $\mathbf{p}$ and the outgoing $\mathbf{p}'$. This equation is the Boltzmann equation and describes the evolution of the distribution function f of a statistical set of particles under a long-range force field $\mathbf{F}$ and elastic binary particle collisions with a differential scattering cross-section $\sigma(\Omega)$.

1.2.2 The Maxwell-Boltzmann distribution

Next we will derive the Maxwell-Boltzmann distribution, which is the equilibrium distribution function that a uniform gas will attain. For this we assume uniformity by neglecting the configuration space coordinate $\mathbf{x}$ and we will also neglect the effect of any long-range force field, i.e. we set $\mathbf{F} = 0$. This does not mean that the analysis that follows applies e.g. only in the absence of gravitational forces, we need to only require that the length-scale over which the gravitational potential changes is much larger than the mean free path of the particles so that collisions clearly dominate over long range forces. If the gas is in equilibrium, then clearly $\mathrm{D}f/\mathrm{D}t = 0$, which makes the left-hand-side of equation (1.27) vanish. Note that this only means that we make the distribution function non-evolving in μ-space, the microscopic particles will still move around and scatter off of each other. For the Boltzmann equation to still hold, also the right-hand-side has thus to vanish which implies that

$$f\, f_1 = f'\, f_1'. \tag{1.28}$$

This means that in-scattering and out-scattering will be in exact balance. Since due to the assumed uniformity of the system, the distribution functions are independent of $\mathbf{x}$ and due to the stationarity also independent of t, we can write $f = f(\mathbf{p})$. Taking the logarithm of the balance condition (1.28), we find

$$\log f(\mathbf{p}) + \log f(\mathbf{p}_1) = \log f(\mathbf{p}') + \log f(\mathbf{p}_1'). \tag{1.29}$$

We shall now make a simple Taylor expansion of this logarithm of the equilibrium distribution function. Up to second order, it must have the form

$$\log f(\mathbf{p}) = C_0 + \mathbf{C}_1 \cdot \mathbf{p} + C_2 \mathbf{p}^2 + \mathcal{O}(p^3). \tag{1.30}$$

We note that this contains terms proportional to the momentum and to the kinetic energy[1], so that equation (1.29) simply reflects energy and momentum conservation in collisions (and higher order terms must

[1]Note that in full generality, the coefficient C_2 would be a matrix but due to the assumed homogeneity and isotropy of the system, we can just assume that the second order term is given by the trace alone.

vanish as they are not assumed to be conserved). The expansion up to second order can be rewritten in a more convenient form as

$$\log f(\mathbf{p}) = -B(\mathbf{p} - \mathbf{p}_0)^2 + \log A, \tag{1.31}$$

where A, B and $\mathbf{p}_0$ are constants that can be easily expressed in terms of the various coefficients C. We can now get rid of the logarithm to find the equilibrium solution for the distribution function as

$$f(\mathbf{p}) = A \exp\left[-B(\mathbf{p} - \mathbf{p}_0)^2\right]. \tag{1.32}$$

We can even go further and determine the constants A and B. We know that the number density of particles is just

$$n = \int \mathrm{d}^3\mathbf{p}\, f(\mathbf{p}) = A\left(\frac{\pi}{B}\right)^{3/2}, \tag{1.33}$$

where we have just carried out the integral to get the second expression. We can also understand the meaning of $\mathbf{p}_0$ as the average momentum of the particles. This can be calculated by formally computing the mean as

$$\langle \mathbf{p} \rangle = \frac{\int \mathrm{d}^3p\, \mathbf{p}\, f}{\int \mathrm{d}^3p\, f} = \frac{A}{n} \int \mathrm{d}^3p\, \mathbf{p} \exp\left[-B(\mathbf{p} - \mathbf{p}_0)^2\right] =: \mathbf{p}_0. \tag{1.34}$$

Clearly the remaining constant B takes the role of the inverse of a dispersion in momentum around the mean momentum $\mathbf{p}_0$. In order for our form to be consistent with the usual form of the Maxwell-Boltzmann distribution, we just have to set $B = (2mkT)^{-1}$ to find

$$f(\mathbf{p}) = n\,(2\pi mkT)^{-3/2} \exp\left[-\frac{(\mathbf{p} - \mathbf{p}_0)^2}{2mkT}\right], \tag{1.35}$$

where now the temperature alone expresses the dispersion of momenta around the mean momentum. This can be easily seen by computing the second moment of f as

$$\left\langle \mathbf{p}^2 \right\rangle - \langle \mathbf{p} \rangle^2 = \frac{\int \mathrm{d}^3p\, \mathbf{p}^2\, f}{\int \mathrm{d}^3p\, f} - p_0^2 = 3mkT. \tag{1.36}$$

We note that after dividing by $2m$, the first term on the left-hand side reflects the mean kinetic energy of a particle in the system, while the second term reflects the kinetic energy due to a particle with the mean momentum $\mathbf{p}_0$, the difference thus must describe the mean internal energy E_{int} of a particle in the system. We see immediately that

$$E_{\text{int}} := \frac{\left\langle \mathbf{p}^2 \right\rangle - \langle \mathbf{p} \rangle^2}{2m} = \frac{3}{2}kT, \tag{1.37}$$

while we call the kinetic energy associated with the mean motion the bulk kinetic energy

$$E_{\text{kin}} := \frac{\langle \mathbf{p} \rangle^2}{2m} = \frac{\mathbf{p}_0^2}{2m}. \tag{1.38}$$

We note that we can obtain certain characteristics of the macroscopic system by taking moments of the distribution function f. The zeroth moment gives us the particle number density n, the first one the mean momentum $\mathbf{p}_0$ and the second gives us the internal energy E_{int}. We will see much more of this in later parts of this lecture.

Background: Moments of a Distribution

You have certainly encountered the notion of moments in basic statistics (or in statistical physics). For a general probability distribution $p(x)$, with $\int p(x)\,\mathrm{d}x = 1$, one calls

$$\mu := \langle x \rangle = \int x\, p(x)\,\mathrm{d}x, \tag{1.39}$$

the mean. This is also the first "raw" moment of the distribution $p(x)$. The raw second moment

$$\mu_2 := \langle x^2 \rangle = \int x^2\, p(x)\,\mathrm{d}x \tag{1.40}$$

is normally not used directly, but instead one uses the central second moment, which is

$$\sigma^2 = \left\langle (x - \langle x \rangle)^2 \right\rangle = \int (x - \langle x \rangle)^2\; p(x)\,\mathrm{d}x = \langle x^2 \rangle - \langle x \rangle^2 \tag{1.41}$$

and this central second moment is called the "variance" of the distribution. The third and fourth raw moments are $\int x^3 p(x)\,\mathrm{d}x$ and $\int x^4\, p(x)\,\mathrm{d}x$, respectively. They are usually given however in a normalised form known as the skewness S and kurtosis K of the distribution:

$$S = \frac{1}{\sigma^3} \int (x - \langle x \rangle)^3\; p(x)\,\mathrm{d}x, \quad \text{and} \quad K = \frac{1}{\sigma^4} \int (x - \langle x \rangle)^4\; p(x)\,\mathrm{d}x. \tag{1.42}$$

For a Gaussian distribution, $S = 0$ and $K = 3$. In fact, a Gaussian distribution is completely described by its mean and its variance. All higher moments can be expressed in terms of these two quantities.

1.2.3 H-theorem and Entropy

The Maxwell-Boltzmann distribution that we have derived in the previous section is the equilibrium solution of the Boltzmann equation. For any initial phase space distribution f, we expect that if collisions occur frequently enough, the Boltzmann equation will drive it towards the equilibrium state described by the Maxwell-Boltzmann distribution. We will demonstrate this next.

The essence of this exercise is the notion of irreversible processes and the generation of entropy. While our Hamiltonian mechanics on the microscopic level (i.e. in Γ-space) is completely reversible, we will see that the macroscopic description in ω-space is not. This can be shown using Boltzmann's infamous H-theorem.

For this, we define the quantity

$$H := \int d^3p\, f\, \log f. \tag{1.43}$$

The H-theorem states that if the distribution function f evolves according to the Boltzmann equation, and external forces are absent, then H for a uniform gas can never increase with time, i.e.

$$\frac{\mathrm{d}H}{\mathrm{d}t} \leq 0. \tag{1.44}$$

The time evolution of H can be easily shown to be given by the rather long expression

$$\begin{aligned}\frac{\mathrm{d}H}{\mathrm{d}t} &= \int \mathrm{d}^3p\ \frac{\partial f}{\partial t}\,(1+\log f)\\ &= \frac{1}{4}\int \mathrm{d}^3p \int \mathrm{d}^3p_1 \int \mathrm{d}\Omega\ \sigma(\Omega)\frac{|\mathbf{p}-\mathbf{p}_1|}{m}\ (f'f'_1 - ff_1)\log\left[\frac{ff_1}{f'f'_1}\right]. \end{aligned} \tag{1.45}$$

Since for any real numbers a and b the relation $(b-a)\log(a/b) \leq 0$ holds, the H-theorem is proven. So now we have to understand why this theorem indeed tells us that collisions will drive the distribution function towards a Maxwell-Boltzmann distribution.

First, we see that in equilibrium H is constant in time, i.e. $\frac{\mathrm{d}H}{\mathrm{d}t} = 0$, since in equilibrium $f'f'_1 = ff_1$, as we have shown above. Therefore, if we start with an arbitrary distribution function f far from equilibrium, the system will have a value of H that is much larger than its equilibrium value. If we are away from equilibrium, the right-hand side of equation (1.45) must be negative and so the system keeps decreasing its value of H until it reaches equilibrium, in which it will follow the Maxwell-Boltzmann distribution. The usual entropy of the system is given by

$$S = -kH + \text{constant}. \tag{1.46}$$

1.2.4 The Moment Equations

In all our derivation we have assumed that the number of particles, their momentum and their energy are conserved. We have also seen at the end of Section 1.2.2 that these three characteristics of the system can be expressed as moments of the distribution function. They will allow us to go to the hydrodynamic description later by reducing further the complexity of our system. While the Boltzmann equation describes the evolution of the phase-space density f in six-dimensional μ-space, by taking moments we reduce the dimensionality to three dimensions since we integrate out the momentum space dimensions. Instead of one equation describing the evolution of a six-dimensional field, we will next obtain a sequence of coupled equations that describe only three-dimensional fields. This comes at the price of multiple equations.

The moments

Unlike before, we will now no longer assume that the system is homogeneous, i.e. the mean momentum is allowed to change over space, and so are the number density and the internal energy. We can summarise the first three moments and their meaning in form in which they are commonly used in hydrodynamics:

$$n(\mathbf{x},t) := \int \mathrm{d}^3p\ f(\mathbf{x},\mathbf{p},t) \qquad \text{is the number density of particles} \tag{1.47}$$

$$\mathbf{v}(\mathbf{x},t) := \frac{1}{mn}\int \mathrm{d}^3p\ \mathbf{p}\, f(\mathbf{x},\mathbf{p},t) \qquad \text{is the velocity field} \tag{1.48}$$

$$e(\mathbf{x},t) := \frac{1}{2mn}\int \mathrm{d}^3p\ \mathbf{p}^2\, f(\mathbf{x},\mathbf{p},t) - \frac{m}{2}\mathbf{v}^2(\mathbf{x},t) \qquad \text{is the internal energy field.} \tag{1.49}$$

In addition, one usually defines the mass density field $\rho(\mathbf{x},t) := m\,n(\mathbf{x},t)$.

And of course one can continue to take higher order moments. There is another property that is somewhat hidden in how we wrote down the moments above. The zeroth moment, the number density, is

obviously a scalar. The first moment, the velocity (or momentum), is a vector. The second moment, the energy, as we wrote it is again a scalar. But in full generality, instead of $\mathbf{p}^2$, we could have multiplied two different Cartesian components of the momentum $p_i\, p_j$, which is a so-called tensor product and can also be written as $\mathbf{p} \otimes \mathbf{p}$. This shows that the second moment is actually a rank-2 tensor (think matrix), and when we wrote it as a scalar, we actually implicitly took the trace of it. The third moment can be built from the tensor product of three momenta $\mathbf{p} \otimes \mathbf{p} \otimes \mathbf{p}$ and would thus be a rank-3 tensor, and so on... This sounds complicated but it will become clear shortly why this is and what it means. So the more simple and formal way would be to write (using Cartesian components)

$$n(\mathbf{x}, t) := \int \mathrm{d}^3p\ f(\mathbf{x}, \mathbf{p}, t) \qquad \text{0th moment} \tag{1.50}$$

$$\pi_i(\mathbf{x}, t) := \int \mathrm{d}^3p\ p_i\, f(\mathbf{x}, \mathbf{p}, t) \qquad \text{1st moment} \tag{1.51}$$

$$\Pi_{ij}(\mathbf{x}, t) := \int \mathrm{d}^3p\ p_i p_j\, f(\mathbf{x}, \mathbf{p}, t) \qquad \text{2nd moment} \ldots \tag{1.52}$$

The first term – rate of change

We now would like to derive evolution equations for these moments. We shall see that one can obtain these by taking moments of the Boltzmann equation. Let's start with the first term of the Boltzmann equation, the simple $\partial f/\partial t$. For the zeroth moment, we would just integrate it over momentum space, and we find

$$\int \mathrm{d}^3p\ \frac{\partial f}{\partial t} = \frac{\partial}{\partial t} \int \mathrm{d}^3p\ f = \frac{\partial n}{\partial t}, \tag{1.53}$$

which is just the rate of change of the zeroth moment. Quite obviously, we can do this for all moments by first multiplying with as many $\mathbf{p}$ as we need and then integrating over momentum space. For the first moment we thus get

$$\int \mathrm{d}^3p\ \mathbf{p}\, \frac{\partial f}{\partial t} = \frac{\partial}{\partial t} \int \mathrm{d}^3p\ \mathbf{p} f = \frac{\partial \boldsymbol{\pi}}{\partial t} = \frac{\partial \rho \mathbf{v}}{\partial t}, \tag{1.54}$$

where we have used that $\mathbf{p}$ and t are independent, and also that $\rho = mn$ in the last equality. So this gives us the rate of change of a momentum density. And of course this applies to all higher moments as well so that the second moment is logically $\frac{\partial \Pi_{ij}}{\partial t}$.

The second term – advection

The second term of the Boltzmann equation is $\frac{\mathbf{p}}{m} \cdot \boldsymbol{\nabla}_{\boldsymbol{x}} f$. For the zeroth moment, we just have to integrate it over momentum space, i.e.

$$\int \mathrm{d}^3p\ \frac{\mathbf{p}}{m} \cdot \boldsymbol{\nabla}_{\boldsymbol{x}} f = \frac{1}{m} \boldsymbol{\nabla}_{\boldsymbol{x}} \cdot \int \mathrm{d}^3p\ \mathbf{p} f = \frac{1}{m} \boldsymbol{\nabla}_{\boldsymbol{x}} \cdot \boldsymbol{\pi} = \boldsymbol{\nabla}_{\boldsymbol{x}} (n\mathbf{v}), \tag{1.55}$$

where in the first equality we have used that $\mathbf{x}$ and $\mathbf{p}$ are independent and so the gradient can be pulled out of the integral and then just inserted definitions. We note that that in the term for the zeroth moment, the first moment appears (because there is already a $\mathbf{p}$ in the equation).

Let's look at what happens when we take the first moment of this term. We look at the component i of it

$$\int \mathrm{d}^3p\ p_i \frac{p_j}{m} \frac{\partial f}{\partial x_j} = \frac{1}{m} \frac{\partial}{\partial x_j} \int \mathrm{d}^3p\ p_i p_j f = \frac{1}{m} \frac{\partial \Pi_{ij}}{\partial x_j}, \tag{1.56}$$

and we see, as before, we get the spatial derivative of the next higher moment. The second moment is then obviously given by

$$\int \mathrm{d}^3p\ p_i p_j \frac{p_k}{m}\frac{\partial f}{\partial x_k} = \frac{1}{m}\frac{\partial}{\partial x_k}\int \mathrm{d}^3p\ p_i p_j p_k f = \frac{1}{m}\frac{\partial \Gamma_{ijk}}{\partial x_k}, \tag{1.57}$$

where Γ_{ijk} is the third moment of the distribution function.

The third term – acceleration

The next term in the Boltzmann equation is only present if we have long-range or external forces $\mathbf{F}(\mathbf{x})$ (i.e. we assume that the force does not depend on the momentum) and is given by $\mathbf{F}\cdot\boldsymbol{\nabla}_{\boldsymbol{p}} f$. Once again, for the zeroth moment, we just integrate over it and find

$$\int \mathrm{d}^3p\ \mathbf{F}\cdot\boldsymbol{\nabla}_{\boldsymbol{p}} f = \mathbf{F}\cdot\int \mathrm{d}^3p\ \boldsymbol{\nabla}_{\boldsymbol{p}} f = \mathbf{F}\cdot\oint_\infty \mathrm{d}\mathbf{S}_{\mathbf{p}}\ f = 0, \tag{1.58}$$

where we have employed Gauss' theorem in momentum space in the second equality so that we integrate over a boundary at infinity in momentum space. Obviously f should vanish there, and so this term must be zero.

Let us next look at the first moment of this term, which can be shown to be (see exercise)

$$\int \mathrm{d}^3p\ p_i \left(F_j \frac{\partial f}{\partial p_j}\right) = -nF_i. \tag{1.59}$$

The second moment turns out to be

$$\int \mathrm{d}^3p\ p_i p_j \left(F_k \frac{\partial f}{\partial p_k}\right) = -(F_i\pi_j + F_j\pi_i). \tag{1.60}$$

This is just a tensorial version of the potential energy change as the particle is accelerated by the force[2].

The last term – collisions

The final term we have in the Boltzmann equation is the collision term $\left[\frac{\partial f}{\partial t}\right]_{\text{coll}}$. Its nature when we take moments is to tell us whether the collisions conserve the respective moment, since formally it behaves exactly like the first term (i.e. we can just pull the integral inside the bracket and the derivative). Since in our case of simple binary elastic collisions all first three moments are conserved, i.e. particle number, momentum and energy, they all vanish in equilibrium. If one would treat particle processes that violate one of these (e.g. reactions between particles that do not conserve the particle number, internal atomic degrees of freedom that can absorb energy) then this term has to be included as a source/sink term to accommodate this. Equivalently, if one can not assume that collisions are in equilibrium, and the underlying distribution function is a Mawell-Boltzmann, then additional terms ("non-ideal" terms) will arise. We will have a look at them shortly.

[2] This can be seen by taking the fundamental Newton relation $F_i = ma_i = \dot{p}_i$. Since we are looking at a quadratic energy term, we want something like $\frac{\partial}{\partial t}(p_i p_j) = p_i F_j + p_j F_i$. Now what's the relation with the potential energy? Let's assume $\mathbf{F} = m\boldsymbol{\nabla}\phi$ where ϕ is the potential, then the potential energy E_p will change if the particle moves a distance $d\mathbf{x}$ by $dE_p = m\boldsymbol{\nabla}\phi\cdot d\mathbf{x}$. If we look at the rate at which it changes, i.e. dE_p/dt, we get $dE_p/dt = m\boldsymbol{\nabla}\phi\cdot\mathbf{v} = \mathbf{F}\cdot\mathbf{v}$ which is just the trace of our expression. So, this just quantifies the rate of change in potential energy.

Putting it all together

Let us put now all the pieces together. The evolution equation for the first three moments are

$$\begin{aligned} \frac{\partial n}{\partial t} + \frac{1}{m}\frac{\partial \pi_i}{\partial x_i} &= 0 \\ \frac{\partial \pi_i}{\partial t} + \frac{1}{m}\frac{\partial \Pi_{ij}}{\partial x_j} &= F_i n \\ \frac{\partial \Pi_{ij}}{\partial t} + \frac{1}{m}\frac{\partial \Gamma_{ijk}}{\partial x_k} &= F_i \pi_j + F_j \pi_i \\ &\vdots \end{aligned} \tag{1.61}$$

These equations fully describe the conservation of mass, momentum and energy (after taking the trace of the third eq.) in our system. They are however not a closed system since the equation for one moment depends on the next moment, so that we have an infinite hierarchy of equations. Without further assumptions this is thus not tractable. We will see how we can close this hierarchy next.

Chapter 2

Hydrodynamic Equations and Phenomenology

As we have seen in Chapter 1, collisions that conserve energy, momentum and the particle number will always drive any arbitrary distribution function towards the Maxwell-Boltzmann distribution function by virtue of the H-theorem. At the same time, we have seen that by taking moments of the Boltzmann equation, we can derive a hierarchy of evolution equations for these moments, given in eq. (1.61). We will next derive the equations of ideal hydrodynamics. These equations one obtains under the assumption of local thermodynamic equilibrium, which is simply the assumption that in every point in space, the distribution function is given by a Maxwell-Boltzmann distribution, however allowing the temperature $T(\mathbf{x})$ to vary spatially. This leads to a truncation of the hierarchy after the second moment, the set of equations becomes closed and thus mathematically tractable.

Next we will introduce the extension to non-ideal hydrodynamics. For this we will relax the local thermodynamic equilibrium condition by allowing the distribution to be close to but not exactly a Maxwell-Boltzmann distribution. We will see that under this condition, new phenomena appear such as thermal conduction and viscosity.

Finally, in this chapter we will look at the hydrodynamic phenomenology arising from these equations, such as shock waves and fluid instabilities.

2.1 Ideal Hydrodynamics

2.1.1 Local Thermodynamic Equilibrium

Under the assumption that collisions occur frequently, i.e. the mean free path of the particles is much smaller than typical length scales of the system, one can assume that in every point $\mathbf{x}$, the collisions have driven the momentum distribution function to a Maxwell-Boltzmann distribution with a spatially varying temperature $T(\mathbf{x})$ and mean momentum $\mathbf{p}_0 = m\mathbf{v}(\mathbf{x})$. This allows us to close the hierarchy of equations. We already calculated the moments of the Maxwell-Boltzmann distribution, so we can just restate them here in spatially varying form. The number density is obviously just $n(\mathbf{x})$, and all higher moments can be expressed in terms of the number density, the mean fluid velocity $\mathbf{v}(\mathbf{x})$ and the

temperature $T(\mathbf{x})$:

$$\pi_i(\mathbf{x}) = \rho v_i \tag{2.1}$$

$$\Pi_{ij}(\mathbf{x}) = m\rho(v_i v_j + \frac{kT}{m}\delta_{ij}) \tag{2.2}$$

$$\Gamma_{ijk}(\mathbf{x}) = m^2\rho\left(v_i v_j v_k + \frac{kT}{m}\left(v_i\delta_{jk} + v_j\delta_{ik} + v_k\delta_{ij}\right)\right), \tag{2.3}$$

where δ_{ij} is the Kronecker-δ symbol (which is defined to be equal to 1 if $i = j$ and zero otherwise). These are actually more general than we need. To simplify our expressions somewhat, we will try to make use of the thermodynamic notions of internal energy and pressure.

Pressure from kinetic theory

Pressure is defined to be the internal resistance of a gas (or fluid) to isotropic compression. For an adiabatic process (i.e. we perform the compression slowly enough so that the entropy remains constant), the pressure P is given by the amount of energy dE required to change the volume of the fluid by an amount dV, i.e. $dE = -P\,dV$. By dimensional arguments, P must thus be an energy density.

Pressure is a result of the random motions of particles. If we were to contain a gas at rest in a fixed volume, then the particles would exert an outward force onto the surface of the container. Let us look at the left boundary in x-direction of the container. The number of particles hitting the face dA_{+x} in a time dt will of course be $\frac{n}{2}\bar{v}_x dA\,dt$ if $\bar{v}_x$ is the typical RMS velocity of a particle in the x-direction. The factor $\frac{1}{2}$ comes from the fact that half of the particles will be moving to the right, and the other half to the right, towards the surface element. A particle of momentum $m\bar{v}_x$ will be reflected by the wall and change its momentum to $-m\bar{v}_x$, the change of momentum is thus $-2m\bar{v}_x$. This imparts an impulse $F_x dt$ on the wall over a time dt given by

$$F_{+x}dt = \frac{n}{2}dA_{+x}\,\bar{v}_x\,dt\;2m\bar{v}_x = mn\bar{v}_x^2\,dA_{+x}\,dt \tag{2.4}$$

Assuming the isotropic random velocity distribution of the Maxwell-Boltzmann distribution, the RMS velocity along only one dimension will be $\bar{v}_x^2 = \frac{1}{3}\frac{\langle\mathbf{p}^2\rangle - \langle\mathbf{p}\rangle^2}{m^2}$. Since pressure is defined as the force exerted per unit area of the surface we have

$$P_{+x} = mn\bar{v}_x^2 = \frac{n}{3m}(\langle\mathbf{p}^2\rangle - \langle\mathbf{p}\rangle^2) = nkT =: P. \tag{2.5}$$

Obviously this does no longer depend on how the surface was oriented, the pressure on any surface will be given by this expression since the random motions are completely isotropic in the Maxwell-Boltzmann case. In full generality, we can however also define a tensor P_{ij} as

$$P_{ij} := \frac{\Pi_{ij}}{m} - \frac{\pi_i\pi_j}{\rho}, \tag{2.6}$$

which in the Maxwell-Boltzmann case takes the trivial form $P_{ij} = nkT\delta_{ij} = P\delta_{ij}$. We can thus simply write

$$\frac{\Pi_{ij}}{m} = \rho v_i v_j + P_{ij} \quad \text{and} \quad \frac{\Pi}{2m} = \operatorname{tr}\frac{\Pi_{ij}}{2m} = \frac{1}{2}\rho\mathbf{v}^2 + \frac{3}{2}P =: \frac{1}{2}\rho\mathbf{v}^2 + \rho\epsilon, \tag{2.7}$$

where $\epsilon := \frac{3}{2}\frac{kT}{m}$ is the internal energy per unit mass associated with a single particle (for a monoatomic ideal gas).

2.1.2 The Equations of Ideal Hydrodynamics

We can insert the results from the previous section now into the moment equations to finally obtain the hydrodynamic equations in terms of three conservation equations for the mass density, the momentum density and the energy density (for which we simply consider only the trace of the equation for the second moment). This yields the so-called conservative form of the hydrodynamic equations

$$\begin{aligned}
\frac{\partial \rho}{\partial t} + \frac{\partial}{\partial x_i}(\rho v_i) &= 0 && (2.8)\\
\frac{\partial}{\partial t}(\rho v_i) + \frac{\partial}{\partial x_j}(\rho v_i v_j) &= -\frac{\partial P}{\partial x_i} + \rho F_i && (2.9)\\
\frac{\partial e}{\partial t} + \frac{\partial}{\partial x_i}(e v_i) &= -\frac{\partial}{\partial x_i}(P v_i) + \rho F_i v_i, && (2.10)
\end{aligned}$$

where $e = \rho\epsilon + \frac{1}{2}\rho v^2$ is the total energy density. The first equation is just the continuity equation, the second is the momentum equation and the third is an equation for the total energy. They can also be written (after some transformations) in primitive form, which means that the equations are expressed in terms of the 'primitive' variables ρ, $\mathbf{v}$ and ϵ instead of the conserved quantities ρ, $\rho\mathbf{v}$ and e. One then finds

$$\begin{aligned}
\frac{\partial \rho}{\partial t} + \frac{\partial}{\partial x_i}(\rho v_i) &= 0 && (2.11)\\
\frac{\partial v_i}{\partial t} + v_j \frac{\partial v_i}{\partial x_j} &= -\frac{1}{\rho}\frac{\partial P}{\partial x_i} + \frac{F_i}{m} && (2.12)\\
\frac{\partial \epsilon}{\partial t} + v_j \frac{\partial \epsilon}{\partial x_j} &= -\frac{P}{\rho}\frac{\partial v_j}{\partial x_j}. && (2.13)
\end{aligned}$$

Here, the second equation is called the Euler equation, and the third is called the internal energy equation.These sets of equations are mathematically equivalent and can be used interchangeably, depending on which ones are easier to apply in the problem at hand.

Background: Conservation laws

We note however that conservation laws, i.e. equations of the form

$$\frac{\partial X}{\partial t} + \boldsymbol{\nabla} \cdot \mathbf{F}_X = S_X, \tag{2.14}$$

where X is a conserved quantity, $\mathbf{F}_X$ the associated flux (of the form $\mathbf{F}_X = X\mathbf{v}$) and S_X the source or sink term for quantity X (i.e. the rate at which X is produced or destroyed in every point) admit an integral form. By integrating over an arbitrary volume V which is fixed in space and time (i.e. does not move), we find by applying Gauss' theorem

$$\begin{aligned}
\frac{\partial}{\partial t}\int_V \mathrm{d}V\ X &= -\int_V \mathrm{d}V\ \boldsymbol{\nabla}\cdot\mathbf{F}_X + \int_V \mathrm{d}V\ S_X\\
&= -\int_{\partial V} \mathrm{d}\mathbf{S}\ \cdot\ \mathbf{F}_X + \int_V \mathrm{d}V\ S_X. && (2.15)
\end{aligned}$$

This means that they can always be written in a form where the rate of change of X in a fixed volume V is given by the integral of the flux over the boundary of that volume and the amount of X produced or destroyed in that volume. Writing the equations in this integral form is typically

Background: Conservation laws (cont)

called the weak form of the hydrodynamic equations, while writing them in the differential form is also called the strong form of the equations. The weak form allows one to study e.g. cases in which the quantity X shows a discontinuity in space as we will see when we discuss shocks.

The adiabatic equation of state

As you might have noticed, the system of equations is now closed and we have three primitive variables ρ, $\mathbf{v}$ and ϵ. The pressure P is related to ϵ through ρ and T. We will now express this relation more directly in order to write also the pressure in terms of primitive variables. First, by eliminating the temperature from the definitions of P and ϵ, we have

$$P = \frac{2}{3}\rho\epsilon \tag{2.16}$$

for our ideal gas of monoatomic particles. The first law of thermodynamics states that the internal energy changes as

$$\mathrm{d}U = -P\,\mathrm{d}V + T\,\mathrm{d}S + \mathrm{d}Q, \tag{2.17}$$

where the first term on the right corresponds to the change of energy due to a change in volume at fixed entropy, the second corresponds to the change due to a change in entropy and the third is due to heat transfer into or out of the system. For a system in isolation $\mathrm{d}Q = 0$. For an adiabatic process also $\mathrm{d}S = 0$ so that we only have $\mathrm{d}U = -P\,\mathrm{d}V$. The total internal energy in the system is

$$U = \frac{3}{2}NkT = \frac{3}{2}PV \quad \text{so that} \quad \mathrm{d}U = \frac{3}{2}\left(P\,\mathrm{d}V + V\,\mathrm{d}P\right) \tag{2.18}$$

Since we had in the adiabatic case $\mathrm{d}U = -P\,\mathrm{d}V$ we have

$$-\frac{5}{2}P\,\mathrm{d}V = \frac{3}{2}V\,\mathrm{d}P \quad \text{which yields} \quad \log\left(\frac{P}{P_0}\right) = -\frac{5}{3}\log\left(\frac{V}{V_0}\right), \tag{2.19}$$

where we have performed a separation of variables followed by an integration in the second equation. Since we can write $\rho = (Nm)/V$, we immediately find the form

$$P = K\,\rho^{5/3}, \quad \text{with} \quad K = \frac{P_0}{\rho_0^{5/3}}. \tag{2.20}$$

This is the so-called polytropic equation of state and is usually written in the more general form $P = K\rho^{\gamma}$, where γ is called the polytropic exponent. Gases and fluids for which the pressure is a function of only the density, i.e. $P = P(\rho)$ are barotropic fluids. For an ideal monoatomic gas we have $\gamma = 5/3$, but this form is indeed more general and can account even for gases that behave differently. One finds, e.g., $\gamma = 1$ for an isothermal gas, which is a gas for which the temperature does not increase when it is compressed, or one finds $\gamma = 4/3$ for a gas of relativistic particles such as photons.

It is important to note that it is only valid for adiabatic processes, i.e. as long as the entropy remains constant. However, if we inject entropy into the system while not changing the volume, then the system will only alter the pre-factor K to a new value K'. After the entropy has been raised, it will evolve along the new adiabatic relation $P = K'\,\rho^{5/3}$.

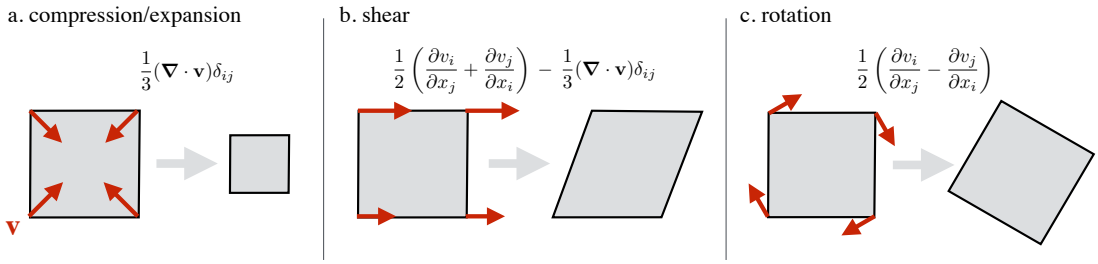

Figure 2.1: The velocity deformation tensor $D_{ij} = \frac{\partial v_i}{\partial v_j}$, indicating the spatial change in the velocity field, can be decomposed into three components: a.) the compression/expansion part, given by the mean of the diagonal elements, $\frac{1}{3}D_{ii}$, b.) the velocity shear, given by the trace-free symmetric part of D_{ij}, and c.) the rotation, given by the anti-symmetric part of D_{ij}. Both shear and rotation preserve the volume of a fluid element and thus cannot act to increase the density.

2.1.3 The fluid velocity field

While a seemingly innocent quantity, the field $\mathbf{v}(\mathbf{x})$ describes the mean velocity with which the fluid (or gas) moves at every point in space. It is the relevant quantity describing the dynamics of the fluid. An import quantity that can be obtained from the fluid velocity field $\mathbf{v}(\mathbf{x})$ is the velocity divergence tensor given by

$$D_{ij} = \frac{\partial v_i}{\partial x_j} \tag{2.21}$$

which combines all possible combinations of velocity-components with directional derivatives. We have already encountered its trace which is one third of the scalar velocity divergence and describes the local compression or expansion of a fluid element

$$\operatorname{tr} D = \boldsymbol{\nabla}\cdot\mathbf{v}. \tag{2.22}$$

It is the quantity that is responsible for a change of density in compressible flow, and vanishes for incompressible flow. More generally, we can decompose D into its symmetric part Λ_{ij} and antisymmetric part Ω_{ij}

$$D_{ij} = \Lambda_{ij} + \Omega_{ij}, \quad \text{with} \quad \Lambda_{ij} = \frac{1}{2}\left(\frac{\partial v_i}{\partial x_j}+\frac{\partial v_j}{\partial x_i}\right), \quad \Omega_{ij} = \frac{1}{2}\left(\frac{\partial v_i}{\partial x_j}-\frac{\partial v_j}{\partial x_i}\right). \tag{2.23}$$

The symmetric part, once one subtracts its trace, describes the shearing of fluid elements at fixed volume (see Figure 2.1), which does not alter the density. The antisymmetric part represents the rotation of fluid elements at fixed volume and can be rewritten as a vector since it only has three independent components. This vector is the vorticity of the flow

$$\boldsymbol{\omega} := \boldsymbol{\nabla}\times\mathbf{v} = \epsilon ijk\Omega_{jk}. \tag{2.24}$$

By taking the curl of the velocity equation, one can derive the vorticity equation which describes the time evolution of the vorticity

$$\frac{\partial\omega}{\partial t} + \boldsymbol{\nabla}\times(\boldsymbol{\omega}\times\mathbf{v}) = \frac{1}{\rho^2}(\boldsymbol{\nabla}\rho)\times(\boldsymbol{\nabla}P) + \boldsymbol{\nabla}\times\mathbf{F}. \tag{2.25}$$

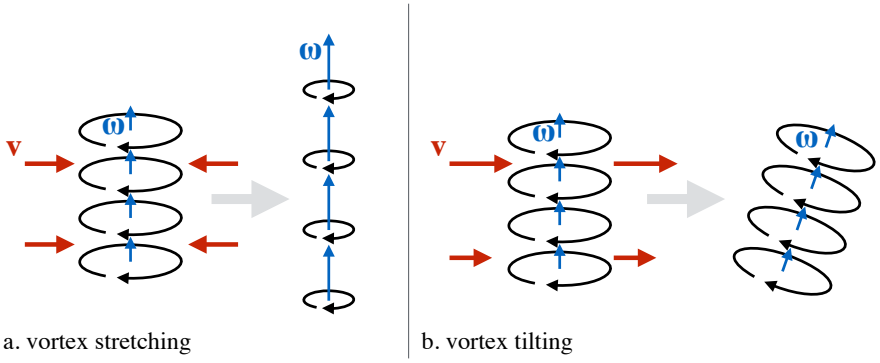

a. vortex stretching b. vortex tilting

Figure 2.2: The effect of the fluid velocity field on a vortex tube (a line of parallel vorticity). Panel a: vortex stretching occurs when the flow is compressed in a direction perpendicular to the vorticity $\boldsymbol{\omega}$, as a consequence, the vorticity increases, but its overall density remains constant. Panel b: vortex tilting occurs when the velocity field has shear. As a result, the vortex tube undergoes an associated rotation.

If the force is conservative, such as the gravitational force, i.e. if $\mathbf{F} = -m\boldsymbol{\nabla}\phi$, then the force term vanishes. In fact, one can show that this equation implies that vorticity is also a conserved quantity and can only be produced by the so-called baroclinc term, which is the first term on the right-hand-side of the equation. For a barotropic fluid, and in particular for a polytropic equation of state $P \propto \rho^{\gamma}$, this term will always vanish so that in this case vorticity is manifestly conserved if the flow is also adiabatic (i.e. no entropy is generated anywhere, which is however not true when shocks occur as we will see later).

When we can assume a barotropic flow under a conservative force, then the vorticity equation reduces simply to

$$\frac{\partial \omega}{\partial t} + \boldsymbol{\nabla} \times (\boldsymbol{\omega} \times \mathbf{v}) = 0. \tag{2.26}$$

After a few vector calculus manipulations and using that $\boldsymbol{\nabla} \cdot \boldsymbol{\omega} = 0$, one can write this as

$$\frac{D\boldsymbol{\omega}}{Dt} = (\boldsymbol{\omega} \cdot \boldsymbol{\nabla})\mathbf{v} - \boldsymbol{\omega}(\boldsymbol{\nabla} \cdot \mathbf{v}). \tag{2.27}$$

This means that vorticity is simply transported by the flow but two additional components arise: the first term on the right represents vortex stretching, the second represents vortex tilting. Vortex stretching means that if a vortex tube (given by ω) is stretched along its axis (i.e. when the flow is divergent along this direction), then the vorticity must increase. Vortex tilting means that if the fluid velocity component perpendicular to the vortex tube changes along the tube, then this will tilt the vorticity. These concepts are important when one studies turbulence.

2.1.4 Gravity and hydrostatic equilibrium

When one considers the self-gravity of the gas, then the density distribution ρ produces a gravitational force $\mathbf{F} = -m\boldsymbol{\nabla}\phi$ where the gravitational potential ϕ is related to the density through Poisson's equation

$$\Delta\phi = 4\pi G\rho. \tag{2.28}$$

In full generality for a self-gravitating system, Poisson's equation has to be solved along with the fluid equations in order to have a complete system including the gravitational force.

A self-gravitating system of finite temperature can be in so-called hydrostatic equilibrium. This is the condition that all velocities vanish, i.e. $\mathbf{u} = 0$ and $\partial\mathbf{u}/\partial t = 0$. From the Euler equation (2.12) it immediately follows that in hydrostatic equilibrium

$$\frac{1}{\rho}\boldsymbol{\nabla} P = -\boldsymbol{\nabla}\phi. \tag{2.29}$$

Due to the isotropic pressure in an ideal gas, such a system will usually assume a spherical symmetry (unless there would be rotation, which would however require non-vanishing velocity). In spherical symmetry, P and ρ are only functions of the radial coordinate r and the differential operators become $\boldsymbol{\nabla} = \mathbf{e}_r \frac{\partial}{\partial r}$ and $\Delta = \frac{1}{r^2}\frac{\partial}{\partial r}(r^2 \frac{\partial}{\partial r})$, where $\mathbf{e}_r$ is the radial unit vector. This combines to the equation of hydrostatic equilibrium in spherical symmetry

$$\frac{\partial \phi}{\partial r} = -\frac{1}{\rho}\frac{\partial P}{\partial r}, \tag{2.30}$$

which after inserting the gravitational force and using Poisson's equation becomes

$$\frac{1}{r^2}\frac{\partial}{\partial r}\left(\frac{r^2}{\rho}\frac{\partial P}{\partial r}\right) = -4\pi G\rho. \tag{2.31}$$

Assuming a barotropic fluid with equation of state $P = K\rho^\gamma$, this equation can be transformed into the famous Lane-Emden equation which was an early model of stars in the 19th century.

For isothermal gas (T=const.), the adiabatic exponent is $\gamma = 1$ so that $P = K\rho$. In this case, the solution to the equations of hydrostatic equilibrium can be shown to be the (singular) isothermal sphere profile, given by

$$\rho(r) = \frac{K}{2\pi G r^2}. \tag{2.32}$$

2.2 Transport Phenomena and Non-Ideal Hydrodynamics

One might question whether the assumption of perfect local thermodynamic equilibrium is always valid for a system. In systems in which the time between collisions is not negligibly short compared to the dynamical time scales (or equivalently, the mean free path is not negligibly small compared to the scales on which density and temperature of the system change, one might want to include the effect of a small departure from the Maxwell-Boltzmann distribution function. We thus go back to the Boltzmann equation and use the following perturbation to the distribution function

$$f(\mathbf{x}, \mathbf{p}, t) = f_M(\mathbf{x}, \mathbf{p}, t) + \delta f(\mathbf{x}, \mathbf{p}, t), \quad \text{where} \quad \delta f \ll f_M, \tag{2.33}$$

and f_M is the Maxwell-Boltzmann distribution. Since for the Maxwell-Boltzmann case, the collisions are in equilibrium, we have $\left[\frac{\partial f_M}{\partial t}\right]_{\text{coll}} = 0$. On the other hand, since δf shall be small, we can assume $Df/Dt = Df_M/Dt$, so that we finally have

$$\frac{\partial f_M}{\partial t} + \frac{\mathbf{p}}{m}\cdot\boldsymbol{\nabla}_{\boldsymbol{x}} f_M + \mathbf{F}\cdot\boldsymbol{\nabla}_{\boldsymbol{p}} f_M = \left[\frac{\partial \delta f}{\partial t}\right]_{\text{coll}}. \tag{2.34}$$

We now apply a trick. Since we know that f_M only depends on the first three moments, which we can express in terms of n, $\mathbf{v}$ and T, we can write $f_M = f_M(n, \mathbf{v}, t)$, then the time derivative of f_M must have the form

$$\frac{\partial f_M}{\partial t} = \frac{\partial f_M}{\partial n}\frac{\partial n}{\partial t} + \frac{\partial f_M}{\partial T}\frac{\partial T}{\partial t} + \frac{\partial f_M}{\partial v_i}\frac{\partial v_i}{\partial t} \tag{2.35}$$

and the spatial gradient must be

$$\boldsymbol{\nabla} f_M = \frac{\partial f_M}{\partial n}\boldsymbol{\nabla} n + \frac{\partial f_M}{\partial T}\boldsymbol{\nabla} T + \frac{\partial f_M}{\partial v_i}\boldsymbol{\nabla} v_i. \tag{2.36}$$

Some steps of calculation (which you can try as an exercise) then gives

$$\frac{1}{f_M}\left[\frac{\partial \delta f}{\partial t}\right]_{\text{coll}} = \frac{1}{T}\frac{\partial T}{\partial x_i}v_i\left(\frac{m}{2kT}\mathbf{v}^2 - \frac{5}{2}\right) + \frac{m}{kT}\Lambda_{ij}\left(v_i v_j - \frac{1}{3}\mathbf{v}^2\delta_{ij}\right), \tag{2.37}$$

where

$$\Lambda_{ij} = \frac{1}{2}\left(\frac{\partial v_i}{\partial x_j} + \frac{\partial v_j}{\partial x_i}\right). \tag{2.38}$$

We then take again the moments of Boltzmann equation, as we have done before, we see that the perturbation δf can be parameterised in terms of two minor modifications: an additional term in the energy equation,

$$\frac{\partial \rho}{\partial t} + \frac{\partial}{\partial x_i}(\rho v_i) = 0 \tag{2.39}$$

$$\frac{\partial}{\partial t}(\rho v_i) + \frac{\partial}{\partial x_j}(\rho v_i v_j) = -\frac{\partial P_{ij}}{\partial x_j} + \rho F_i \tag{2.40}$$

$$\frac{\partial e}{\partial t} + \frac{\partial}{\partial x_i}(e v_i) = -\frac{\partial}{\partial x_i}(P_{ij} v_j) + \frac{\partial}{\partial x_i}\left(\kappa\frac{\partial T}{\partial x_i}\right) + \mathbf{F}\cdot(\rho\mathbf{v}), \tag{2.41}$$

and the 'pressure' P_{ij} is now manifestly tensorial and has the form

$$P_{ij} = P\delta_{ij} + \sigma_{ij}, \tag{2.42}$$

where σ_{ij} is the viscous stress tensor

$$\sigma_{ij} = -2\mu\left(\Lambda_{ij} - \frac{1}{3}\delta_{ij}\boldsymbol{\nabla}\cdot\mathbf{v}\right) - \zeta\delta_{ij}\boldsymbol{\nabla}\cdot\mathbf{v}. \tag{2.43}$$

The Euler equation with included viscosity is called the Navier-Stokes equation (which can be trivially derived by going to the primitive form of the equations). Together the set of equations is said to provide the equations of non-ideal hydrodynamics. In summary: what has happened in our derivation from kinetic theory is that the new fields σ_{ij} and κ capture the corrections to the moment equations due to the deviation from the Maxwell-Boltzmann distribution. They provide new physical phenomenology that we will discuss next. Typically, the new fields derive from deviations from thermodynamic equilibrium and/or the collision term and have to be measured except in extremely simple cases (such as hard sphere collisions or other relatively simple interactions).

Heat conduction and thermal diffusivity

The new term that was added is the correction term to the energy equation of the form

$$\frac{\partial}{\partial x_i}\left(\kappa\frac{\partial T}{\partial x_i}\right) \tag{2.44}$$

and it describes heat conduction with a thermal conductivity κ, which reflects the notion that temperature gradients will flatten and attempt to approach a more uniform Maxwell-Boltzmann distribution. If

one can assume that κ is a simple constant, then this term becomes $\kappa\Delta T$, and one can easily show that in a fluid at rest (neglecting external forces and viscosity for the moment) the energy equation can be written as

$$\frac{\partial T}{\partial t} = \frac{2\kappa}{3nk}\Delta T, \tag{2.45}$$

which is just the heat equation with a thermal diffusivity $\alpha = \frac{2\kappa}{3nk}$.

Viscosity and the Reynolds number

Viscosity simply modifies the pressure tensor P_{ij} and represents a resistance of the fluid to shear and to compression. The shear viscosity comes from a resistance of the fluid to shearing motion. The tensor

$$\Lambda_{ij} - \frac{1}{3}\delta_{ij}\boldsymbol{\nabla}\cdot\mathbf{v} \tag{2.46}$$

is just the symmetric trace-free part of the velocity gradient tensor D_{ij}. Remembering that the trace of the velocity gradient tensor is $\boldsymbol{\nabla}\cdot\mathbf{v}$ and represents compression and expansion, the trace-free symmetric part describes a shearing motion that does not change the volume. The resistance to such motion is proportional to the shear viscosity μ and means that viscous forces will oppose such shearing motions. It is common to define also the kinematic viscosity ν as

$$\nu = \frac{\mu}{\rho} \tag{2.47}$$

since μ appears in the momentum equation, there is an implicit dependence on density, which is scaled out in the kinematic viscosity. For this reason, μ is often also called dynamic viscosity. The importance of viscous effects in a fluid can be quantified by the dimensionless Reynolds number, which is defined as

$$\mathcal{R} = \frac{\rho v L}{\mu} = \frac{vL}{\nu}, \tag{2.48}$$

where ρ is the mass density, v is the fluid velocity, and L is a typical length scale in the system. In Figure 2.3, you can see the effect of an increasing Reynolds number on the flow around an obstacle (whose extent we can take as the 'typical' length scale L). At low flow velocities, the Reynolds number is low and the flow is laminar. The properties of the flow change as the Reynolds number increases (by increasing the flow velocity). For reasonably high Reynolds numbers such a flow produces the so-called Kármán vortex street behind the obstacle which illustrates the transition to turbulence, which we will discuss later in Section 2.8

In addition to kinematic viscosity, in compressible media, there can also be a different kind of viscosity associated with compression and expansion, i.e. proportional to the trace of the velocity gradient tensor. This is the bulk viscosity ζ (or sometimes called "volume viscosity"). It vanishes for incompressible media but it can be of importance when gases are rapidly compressed, such as in shock waves.

2.3 Application: Viscous accretion disks

2.3.1 The origin of disks and basic disk dynamics

Viscosity is a subdominant phenomenon in most astrophysical gas dynamics, it however plays an important role in simplified models of accretion disks around stars, planets and even black holes. For this

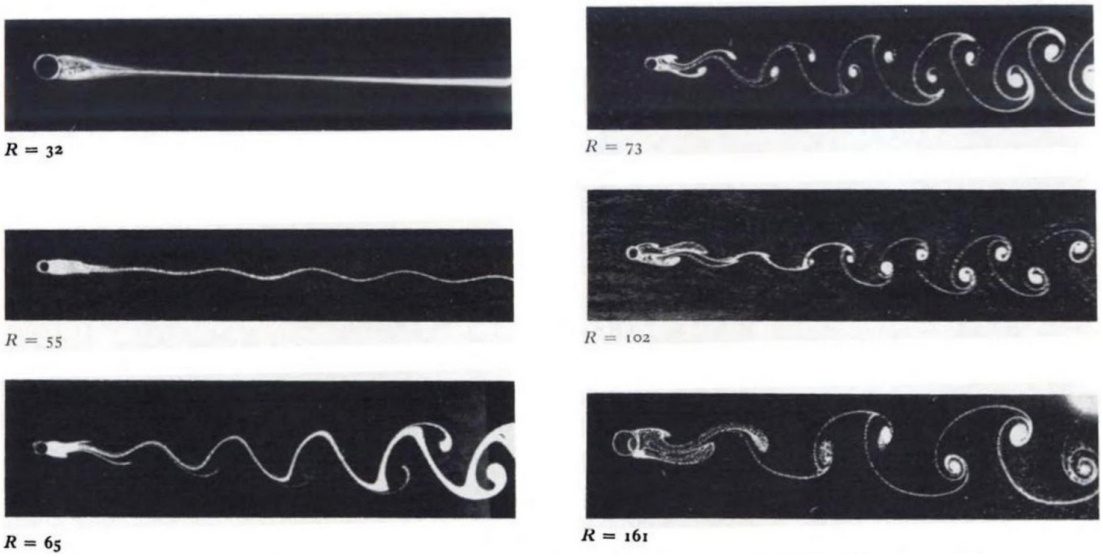

Figure 2.3: Flow around a body with increasing Reynolds number. For $\mathcal{R} \gtrsim 70$, the Kármán vortex street develops, while for low $\mathcal{R}$, the flow is completely laminar. [Image reproduced from Batchelor (1967)]

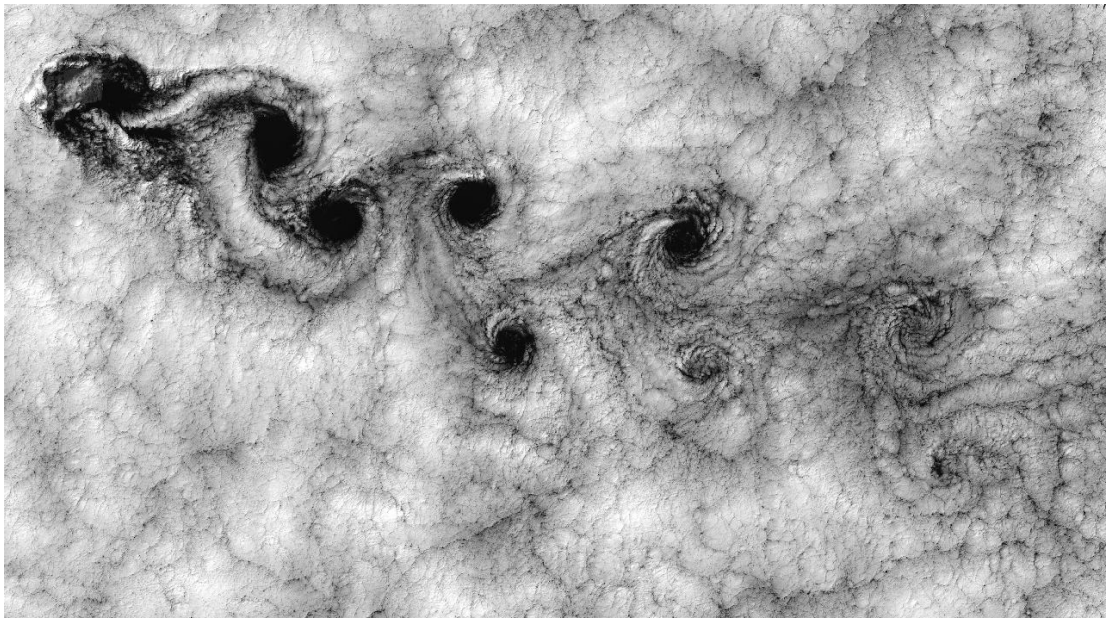

Figure 2.4: This image of clouds off the Chilean coast near the Juan Fernandez Islands (also known as the Robinson Crusoe Islands) was taken by the Landsat 7 satellite on September 15, 1999. It shows the Kármán vortex street from Fig. 2.3 in the clouds downwind from the Island. [Image courtesy NASA]

reason, we will discuss these systems in this section. Disks form in many astrophysical contexts: disk galaxies, protostellar disks, circumplanetary disks, accretion disks around black holes, ... This is always due to the same underlying principle: the material forming the disk usually starts out in some other form, think of a dilute cloud of gas made up from more or less randomly moving gas particles. Such a system will also have at least some angular momentum, either with respect to its own center of gravity, or with respect to another more massive object towards which it is falling. Since angular momentum is conserved, if the cloud collapses under its own gravity its rotational velocity must increase. Collisions of particles in the direction perpendicular to the axis of rotation however do not change the angular momentum, but will eventually cancel all bulk motion and convert it into internal energy. This means that collapse of a gaseous object of nonzero angular momentum will always form an oblate structure. If the gas is able to lose internal energy by a cooling process, this oblate object can become thinner and thinner turning it into a disk. A disk is thus rotationally supported against gravity in its radial direction and pressure supported in the direction perpendicular to the disk.

For a disk to be rotationally supported, it means that at all radii the gravitational force has to provide the centripetal force which means that for a fluid element of mass m at radius r in cylindrical or spherical symmetry

$$m\, r\Omega^2 = \frac{G\, M(<r)\, m}{r^2}, \tag{2.49}$$

where $\Omega(r)$ is the angular velocity ($v_\phi = r\Omega$), and $M(<r)$ is the total mass enclosed in the radius r. If we can assume that all the mass is exactly at the centre at $r = 0$, then we obtain the relation for Keplerian motion around a central body of mass M

$$\Omega(r) = \sqrt{\frac{GM}{r^3}}. \tag{2.50}$$

We will describe the disk in cylindrical coordinates (r, ϕ, z), so we have to re-write our fluid equations in cylindrical coordinates. We can assume that the disk remains a perfect disk by setting $v_z = 0$ and $\partial/\partial\phi = 0$. The gradient and the divergence operator in cylindrical coordinates are

$$\boldsymbol{\nabla} = \mathbf{e}_r \frac{\partial}{\partial r} + \mathbf{e}_\phi \frac{1}{r}\frac{\partial}{\partial \phi} + \mathbf{e}_z \frac{\partial}{\partial z}, \quad \boldsymbol{\nabla}\cdot\mathbf{A} = \frac{1}{r}\frac{\partial}{\partial r}\left(r\, A_r\right) + \frac{1}{r}\frac{\partial}{\partial\phi}A_\phi + \frac{\partial}{\partial z}A_z. \tag{2.51}$$

For a stable perfect disk, using ideal hydrodynamics, we thus have the continuity equation

$$\frac{\partial \rho}{\partial t} + \frac{1}{r}\frac{\partial}{\partial r}\left(r\rho v_r\right) = 0. \tag{2.52}$$

If we neglect pressure (i.e. we assume a thin disk), the Euler equation becomes

$$\frac{\partial v_r}{\partial t} + v_r\frac{\partial v_r}{\partial r} - \frac{v_\phi^2}{r} = F_r \tag{2.53}$$

$$\frac{\partial v_\phi}{\partial t} + v_r\frac{\partial v_\phi}{\partial r} + \frac{v_r\, v_\phi}{r} = 0. \tag{2.54}$$

Since the only quantity involving z is the density, we can define the surface density $\Sigma = \int \mathrm{d}z\ \rho$ and express everything through that. The rate of mass flow in the radial direction will then be given by

$$\dot{M}(r) = -2\pi r \Sigma v_r. \tag{2.55}$$

This is the quantity that we are interested in, since it describes the so-called accretion rate onto the central body if we measure it at its location $r = 0$. The continuity equation in terms of Σ is of course

$$\frac{\partial \Sigma}{\partial t} + \frac{1}{r}\frac{\partial}{\partial r}\left(r\Sigma v_r\right) = 0. \tag{2.56}$$

The angular velocity is related to v_ϕ as $\Omega = v_\phi/r$. This means we can combine the continuity equation, after multiplying by rv_ϕ, and the Euler equation, after multiplying by r, into the single equation

$$\frac{\partial}{\partial t}\left(\Sigma r^2\Omega\right) + \frac{1}{r}\frac{\partial}{\partial r}\left(\Sigma r^3\Omega v_r\right) = 0 \tag{2.57}$$

We note that this is just a conservation law for the angular momentum density $\rho\mathbf{r}\times\mathbf{v}$. If we integrate this over z, then we get an angular momentum surface density

$$\ell = r^2\Sigma\Omega. \tag{2.58}$$

We can thus write

$$\frac{\partial \ell}{\partial t} + \frac{1}{r}\frac{\partial}{\partial r}\left(r\ell v_r\right) = 0. \tag{2.59}$$

We now want to look for a steady state (or equilibrium) solution. For this we put the time derivatives of equations (2.56) and (2.59) to zero and integrate with respect to the radius to find

$$r\Sigma v_r = C_1, \quad \text{and} \quad r\ell v_r = C_2, \tag{2.60}$$

where C_1 and C_2 are integration constants. We can use the first expression to find that (using eq. (2.55))

$$\dot{M} = -2\pi r\Sigma v_r = -2\pi C_1, \tag{2.61}$$

which means that for a steady state disk, the accretion rate is constant (at all radii)! The second condition, using eq. (2.58) and (2.50) means for a non-viscous disk

$$C_2 = r^3\Sigma\Omega v_r = \sqrt{GM}\Sigma v_r r^{3/2} = \sqrt{GM}r^{1/2}C_1, \tag{2.62}$$

which clearly cannot be constant, unless $v_r = 0$. This is completely expected since in ideal hydrodynamics, there is no angular momentum transport and so a steady state disk must just be a Keplerian disk with vanishing radial velocity. We have introduced this complicated formalism in order to have it easier with the next step we will make. We will now show that when viscosity is included, there is indeed momentum transport, and we will get a constant non-zero accretion rate for such a disk.

2.3.2 Accretion Disks

The inclusion of viscosity changes the picture dramatically. Since $v_\phi = r\Omega = \sqrt{GM/r}$, fluid elements at different radii rotate at different velocities – this is called differential rotation. This means that if there is non-zero viscosity, the shear will be able to transport angular momentum. To demonstrate this, we just have to add the viscous term from the Navier-Stokes equation. The viscous term that we have to add to the Euler equation is

$$\frac{1}{\rho}\frac{\partial}{\partial x_j}\left(\mu S_{ij}\right) = \frac{1}{\rho}\frac{\partial}{\partial x_j}\left(\nu\rho S_{ij}\right), \tag{2.63}$$

where S_{ij} is the trace-subtracted velocity shear tensor. Since we have to use cylindrical coordinates, we have to express this now in those. A short calculation shows that under our assumptions that v_ϕ and v_r are only a function of radius, after integration over z the non-viscous equation for angular momentum conservation (2.59) becomes now

$$\frac{\partial \ell}{\partial t} + \frac{1}{r}\frac{\partial}{\partial r}\left(r\ell v_r\right) = \frac{1}{r}\frac{\partial}{\partial r}\left(\nu\Sigma r^3\frac{d\Omega}{dr}\right), \tag{2.64}$$

where we have used the relation between v_ϕ and Ω. For a disk in equilibrium, we thus get a new expression for the second constant of integration C_2 of the form

$$r\ell\left(v_r - \nu\frac{1}{\Omega}\frac{d\Omega}{dr}\right) = C_2. \tag{2.65}$$

We can now impose a boundary condition. A reasonable choice would be to assume that at some radius r_*, e.g. the surface of the accreting object, the accreting material is dragged into a rigid rotation so that $d\Omega/dr = 0$ at r_*., this determines C_2, so that we get

$$C_2 = -\frac{\dot{M}}{2\pi}r_*^2\Omega(r_*) = -\frac{\dot{M}}{2\pi}\sqrt{GMr_*}, \tag{2.66}$$

which defines the value of this constant. Since $\Omega = (GM/r^3)^{1/2}$, we have $\Omega^{-1}\, d\Omega/dr = -\frac{3}{2}r$. Putting everything together, we find

$$\frac{\dot{M}}{3\pi}\left[1 - \left(\frac{r_*}{r}\right)^{1/2}\right] = \nu\Sigma. \tag{2.67}$$

This is the famous result of Shakura & Sunyaev (1973) and it shows that the accretion rate is directly proportional to the viscosity.

By losing angular momentum through viscosity, material is thus transported inward until it ends up in the central object. This process is called accretion. Obviously, the energy that is lost as the material is transported inward must go into internal energy. If we assume that the disk can effectively radiate away all that energy, it is possible to calculate the energy in radiation that such an accretion disk produces. If one calculates the respective term in the energy equation, and transforms it to cylindrical coordinates, using our usual assumption one finds

$$\frac{dE}{dt} = \nu\Sigma r^2\left(\frac{d\Omega}{dr}\right)^2. \tag{2.68}$$

We can insert our result for the accretion rate from above as well as the definition of Ω to find the rate at which the disk dissipates energy.

$$\frac{dE}{dt} = -\frac{GM\dot{M}}{\frac{4\pi}{3}r^3}\left[1 - \left(\frac{r_*}{r}\right)^{1/2}\right] \tag{2.69}$$

If we assume that all this energy is radiated away, we can calculate the total luminosity (i.e. energy per unit time) of the disk by integrating over the whole disk, i.e. from r_* to infinity as

$$L = \int_{r_*}^{\infty}\left(-\frac{dE}{dt}\right)2\pi r\,\mathrm{d}r = \frac{GM\dot{M}}{2r_*}. \tag{2.70}$$

This means that the disk has a luminosity that is proportional to the gravitational potential at the surface of the accreting object as well as the accretion rate. An important argument by Shakura & Sunyaev was that the physical viscosity of the disk gas is not high enough to explain the luminosities of disks around X-ray binary stars. They suggested that the viscosity is strongly boosted by a high level of turbulence in the disk. More recent results demonstrate that magnetic fields in the disk can trigger turbulence that then leads to a viscosity high enough to explain the values necessary.

2.4 Gas Dynamics

In this section, we will now study phenomena occurring in compressible inviscid flow. Almost all situations that we encounter in astrophysics are in this regime, so the phenomenology we develop will be applicable to a wide variety of astrophysical systems.

2.4.1 Acoustic Waves

In compressible flows, perturbations in the flow propagate with the speed of sound as we will see next. To demonstrate this, we will consider a homogeneous gas of density $\rho_0 = \text{const}$ and pressure $P_0 = \text{const}$ at rest, i.e. $\mathbf{v}_0 := 0$ in the absence of any external force. Suppose now that we introduce a small perturbation in pressure $P_1(\mathbf{x}, t)$ and density $\rho_1(\mathbf{x}, t)$. These perturbations will give rise to a perturbation to the velocity field $\mathbf{v}_1(\mathbf{x}, t)$. Inserting the perturbed fields into the continuity and the Euler equation, we find

$$\frac{\partial \rho_1}{\partial t} + \frac{\partial}{\partial x_i}\left[(\rho_0 + \rho_1)\, v_{1,i}\right] = 0 \tag{2.71}$$

$$\frac{\partial v_{1,i}}{\partial t} + v_{1,j}\frac{\partial v_{1,i}}{\partial x_j} = -\frac{1}{\rho_0 + \rho_1}\frac{\partial P_1}{\partial x_i}. \tag{2.72}$$

We will now assume that the perturbations are small compared to the unperturbed solution. For this we assume that the unperturbed fields, ρ_0 and P_0 are $\mathcal{O}(1)$ and the perturbed fields ρ_1, P_1 and u_1 are $\mathcal{O}(\epsilon)$, where $\epsilon \ll 1$. We then see that products of two unperturbed fields are also $\mathcal{O}(1)$, the product of an unperturbed field with a perturbed one becomes $\mathcal{O}(\epsilon)$ while the product of two perturbed fields becomes $\mathcal{O}(\epsilon^2)$, which means that the latter will be much smaller than the previous ones. As long as $\epsilon \ll 1$, we can thus neglect terms of order ϵ^2. This procedure is called linearisation. The linearised set of equations is thus

$$\frac{\partial \rho_1}{\partial t} + \rho_0\frac{\partial v_{1,i}}{\partial x_i} = 0 \tag{2.73}$$

$$\rho_0\frac{\partial v_{1,i}}{\partial t} = -\frac{\partial P_1}{\partial x_i}. \tag{2.74}$$

We note that we can combine these two equations into one single equations if we take the time derivative of the first and the spatial derivative of the second, i.e.

$$\frac{\partial^2 \rho_1}{\partial t^2} + \rho_0\frac{\partial^2 v_{1,i}}{\partial t \partial x_i} = 0 \tag{2.75}$$

$$\rho_0\frac{\partial^2 v_{1,i}}{\partial x_i \partial t} = -\frac{\partial^2 P_1}{\partial x_i^2} \tag{2.76}$$

$$\Rightarrow \quad \frac{\partial^2 \rho_1}{\partial t^2} - \frac{\partial^2 P_1}{\partial x_i^2} = 0 \tag{2.77}$$

This equation already almost looks like a wave equation, if not both ρ_1 and P_1 appeared. However, we can find a relation between the two since for a barotropic gas $P = P(\rho)$ and thus

$$P_0 + P_1 = P(\rho_0) + \left.\frac{dP}{d\rho}\right|_{\rho_0}\rho_1 \quad \Rightarrow \quad P_1 = \left.\frac{dP}{d\rho}\right|_{\rho_0}\rho_1 =: c_s^2\rho_1, \tag{2.78}$$

where we denote the square-root of the derivative as $c_s := \sqrt{dP/d\rho}$ at density ρ_0. Since $\rho_0 = \text{const.}$, we can assume that also $c_s = \text{const}$. Then our equation (2.77) simply becomes

$$\left(\frac{\partial^2}{\partial t^2} - c_s^2 \nabla^2\right) \rho_1 = 0, \tag{2.79}$$

which is clearly a wave equation with a wave propagation speed c_s. It describes the propagation of acoustic sound waves with sound speed c_s. For a polytropic equation of state, we can compute the adiabatic sound speed to be

$$c_s = \sqrt{\gamma K \rho_0^{\gamma-1}} = \sqrt{\gamma \frac{P_0}{\rho_0}} = \sqrt{\frac{\gamma k}{m} T_0}, \tag{2.80}$$

where the temperature $T_0 = \frac{m}{k} P_0/\rho_0$.

Since the wave equation is linear, as in electrodynamics, the principle of a superposition of plane waves holds, and the solutions are of the form

$$\rho_1(\mathbf{x}, t) = \sum_{\mathbf{k}} \tilde{\rho}_1(\mathbf{k}) \, \exp\left[i(\mathbf{k} \cdot \mathbf{x} - \omega t)\right], \tag{2.81}$$

where $\tilde{\rho}_1(\mathbf{k})$ is the amplitude of the wave with wave number $\mathbf{k}$. A substitution of this into the wave equation yields a dispersion relation

$$\omega^2 = c_s^2 \mathbf{k}^2. \tag{2.82}$$

Acoustic waves are thus non-dispersive, i.e. as long as the perturbations are small, they will just propagate as waves that maintain their shape as they travel through the homogeneous unperturbed gas. Before we end this subsection, we note that we of course also have a linear wave equation for the velocity perturbations of the form

$$\left(\frac{\partial^2}{\partial t^2} - c_s^2 \nabla^2\right) \mathbf{v}_1 = 0. \tag{2.83}$$

It is easy to show that the velocity wave and the density wave have a phase shift of $\pi/2$ with respect to each other.

2.4.2 Shock Waves

In the previous section we assumed that the perturbations are small. Naturally, when they cannot be considered small, the analysis in terms of linear acoustic waves does no longer apply and a new phenomenon – shock waves – emerges.

Wave steepening

We have seen that velocity perturbations propagate as acoustic waves when they are small. When they can no longer be considered small, we will have to consider the full Euler equation. Let us neglect the pressure term for the moment, then in one dimension, the Euler equation is simply given by

$$\frac{\partial v}{\partial t} + v \frac{\partial v}{\partial x} = 0. \tag{2.84}$$

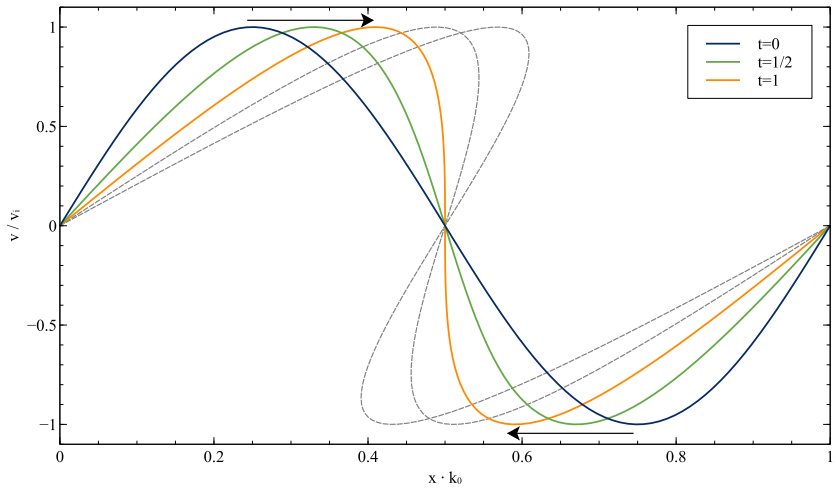

Figure 2.5: The steepening of a sinusoidal velocity perturbation due to the non-linear terms in the Burgers' equation. At time $t = 1$, a vertical gradient has developed, and at later times, fluid elements from the left and the right will have moved into the same central region, leading to a velocity field $v(x, t)$ that is no longer single-valued. This shows the origin of shock waves.

This equation is called Burgers' equation. We can understand how the fluid moves in this case through the method of characteristics that we have in fact employed multiple times before. To this end, we want to follow a fluid element as it moves on a trajectory $x(t)$ with the fluid (the "characteristic curve") so that $\dot{\mathbf{x}}(t) = \mathbf{v}$. As before, this leads us to the Lagrangian derivative, i.e. calculating the total derivative of $\mathbf{v}(\mathbf{x}(t), t)$ gives us

$$\frac{D\mathbf{v}}{Dt} = \frac{\partial \mathbf{v}}{\partial t} + (\dot{\mathbf{x}} \cdot \boldsymbol{\nabla})\mathbf{v} = \frac{\partial \mathbf{v}}{\partial t} + (\mathbf{v} \cdot \boldsymbol{\nabla})\mathbf{v}, \tag{2.85}$$

which means that Burgers' equation is equivalent to

$$\frac{Dv}{Dt} = 0, \tag{2.86}$$

which simply means that in the absence of pressure forces, every fluid element keeps moving with its initial velocity. We had seen in the section before that for small perturbations, the fluid velocities just follow a wave equation, which means that they have e.g. solutions of the form $v \propto \sin(k_0(x \mp c_s t))$, so that the characteristics are straight lines of the form $x \pm c_s t = \text{const}$.

A general perturbation of this form (i.e. no longer assuming that it be small), will however undergo wave steepening due to the nonlinear terms in the Euler equation as soon as the pressure force drops. In Figure 2.5, we show the evolution of a sinusoidal velocity perturbation in the absence of pressure as described by Burgers' equation. Fluid elements at higher velocity will start to overtake the slower ones leading to a steepening of the wave until at $t = 1$, a vertical velocity gradient emerges. It is clear that the steepening is a results of the non-linear term $v_j \partial_j v_i$. At later times, the fluid velocity field becomes multi-valued in the absence of pressure forces. Generally however, the pressure will be nonzero and, as we will see next, a shock wave develops in that case.

Shock Waves and Jump Conditions

We have just seen how a smooth initial condition can steepen into a solution that will develop a discontinuity. In the theory of discontinuous solutions of the hydrodynamic equations, one expresses such a situation in terms of a left and a right state, where both states are assumed to initially have constant density, velocity and pressure, i.e. we have a left state $S_L = (\rho_L, P_L, v_L)$ and a right state $S_R = (\rho_R, P_R, v_R)$. Assuming that both $v_L > 0$ and $v_R > 0$ and $v_L > v_R$ a shock will develop. The left state is typically called the upstream state, the right one the downstream state. The solution to the fluid equations under discontinuous two-state initial conditions is called a Riemann problem. Remembering the conservative form of the fluid equations, it is clear that even if the fluid variables are discontinuous, the fluxes of the conserved quantities must match at the interface between the two states, i.e.

$$\begin{aligned} \rho_L v_L &= \rho_R v_R && (2.87)\\ P_L + \rho_L v_L^2 &= P_R + \rho_R v_R^2 && (2.88)\\ E_L v_L &= E_R v_R. && (2.89) \end{aligned}$$

We now introduce the shock velocity v_S and require that the fluxes through the moving shock front are given by the difference of the respective left and right fluxes (in fact this can be rigorously derived for general conservation laws), i.e.

$$\begin{aligned} v_s(\rho_R - \rho_L) &= \rho_R v_R - \rho_L v_L && (2.90)\\ v_s(\rho_R v_R - \rho_L v_L) = &= (P_R + \rho_R v_R^2) - (P_L + \rho_L v_L^2) && (2.91)\\ v_s(E_R - E_L) &= \left[\rho_R v_R \left(e_R + \frac{1}{2}u_R^2 + \frac{P_R}{\rho_R}\right)\right] - \left[\rho_L v_L \left(e_L + \frac{1}{2}u_L^2 + \frac{P_L}{\rho_L}\right)\right]. && (2.92) \end{aligned}$$

These conditions, relating pre- and post-shock quantities are called Rankine-Hugoniot conditions. Some algebra then gives us the shock velocity as

$$v_s = v_L + c_L\sqrt{1 + \frac{\gamma+1}{2\gamma}\left(\frac{P_R}{P_L} - 1\right)}, \tag{2.93}$$

where $c_L = \sqrt{\gamma P_L/\rho_L}$ is the (upstream) sound speed.

For a stationary shock, i.e. $v_s = 0$, one finds the simpler conditions

$$\begin{aligned} \frac{\rho_R}{\rho_L} &= \frac{(\gamma+1)M^2}{2 + (\gamma-1)M^2} && (2.94)\\ \frac{P_R}{P_L} &= \frac{2\gamma M^2 - (\gamma-1)}{\gamma+1}, \quad \text{where} \quad M = \frac{v_L}{c_L} && (2.95) \end{aligned}$$

is the Mach number of the shock, i.e. the fluid velocity in units of the sound speed. For a shock wave one always has $M > 1$. It is easy to see that in the limit of $M \to \infty$, the relation between pre- and post-shock density becomes

$$\frac{\rho_R}{\rho_L} \to \frac{\gamma+1}{\gamma-1}, \tag{2.96}$$

which for an ideal monoatomic gas ($\gamma = 5/3$) becomes $\rho_R/\rho_L \to 4$ meaning that the maximum compression in such a gas due to the shock is 4. Figure 2.6 shows the shock waves produced by a jet moving at supersonic speed i.e. $M > 1$, through air. The shock waves it produces propagate away from the

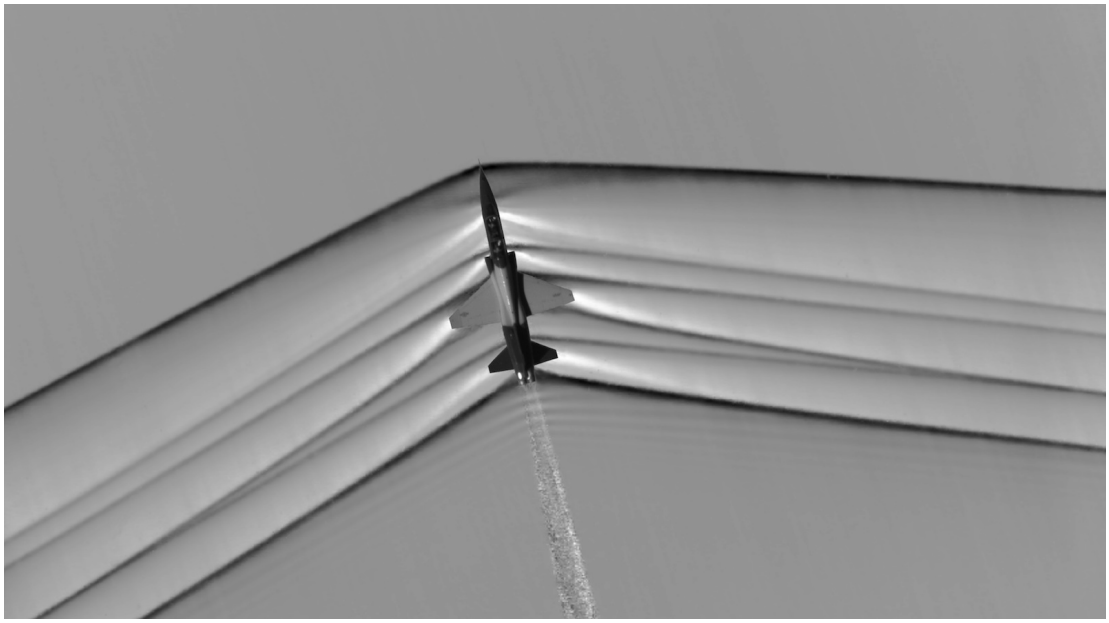

Figure 2.6: Schlieren image of a jet plane flying at supersonic velocity over the Mojave desert. Clearly seen can be seen a sequence of compressive shock waves and associated rarefaction waves, also the turbulent wake left by the jet engine is revealed. [Image credit: NASA Photo]

plane with the shock velocity, which one can assume to be constant. This phenomenon thus produces a cone-shaped shock front trailing from the plane. The shock front has an angle of $\sin \mu = M^{-1}$ with respect to the vector pointing against the direction of motion.

The general Riemann problem in three variables (ρ, P, v) in fact can produce three wave-like features: (1) a shock wave, (2) a rarefaction wave, and (3) a contact discontinuity. Discussing them is however beyond the scope of this introductory course.

2.4.3 Blast Waves and Supernovae

An important example for a shock wave phenomenon is given by the solution for a blast wave such as the one produced in a supernova explosion. A supernova explosion occurs at the end of the life of massive stars when nuclear fusion processes die out, after which the star collapses and then undergoes an explosion due to runaway nuclear fusion in the highly compressed stellar matter, expelling the stellar material to large radii into the interstellar medium. A simple model for such an explosive process is thus by assuming that a large amount of energy E is suddenly released in a point at $r = 0$ which is then left to expand into the surrounding medium of density ρ. One can further assume that the pressure in the ambient medium is negligible compared to the pressure inside the blast wave, i.e. we set $P = 0$ in the ambient medium.

There is an elegant way to solve this problem by exploiting that its solutions are self-similar, i.e. expressed in the right quantities, the solutions at later times are just scaled versions of the solution at early times. Such self-similar solutions can usually be easily found by dimensional analysis. We are interested in the location of the shock front r_s as a function of time t. The only free parameters in the

Figure 2.7: The SNR 0509-67.5 supernova remnant in the Large Magellanic Cloud. Its diameter is about 7 parsecs, and it is expanding at about 5000 km/s. The explosion was seen ca. 400 years ago on earth. The green-blue haze shows X-ray emission from the post-shock heated gas, while the red shows emission in optical wavelengths from the actual shock front. [Image Credit: X-ray: NASA/CXC/SAO/J.Hughes et al, Optical: NASA/ESA/Hubble Heritage Team (STScI/AURA)]

problem are the energy of the blast E and the density of the ambient medium ρ. The units of energy are mass $\times$ length^2 $\times$ time^{-2} and those of density are mass $\times$ length^{-3}. We can thus obviously combine E, ρ and t in exactly one way to obtain a length-scale. Let us call this length-scale λ and we have

$$\lambda = (Et^2/\rho)^{1/5} \tag{2.97}$$

We were originally interested in the radius $r(t)$ of the radial location of a shell of gas inside the spherical blast. In order to obtain a self-similar solution, we will now express this radius in units of λ, i.e. we write

$$\xi = \frac{r}{\lambda} = r\left(\frac{\rho}{Et^2}\right)^{1/5}. \tag{2.98}$$

For the solution to be self-similar, we must have $\xi = \text{const}$, so that we can label every shell by its value of $\xi = \xi_0$ in that case and obtain the self-similar solutions

$$r(t) = \xi_0\left(\frac{Et^2}{\rho}\right)^{1/5}. \tag{2.99}$$

The velocity of expansion of the blast wave is then simply

$$v_s(t) = \frac{dr_s}{dt} = \frac{2}{5}\xi_0\left(\frac{E}{\rho t^3}\right)^{1/5}. \tag{2.100}$$

We thus have that the blast wave expands as $t^{2/5}$ and the velocity of the blast decreases as $t^{-3/5}$. This self-similar solution for a spherical blast wave is called a Sedov-Taylor blast wave and was independently found by Sedov and Taylor in the 1940s in the context of the explosions of atomic bombs. It turns out that these self-similar solutions are excellent approximations throughout the early phases of both nuclear explosions as well as supernova explosions (see Figure 2.7). In order to find the equations determining the radial dependence of ρ, v and P in terms of the self-similar variable ξ.

Let us take the Rankine-Hugoniot condition for a stationary shock wave (i.e. it applies in the frame of the shock) and assume a very high Mach number. Then we can apply eq. (2.95) in the limit $M \to \infty$, i.e. we can write

$$\rho_R = \left(\frac{\gamma+1}{\gamma-1}\right)\rho_L, \quad v_R = \frac{2}{\gamma+1}v_s, \quad P_R = \frac{2}{\gamma+1}\rho_L v_s^2. \tag{2.101}$$

We now want to express the solutions in terms of dimensionless self-similar functions, i.e. we write

$$\rho(r,t) = \rho_R\,\rho(\xi), \quad v(r,t) = v_R\frac{r}{r_s}v(\xi), \quad P(r,t) = P_R\left(\frac{r}{r_s}\right)^2 P(\xi). \tag{2.102}$$

Using the jump conditions, we can then write

$$\rho(r,t) = \rho_L\,\frac{\gamma+1}{\gamma-1}\rho(\xi), \quad v(r,t) = \frac{4}{5(\gamma+1)}\frac{r}{t}v(\xi), \quad P(r,t) = \frac{8\rho_L}{25(\gamma+1)}\left(\frac{r}{t}\right)^2 P(\xi). \tag{2.103}$$

We also have the boundary condition that at the shock front location $\xi = \xi_0$ and $\rho(\xi_0) = v(\xi_0) = P(\xi_0) = 1$.

Next we have to rewrite the hydrodynamic equations in spherical symmetry

$$\frac{\partial\rho}{\partial t} + \frac{1}{r^2}\frac{\partial}{\partial r}\left(r^2\rho v\right) = 0 \tag{2.104}$$

$$\frac{\partial v}{\partial t} + v\frac{\partial v}{\partial r} = -\frac{1}{\rho}\frac{\partial P}{\partial r} \tag{2.105}$$

$$\left(\frac{\partial}{\partial t} + v\frac{\partial}{\partial r}\right)\log\frac{P}{\rho^\gamma} = 0 \tag{2.106}$$

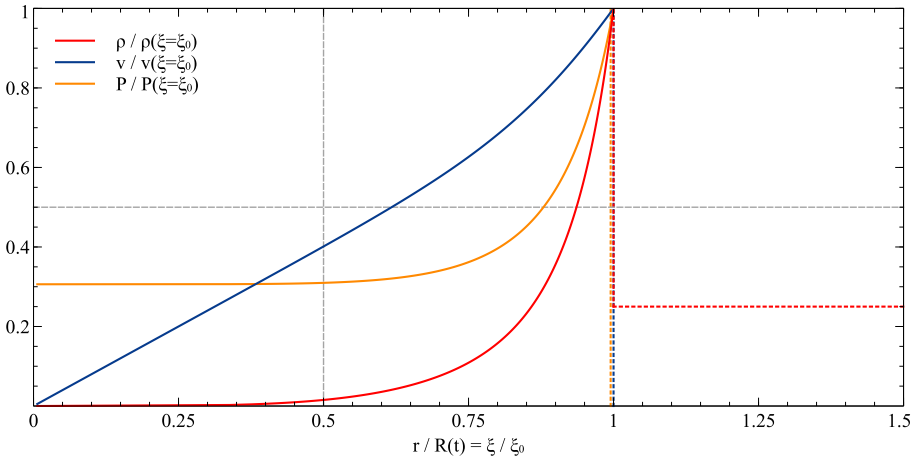

Figure 2.8: Analytic solutions for a Sedov-Taylor blast wave for a $\gamma = 5/3$ gas. The radial coordinate is given relative to the position of the shock front, the fluid quantities are in units of their respective values at the shock front location.

in terms of the ξ. We first use that we can write

$$\frac{\partial}{\partial t} = -\frac{2}{5}\frac{\xi}{t}\frac{d}{d\xi}, \quad \text{and} \quad \frac{\partial}{\partial r} = \frac{\xi}{r}\frac{d}{d\xi}. \tag{2.107}$$

This finally gives us a set of ordinary differential equations

$$-\xi\frac{d\rho}{d\xi} + \frac{2}{\gamma+1}\left[3\rho v + \xi\frac{d}{d\xi}(\rho v)\right] = 0 \tag{2.108}$$

$$-v - \frac{2}{5}\xi\frac{dv}{d\xi} + \frac{4}{5(\gamma+1)}\left[v^2 + v\xi\frac{dv}{d\xi}\right] = -\frac{2}{5}\frac{\gamma-1}{\gamma+1}\frac{1}{\rho}\left(2P + \xi\frac{dP}{d\xi}\right) \tag{2.109}$$

$$\xi\frac{d}{d\xi}\left(\log\frac{P}{\rho^\gamma}\right) = \frac{5(\gamma+1)-4v}{2v-(\gamma+1)}. \tag{2.110}$$

This means by exploiting the self-similar nature of the solution, we have reduced the set of partial differential equations (i.e. in terms of r and t) to a set of ordinary differential equations in terms of the single independent variable ξ! In fact, Sedov has shown that this system in fact has an analytical solution, which is however rather lengthy to write down. Alternatively, one can simply solve the set of ordinary differential equations above by numerical means. The solutions in the case of an ideal monoatomic gas are shown in Figure 2.8. One sees nicely how the gas is compressed by the maximum ratio of 4 in the shock. The shock-front itself is very narrow, the density asymptotes to zero towards the origin of the explosion, while the shock produces a constant pressure behind it and an almost linear velocity profile.

2.4.4 Spherical Accretion Flows and Winds

We will consider in this Section one more simple case that is often used as a basis in more sophisticated astrophysical models of the accretion of material onto a central mass or the spherical ejection of mass

from a spherical object. They are mathematically equivalent and just differ in the sign of the velocity, being directed either inward or outward. The spherical accretion model is somewhat academic since it assumes that angular momentum is small enough in order to prevent the formation of an accretion disk. Despite this simplification, this model is commonly used as a crude estimate of the accretion rate of objects, in particular black holes, from an ambient medium.

For this analysis, we will consider a steady spherical flow, so that the radial velocity of the gas is independent of time. Under such conditions, the mass flux (either inward or outward) must be given by

$$\dot{M} = 4\pi r^2 \rho v = \text{const}, \tag{2.111}$$

which we can insert into the spherical continuity equation, for which with $\partial\rho/\partial t$

$$\frac{2}{r} + \frac{1}{\rho}\frac{d\rho}{dr} + \frac{1}{v}\frac{dv}{dr} = 0 \tag{2.112}$$

The Euler equation in spherical coordinates after setting $\partial v/\partial t = 0$ and assuming that the gravitational field is produced by a central mass M

$$\rho v \frac{dv}{dr} = -\frac{dp}{dr} - \frac{GM}{r^2}\rho. \tag{2.113}$$

Using that $dp/dr = c_s^2\, d\rho/dr$, we can eliminate ρ and find the single equation

$$\left(v - \frac{c_s^2}{v}\right)\frac{dv}{dr} = \frac{2c_s^2}{r} - \frac{GM}{r^2}. \tag{2.114}$$

We see that $v = c_s$ (i.e. the point where the flow transitions from sub- to super-sonic) at a radius

$$r = r_c = \frac{GM}{2c_s^2}. \tag{2.115}$$

This point is called the sonic point since the gas is transonic there. If we assume that the sound speed is constant, we can immediately find the transonic mass flux to be

$$\dot{M} = \pm 4\pi r_c^2 \rho c_s = \pm\pi \frac{G^2M^2}{c_s^3}\rho. \tag{2.116}$$

If the central mass has a velocity V with respect to the ambient medium, then the transonic flux is changed to be

$$\dot{M} = \pm 4\pi r_c^2 \rho c_s = \pm\pi \frac{G^2M^2}{(V^2 + c_s^2)^{3/2}}\rho. \tag{2.117}$$

For the case of accretion ($\dot{M} < 0$), these two formulae are known as the equations describing Bondi-Hoyle accretion after the names of the researchers who first developed this approximation.

2.5 Hydrodynamic Instabilities

Clearly, the most interesting hydrodynamic phenomena are not only those that describe an equilibrium state. In this section, we will investigate various of the many instabilities that can arise when a system in equilibrium is perturbed. Since perturbations will naturally occur in a system, we have to distinguish between stable equilibria, where the perturbation only causes oscillations around the equilibrium state, and unstable equilibria, where the perturbation can radically alter the state of the system.

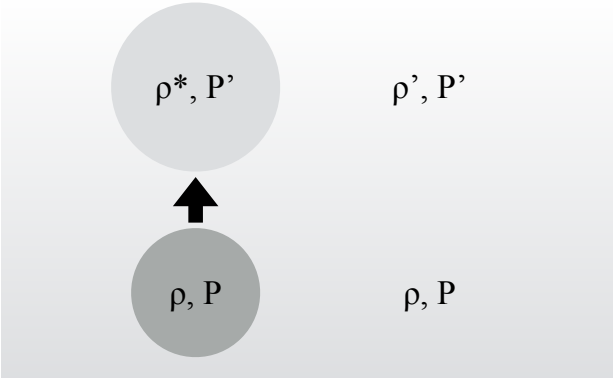

Figure 2.9: Convective instability: displacement of a blob of gas in a stratified medium. The blob will rise buoyantly if $\rho^* < \rho'$, otherwise it will sink back to its original position.

2.5.1 Convective Instability

We begin our analysis of unstable systems with a perfect gas that is hydrostatic equilibrium in a (locally) uniform gravitational field. For simplicity let gravity act in the z-direction, so that for symmetry reasons, we can assume $\rho(z)$ and $P(z)$ to be a function of z only. Let us assume that at some initial height z, a blob of gas has the same density ρ and pressure P as its ambient medium, but a perturbation displaces it upward, where the ambient medium has density ρ' and pressure P' (see Figure 2.9 for an illustration). The blob remains in pressure equilibrium, but if we assume that it has moved upward in an adiabatic way, then it might not in general have the same density as the ambient medium. Let us call the density inside the blob at the new position ρ^*. If $\rho^* < \rho'$, then the displaced blob of gas is said to be buoyant and will continue to rise, while if $\rho^* < \rho'$, then the system is stable, and the blob will sink back to its initial position. To determine whether the system is convectively unstable, we thus have to calculate the density at the displaced position and compare it to the ambient density.

For an adiabatic process, the new density must be given by

$$\rho^* = \rho \left(\frac{P'}{P} \right)^{1/\gamma}. \tag{2.118}$$

We next assume that hydrostatic equilibrium in the ambient medium requires a pressure gradient dP/dz, so that if the blob is displaced by a distance Δz, we can write the pressure at the higher position as

$$P' = P + \frac{dP}{dz} \Delta z. \tag{2.119}$$

Using the binomial theorem, we can write $(1+x)^{1/\gamma} \simeq 1 + x/\gamma + \mathcal{O}(x^2)$, so that for the density inside the adiabatically risen blob

$$\rho^* = \rho + \frac{\rho}{\gamma P} \frac{dP}{dz} \Delta z. \tag{2.120}$$

We now have to compare this to the density at the higher position in the ambient medium. It is given by

$$\rho' = \rho + \frac{d\rho}{dz} \Delta z \tag{2.121}$$

where we can use $P = nkT$ and thus $\rho = mP/kT$, so that $d\rho = mdP/kT - mPdT/kT^2$ which can then be put together to yield

$$\rho' = \rho + \frac{\rho}{P}\frac{dP}{dz}\Delta z - \frac{\rho}{T}\frac{dT}{dz}\Delta z. \tag{2.122}$$

The difference between the density inside the blob of gas and the ambient medium is then

$$\rho^* - \rho' = \left[-\left(1 - \frac{1}{\gamma}\right)\frac{\rho}{P}\frac{dP}{dz} + \frac{\rho}{T}\frac{dT}{dz}\right]\Delta z. \tag{2.123}$$

If we set things up so that dT/dz and dP/dz are both negative (as would be the case if gravity is in the negative z-direction), then the atmosphere is stable if

$$\left|\frac{dT}{dz}\right| < \left(1 - \frac{1}{\gamma}\right)\frac{T}{P}\left|\frac{dP}{dz}\right| \tag{2.124}$$

This criterion simply states that if the temperature gradient is steeper than the critical value, given by the right-hand-side, then the atmosphere is convectively unstable and any perturbation will cause convection to happen. This criterion was first developed by Schwarzschild in 1906 and is thus also called the Schwarzschild stability criterion.

One can even approximate the equation of motion of the blob from Newton's law as

$$\rho^*\frac{d^2}{dt^2}\Delta z = -(\rho^* - \rho')g, \tag{2.125}$$

if one assumes the blob to be small so that one can neglect its interaction with the ambient gas. Substituting eq. (2.123), one finds

$$\frac{d^2}{dt^2}\Delta z + N^2\Delta z = 0, \tag{2.126}$$

which is a second order equation in time, meaning that depending on whether N^2 is positive or negative, meaning that it is either oscillating or a damped motion. In the oscillating case, the frequency is given by

$$N = \sqrt{\frac{g}{T}\left[\frac{dT}{dz} - \left(1 - \frac{1}{\gamma}\right)\frac{T}{P}\frac{dP}{dz}\right]}, \tag{2.127}$$

which is also called the Brunt-Väisälä frequency and gives the frequency of oscillation of the blob of gas in the ambient medium. Such convective motion is an important means of heat transport in stratified atmospheres and particularly in stars.

2.5.2 Perturbations at an interface

The next class of fluid instabilities occur at a perturbed interface between two fluid phases. For simplicity let us consider the situation in two dimensions and assume that the two phases are separated at $y = 0$ in the y-direction, and initially uniform in the x-direction. We then have $\rho(y < 0) = \rho$ and $\rho(y > 0) = \rho'$ with different velocities. The situation we are thinking of is the one illustrated in Figure 2.10.

We will neglect vorticity ($\boldsymbol{\nabla} \times \mathbf{v} = 0$ and assume an incompressible fluid $\boldsymbol{\nabla} \cdot \mathbf{v} = 0$ in this simplified model, so that we can write $\mathbf{v} = -\boldsymbol{\nabla}\phi$ for the full fluid velocity. Such a flow is called a potential flow. In this case, the Euler equation becomes

$$-\boldsymbol{\nabla}\frac{\partial\phi}{\partial t} + \boldsymbol{\nabla}\left(\frac{1}{2}v^2\right) = -\boldsymbol{\nabla}\left(\frac{P}{\rho}\right) - \boldsymbol{\nabla}\Phi, \tag{2.128}$$

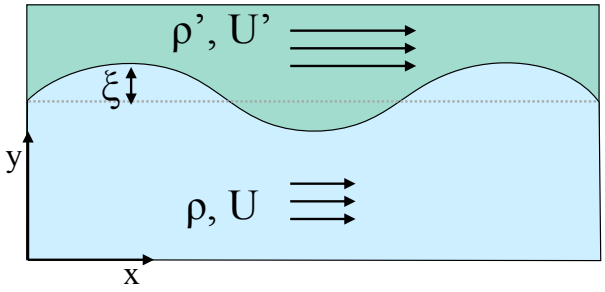

Figure 2.10: Perturbation at the interface between two fluid phases.

where Φ is the gravitational potential. This equation can trivially be integrated, and leaves a time-dependent integration constant $F(t)$, i.e.

$$-\frac{\partial \phi}{\partial t} + \frac{1}{2}v^2 + \frac{P}{\rho} + \Phi = F(t). \tag{2.129}$$

We shall now assume that the two fluids have uniform velocities U and U' in the x-direction. In the absence of viscosity, such a situation is a steady state solution of the fluid equations. We will now consider a small perturbation ξ of the interface between the two phases, i.e. the position of the interface shall be at $y = \xi(x,t)$. We want to investigate now whether this perturbation grows, decays or oscillates with time.

Since we have a pure potential flow by assumption, the velocity potential below the interface can be written as

$$\phi = -Ux + \delta\phi, \tag{2.130}$$

where U gives then the uniform velocity U in the x-directions and $\delta\phi$ is the perturbation satisfying $\nabla^2\delta\phi = 0$ (since $\boldsymbol{\nabla} \cdot v = 0$). Equivalently, we have above the interface

$$\phi' = -U'x + \delta\phi'. \tag{2.131}$$

We want to follow the motion of the interface function $\xi(x,t)$. The vertical velocity is just $-\partial\delta\phi/\partial y$ and it is also given by the Lagrangian derivative of the displacement $D\xi/Dt$, so we equate the two and keep only terms up to linear order to find for the lower fluid

$$-\frac{\partial \delta\phi}{\partial y} = \frac{\partial \xi}{\partial t} + U\frac{\partial \xi}{\partial x} \tag{2.132}$$

where the second term arises because U is along the x-direction and terms $\frac{\partial\delta\phi}{\partial y}\frac{\partial\xi}{\partial y}$ can be neglected since they are quadratic in the perturbations. Equivalently, we obtain for the fluid above the surface

$$-\frac{\partial \delta\phi'}{\partial y} = \frac{\partial \xi}{\partial t} + U'\frac{\partial \xi}{\partial x}. \tag{2.133}$$

Since we are dealing with linear partial differential equations now, we can make the usual plane wave ansatz and write

$$\xi(x,t) = A\exp\left[i(kx - \omega t)\right]. \tag{2.134}$$

This ansatz, together with Laplace's equation for the velocity potentials $\nabla^2\delta\phi = 0$ implies that then we have to write

$$\delta\phi(x,y,t) = B\exp\left[i(kx-\omega t)+ky\right] \quad \text{and} \tag{2.135}$$

$$\delta\phi'(x,y,t) = B'\exp\left[i(kx-\omega t)-ky\right]. \tag{2.136}$$

Inserting this into the equations above, we find

$$i(-\omega+kU)A = -kB, \quad \text{and} \tag{2.137}$$

$$i(-\omega+kU')A = kB'. \tag{2.138}$$

We can derive the pressure in the upper and lower fluid using the equation for the time evolution of the velocity potential, eq. (2.129), i.e. in the lower fluid

$$P = -\rho\left(-\frac{\partial\delta\phi}{\partial t}+\frac{1}{2}v^2+g\xi\right)+\rho F(t), \tag{2.139}$$

where we have used the approximation $\Phi = g\xi$, i.e. $g = \partial\Phi/\partial y|_{y=0}$. One can derive the equivalent expression for the fluid above the interface, and requiring that the two fluids are in pressure equilibrium at the interface then implies that

$$\rho\left(-\frac{\partial\delta\phi}{\partial t}+\frac{1}{2}v^2+g\xi\right) = \rho'\left(-\frac{\partial\delta\phi'}{\partial t}+\frac{1}{2}v'^2+g\xi\right)+K(t), \tag{2.140}$$

where $K(t) = \rho F(t)-\rho' F'(t)$ which we can safely assume to be constant in time. Under this condition, K can be found for the unperturbed solution, in which case

$$K = \frac{1}{2}\rho U^2 - \frac{1}{2}\rho' U'^2. \tag{2.141}$$

We also need the square of the total fluid velocity v^2, which is

$$v^2 = (U\mathbf{e}_x - \boldsymbol{\nabla}\delta\phi)^2 = U^2 - 2U\frac{\partial\delta\phi}{\partial x} \tag{2.142}$$

up to linear order in the perturbations. If we insert this into eq. (2.140), we have

$$\rho\left(-\frac{\partial\delta\phi}{\partial t}-U\frac{\partial\delta\phi}{\partial x}+g\xi\right) = \rho'\left(-\frac{\partial\delta\phi'}{\partial t}-U'\frac{\partial\delta\phi'}{\partial x}+g\xi\right). \tag{2.143}$$

If we insert the ansatz for the solutions of ϕ and ξ into this, we finally find

$$\rho\left[-i(-\omega+kU)B+gA\right] = \rho'\left[-i(-\omega+kU')B'+gA\right]. \tag{2.144}$$

Using the relations between A and B and B', we can further simplify this as

$$\rho\left(-\omega+kU\right)^2+\rho'\left(-\omega+kU'\right)^2 = kg(\rho-\rho'). \tag{2.145}$$

This is a quadratic equation, and we can write its solution as the well-known dispersion relation of linear fluid interface instabilities

$$\frac{\omega}{k} = \frac{\rho U+\rho' U'}{\rho+\rho'} \pm \left[\frac{g}{k}\frac{\rho-\rho'}{\rho+\rho'}-\frac{\rho\rho'(U-U')^2}{(\rho+\rho')^2}\right]^{1/2}. \tag{2.146}$$

It is clear that when ω is a purely real number, the perturbations will correspond to simple oscillations (or acoustic waves), while as soon as ω has a non-zero imaginary part, the perturbations will grow. Whether such unstable solutions exist clearly depends on whether the term under the square root is positive or negative which can be used to distinguish regimes of stability and instability. This very general result can be applied to many relevant cases, which we will consider next.

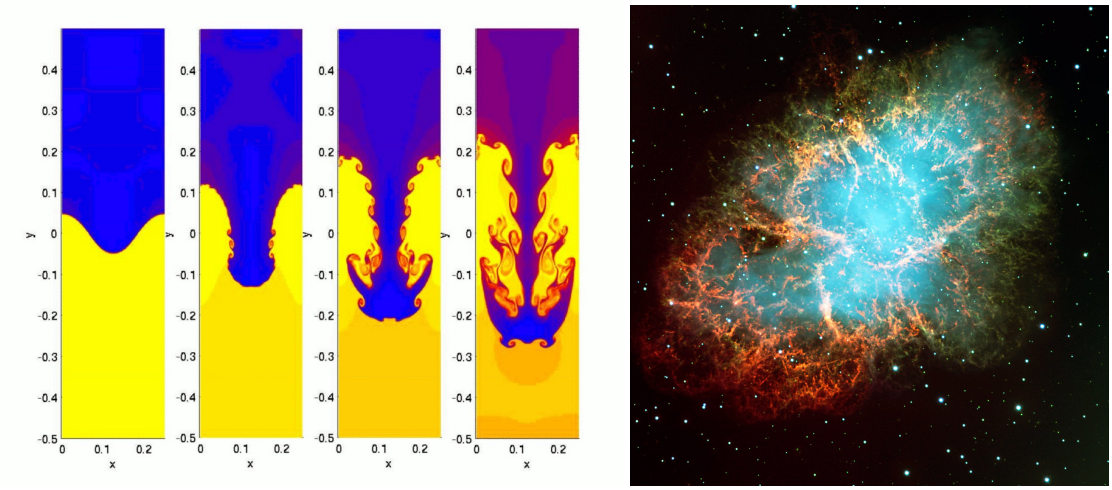

Figure 2.11: **Left:** Rayleigh-Taylor instability in a numerical simulation of a heavier fluid on top of a lighter fluid with a sinusoidally perturbed interface [Image credit: Li and Li, U.S. DoE]. **Right:** Rayleigh-Taylor instability at the surface of the supernova bubble in the Crab nebula.[Image copyright by NASA/ESA, J. Hester and A. Loll.]

2.5.3 Surface gravity waves

The simplest application we can consider is for two fluids at rest, with the lighter fluid above the heavier fluid, i.e. $U = U' = 0$ and $\rho > \rho'$. For a perturbation of the interface between them, the dispersion relation gives

$$\frac{\omega}{k} = \pm\sqrt{\frac{g}{k}\frac{\rho - \rho'}{\rho + \rho'}}. \tag{2.147}$$

Since k is a real number, then also ω is a real number in this case. This means that the waves are simply propagating on the surface without growing or damping out. Such waves are called surface gravity waves and their phase velocity ω/k depends on the wave number k so that they do not maintain their shape if they are made up from multiple waves but instead disperse. In the case of the lighter fluid being air, and the lower being water, we can safely assume $\rho' \ll \rho$, so that $\omega = \pm\sqrt{gk}$. This is a very simplified picture however since it implicitly assumes that the water depth is infinite, so that no breaking of the wave can occur. Also, non-linear effects can lead to some non-dispersive surface gravity waves. Such waves are called solitons and they occur in various physical situations with the common property that their shape remains fixed over time.

2.5.4 Rayleigh-Taylor Instability

Unlike in the previous case, we can now take the heavier fluid to sit on top of the lighter fluid. We expect that gravity tries to pull down the heavier fluid so that this situations should be unstable to perturbations. You can verify yourself that for an unperturbed interface, this situation is hydrostatic! In the case that $\rho < \rho'$, we find that ω is imaginary. If ω is imaginary, then

$$\xi \propto \exp(|\omega|t), \tag{2.148}$$

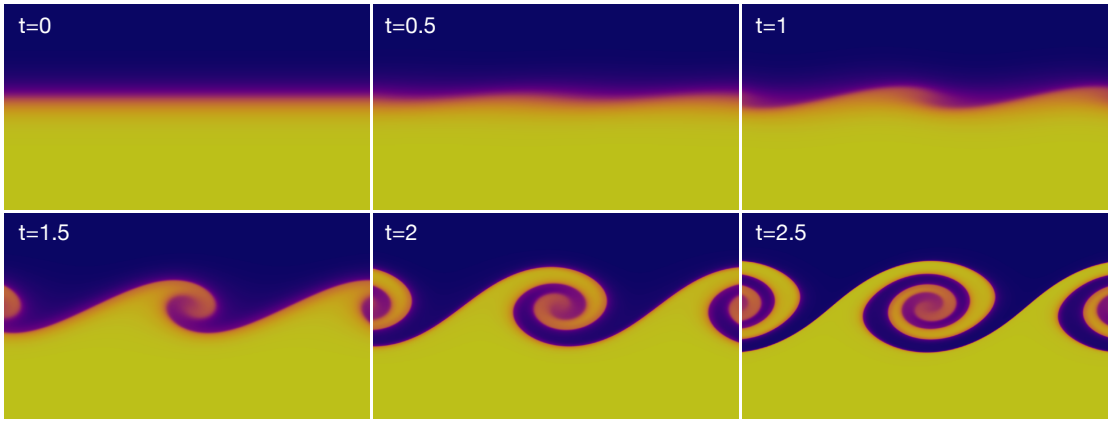

Figure 2.12: Numerical simulation of the non-linear evolution of the Kelvin-Helmholtz instability over time. The interface between the two phases (indicated by differently coloured dyes in yellow and blue, the blue coloured fluid is moving to the right) is initially smooth and the perturbation is tiny, but grows rapidly into the characteristic rolls. [Images courtesy Michaël Michaux, Lagrange/UCA]

so that we expect the perturbation to grow as expected. This phenomenon is called the Rayleigh-Taylor instability. Note that in our analysis, we assumed the gravitational acceleration to be constant, so the analysis is equally applicable if a lighter fluid is being accelerated against a heavier fluid. This situation naturally occurs at the surface of a supernova explosion bubble, so that Rayleigh-Taylor instability is also expected to occur for the boundary of the bubble, and can indeed be clearly seen in older supernova remnants, such as e.g. the Crab nebula. The Rayleigh-Taylor instability leads to prominent "fingers" of dense fluid penetrating the lighter fluid (see Figure 2.11).

2.5.5 Kelvin-Helmholtz Instability

Another very common instability arises when U and U' are non-zero, but when we require $\rho > \rho'$ so that the system is Rayleigh-Taylor stable. From eq. (2.146) we see immediately that ω can have an imaginary part if the expression under the square root is negative, i.e. when

$$\rho\rho'(U - U')^2 > (\rho^2 - \rho'^2)\frac{g}{k}. \tag{2.149}$$

We note immediately that this instability is also present if $g = 0$, in which case it reduces to $(U - U')^2 > 0$ meaning that any relative velocity will trigger it in that case! This instability is called the Kelvin-Helmholtz instability and it causes the interface between two fluids that are sheared against each other to become unstable and develop characteristic roll patterns as shown in Figure 2.12. The simplest example is the emergence of water waves from wind blowing over the surface, but this instability is in fact extremely common in astrophysical situations whenever the interface between two phases which are moving at relative velocities is perturbed, see Figure 2.13.

2.5.6 Jeans Instability

Arguably the most important instability in astrophysics arises from the counter-play of gravity and pressure. Assume we have homogeneous self-gravitating medium whose density we perturb. Whether

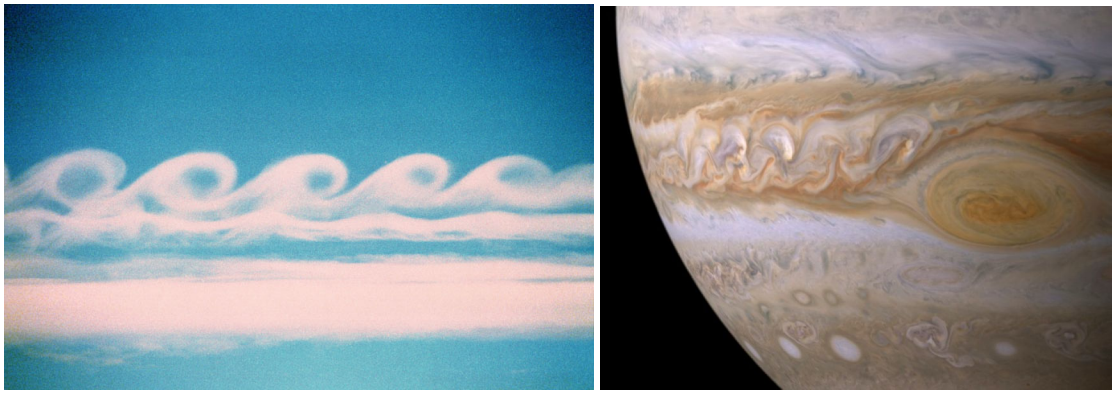

Figure 2.13: **Left:** Kelvin-Helmholtz instability in clouds due to two layers of air moving at relative velocities at the cloud layer [Image credit: internet, unknown]. **Right:** Kelvin-Helmholtz instability in clouds on Jupiter [Image copyright by NASA]

gravity will cause a runaway growth of density (over-dense region attracting more and more gas) depends on the pressure force. If pressure is large enough, we will only see the acoustic oscillations that we discussed earlier. If pressure is too low to achieve this, the gas will however undergo the Jeans instability. The analysis goes along the lines of our analysis of acoustic waves with the addition of gravity.

We thus start from the linearised perturbed equations (2.73) and (2.74) that we reproduce here to avoid page-flipping:

$$\frac{\partial \rho_1}{\partial t} + \rho_0 \frac{\partial v_{1,i}}{\partial x_i} = 0 \tag{2.150}$$

$$\rho_0 \frac{\partial v_{1,i}}{\partial t} = -\frac{\partial P_1}{\partial x_i}, \tag{2.151}$$

where quantities with index '1' refer to the perturbation, and those with '0' to the unperturbed quantities. We now have to supplement this with Poisson's equation for the perturbation of the gravitational force (note that this is in fact subtle since the system of equations at constant density is actually inconsistent):

$$\nabla^2 \Phi_1 = 4\pi G \rho_1. \tag{2.152}$$

And we also have to add the gravitational force to the Euler equation (2.151), so that we get, after rewriting the pressure gradient as a density gradient using the sound speed c_s

$$\rho_0 \frac{\partial v_{1,i}}{\partial t} = -c_s^2 \frac{\partial \rho_1}{\partial x_i} - \rho_0 \frac{\partial \Phi_1}{\partial x_i}. \tag{2.153}$$

We note that once again, we can re-write this as a single second order equation of the form

$$\left(\frac{\partial^2}{\partial t^2} - c_s^2 \nabla^2 \right) \rho_1 - \rho_0 \nabla^2 \Phi_1 = 0, \tag{2.154}$$

which conveniently also allows us to directly insert Poisson's equation (2.152) to finally find

$$\left(\frac{\partial^2}{\partial t^2} - c_s^2 \nabla^2 - 4\pi G \rho_0 \right) \rho_1 = 0. \tag{2.155}$$

Since this is a linear partial differential equation, we can make our usual plane wave ansatz, i.e. we set $\rho_1 = A \exp[i(\mathbf{k}\cdot\mathbf{x} - \omega t)]$ to obtain the dispersion relation

$$\omega^2 = c_s^2(k^2 - k_J^2), \tag{2.156}$$

where we define

$$k_J^2 = \frac{4\pi G\rho_0}{c_s^2}. \tag{2.157}$$

We see immediately that when $k < k_J$, then ω becomes imaginary, which results in density perturbations to grow exponentially. On the other hand, if $k < k_J$, then the mode of wave number k is stable and will just cause oscillations (or acoustic waves). The wave number k_J can of course be expressed in terms of a wave length $\lambda_J = 2\pi/k_J$, so that this statement means that in a self-gravitating gas of background density ρ_0 with sounds speed c_s, perturbations on wavelengths longer than λ_J overcome pressure forces and will collapse. The length λ_J is called the Jeans length. Since it corresponds directly to a mass on the unperturbed background, one defines also

$$M_J = \frac{4\pi}{3}\rho_0\lambda_J^3 \tag{2.158}$$

as the Jeans mass which tells us directly whether a perturbation of mass M_J in a medium at mean density ρ_0 with a sound speed c_s will undergo gravitational collapse.

2.6 Multi-species, ionisation and radiative cooling

We have neglected in our analysis so far that in the typical astrophysical environment, a gas will not be made up just from one single particle type. Moreover, depending on temperature and density, atoms in the gas can be neutral or ionised. And a further complication is that radiative processes enter the picture which can remove internal energy out of the system. In this section, we will provide the relevant formulae to deal with these situations. The physical details on these processes would require a separate course, so that we just provide a set of tools.

2.6.1 Average treatment of multi-species gases

You might have wondered why we have often assumed that the particle mass in our exercises was taken to be $\sim 1.2\, m_H$ the mass of a hydrogen atom m_H. In fact this was well motivated as we will see now. The underlying idea is that when we have a multi-species gas, such as one consisting of Hydrogen, Helium and other heavier elements, collectively called metals in astrophysics, it is most of the time very reasonable to assume that they are in mutual equilibrium so that they have the same temperature and mean velocity. If this is the case, we can write the mean mass of the fluid particles by

$$\bar{m} = \mu\, m_H, \tag{2.159}$$

where μ is defined to be the mean molecular weight in units of the mass of a Hydrogen atom. Naturally, the mean molecular weight depends both on the composition of the gas in terms of its atoms, but also on the ionisation state – think that when a gas gets ionised, the number of particles increases, but not their mass, so the mean particle mass has to drop. We can then write for a *completely neutral gas*

$$\bar{m}_{\text{neutral}} = \frac{\sum_j N_j m_j}{\sum_j N_j} \quad \Rightarrow \mu_{\text{neutral}} = \frac{\sum N_j A_j}{\sum_j N_j}, \tag{2.160}$$

where N_j is the number of atoms of species j, m_j their mass, and $A_j := m_j/m_H$ is the mass of atoms of species in units of the mass of a hydrogen atom. Similarly, one can write down the mean molecular weight for an ionised gas

$$\mu_{\text{ionised}} = \frac{\sum_j N_j A_j}{\sum_j N_j (1+z_j)}, \tag{2.161}$$

where z_j is the number of free electrons due to species j, so that $1+z_j$ is the number of electrons plus the nucleus. It is common now to rewrite these formulae somewhat, so that they can be expressed in terms of the fraction of the total mass in species j. For this one cosiders

$$\frac{1}{\mu m_H} = \frac{\sum_j (1+z_j) N_j}{\sum N_j m_j} = \frac{\text{total number of particles}}{\text{total mass of gas}} \tag{2.162}$$

$$= \sum_j \frac{(1+z_j)N_j}{N_j A_j m_H} X_j = \sum_j \frac{1+z_j}{A_j m_h} X_j, \tag{2.163}$$

where we set $X_j = N_j m_j / \sum_i N_i m_i$ as the mass fraction of atoms of type j. We thus have

$$\frac{1}{\mu} = \sum_j \frac{1+z_j}{A_j} X_j. \tag{2.164}$$

For a neutral gas this becomes simply

$$\frac{1}{\mu_{\text{neutral}}} \simeq X + \frac{1}{4}Y + \left\langle \frac{1}{A} \right\rangle Z, \tag{2.165}$$

where X is the mass fraction of the gas in hydrogen, Y the fraction in Helium and Z in heavier elements. The fraction Z is also called the metallicity of the gas. For the solar environment one finds $< 1/A > \sim 1/15.5$. On the other hand, for a fully ionised gas, one has

$$\frac{1}{\mu_{\text{ionised}}} \simeq 2X + \frac{3}{4}Y + \left\langle \frac{1+z}{A} \right\rangle Z, \tag{2.166}$$

where one finds in fact that $< (1+z)/A > \simeq 1/2$ to a very good approximation. For the solar neighbourhood one has $X = 0.70, Y = 0.28, Z = 0.02$, while for primordial gas in the early Universe has $X = 0.76, Y = 0.24, Z \sim 0$.

2.6.2 Equilibrium ionisation

In order to evaluate the cooling function above, we need the degree of ionisation of a gas. Ionisation is a bound-free transition, meaning that the end state is to a continuum of energies, because the freed electron's energy is given purely by its (continuous) kinetic energy $E_e = p^2/2m_e$, where m_e is the mass of the electron. Assuming that the energy needed for ionisation from state r is χ_r, we have that a photon of energy $E_\nu := h\nu > \chi_r$ will produce an electron where the excess energy beyond χ_r goes into its momentum, such that

$$h\nu = \chi_r + \frac{p^2}{2m_e}. \tag{2.167}$$

Under the condition of thermodynamic equilibrium, the degree of ionisation can only depend on the density and temperature of the gas. We shall compute this next.

Assume a two-state system with states A and B, then in thermodynamic equilibrium, the relative occupation numbers of the states A and B are

$$\frac{N_B}{N_A} = \frac{g_B}{g_A} \exp\left[-\frac{E_B - E_A}{kT}\right], \tag{2.168}$$

where E_A and E_B are the energies of the states and g_A and g_B their respective statistical weights. Let us assume now that A is the un-ionised state, and B is the ionised state, then

$$E_B - E_A = \chi_r + \frac{p^2}{2m_e}. \tag{2.169}$$

The statistical weight of the un-ionised state is just that of the respective atomic state of ionisation degree i: $g_A = g_i$, while that for the ionised state, atomic state of ionisation degree $i+1$: g_{i+1}, multiplied by the number of possible states of the free electron. The number of possible state of the free electron is given by the volume of the six-dimensional phase space accessible to the electron in units of Planck's constant h, multiplied by 2 due to the two possible spin states of an electron, i.e. we have

$$g_B = 2g_{i+1}\frac{\mathrm{d}^3x\mathrm{d}^3p}{h^3} = 2g_{i+1}\frac{V_e 4\pi p^2 \mathrm{d}p}{h^3}, \qquad \text{where} \quad V_e = \frac{1}{n_e}. \tag{2.170}$$

Integrating over all states, we thus have

$$\begin{aligned}
\frac{n_{i+1}}{n_i} &= \frac{g_{i+1}}{g_i}\frac{2}{n_e h^3}\int_0^\infty \exp\left[-\left(\chi + \frac{p^2}{2m_e}\right)/kT\right] 4\pi p^2\,\mathrm{d}p & (2.171)\\
&= \frac{g_{i+1}}{g_i}\frac{2}{n_e h^3}\exp\left[-\chi/kT\right]\int_0^\infty \exp\left(-p^2/2m_e kT\right) 4\pi p^2\,\mathrm{d}p & (2.172)\\
&= \frac{g_{i+1}}{g_i}\frac{2}{n_e h^3}\left(2\pi m_e kT\right)^{3/2}\exp\left[-\chi/kT\right] & (2.173)
\end{aligned}$$

where we used that $\int \exp\left(-y^2/a\right) y^2 \mathrm{d}y = \frac{1}{4}a^{3/2}\sqrt{\pi}$. This result is the famous Saha equation.

While in physics and chemistry, the ionisation state of an atom is usually indicated as, e.g., He, He^+ and He^{2+} for neutral, singly and doubly ionised Helium, respectively. In astronomy, these ionisation states are labelled with Roman numerals as HeI, HeII and HeIII, respectively, so that e.g. HI is neutral hydrogen. For the most abundant elements hydrogen and helium, we have the values

- Hydrogen, HI→HII: χ=13.6 eV, $2g_{i+1}/g_i = 1$
- First ionisation of Helium, HeI→HeII: χ=25.5 eV, $2g_{i+1}/g_i = 4$
- Second ionisation of Helium, HeII→HeIII: χ=54.2 eV, $2g_{i+1}/g_i = 1$

In the case of hydrogen, the ionisation fraction x_H is given by the ratio

$$x_\mathrm{H} = \frac{n_\mathrm{HII}}{n_\mathrm{H}} = \frac{n_\mathrm{HII}}{n_\mathrm{HI} + n_\mathrm{HII}}, \quad \text{and} \quad n_\mathrm{HII} = n_e \tag{2.174}$$

by charge conservation, so that one can write

$$\frac{x_\mathrm{H}^2}{x_\mathrm{H} - 1} = \frac{(2\pi m_e)^{3/2}}{h^3}\frac{(kT)^{5/2}}{P}\exp\left[-\frac{13.6\,\mathrm{eV}}{kT}\right], \tag{2.175}$$

In astronomy, the neutral state of Hydrogen is labelled as HI, while the ionised state is labelled HII. Note that the Saha equation describes the collisional equilibrium ionisation in a gas. Gas can also be photo-ionised by a source emitting photons with an energy above the ionisation energy. For this reason, the Saha equation does not describe the ionisation of HII regions around young stars.

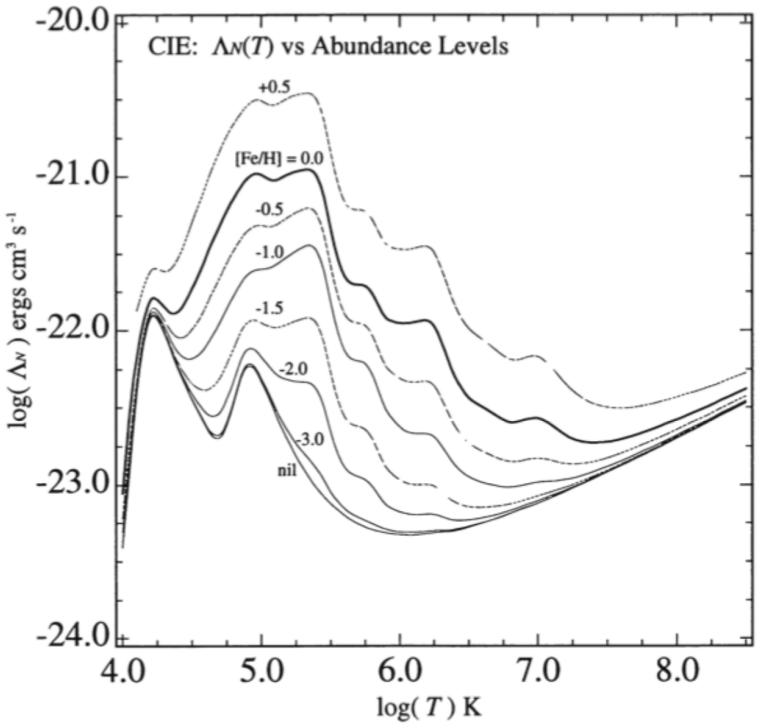

Figure 2.14: The volumetric cooling function $\Lambda(T)$ based on the detailed calculations of Sutherland & Dopita (1993). The different curves correspond to different metallicities from super-solar (top-most curve), to primordial composition with zero metallicity (bottom-most curve).

2.6.3 The cooling function

A full treatment of radiative processes is beyond the scope of this course, but radiative cooling has such an important role in astrophysics that we cannot leave it out. It is the simplest form of a radiative process, where internal energy of a gas is converted into radiation which then leaves the system without being re-absorbed. Such a situation is called optically thin. The processes that can lead to the emission of a photon from an interaction between gas particles are manifold. The most relevant atomic processes are the following two-body processes

1. Collisional excitation: particle collisions excite an electron in an atom, which subsequently de-excites under emission of a photon ("bound-bound transition").
2. Collisional ionisation: particle collisions lead to the removal of a bound electron, removing an amount of energy equal to at least the ionisation energy from the system. ("bound-free transition")
3. Recombination: an ionised atom can capture a free photon and will emit a photon. ("free-bound transition")
4. Bremsstrahlung: in ionised gases, free electrons can be accelerated/decelerated by ions leading to the emission of Bremsstrahlung. ("free-free transition")

While the exact energy balance of these processes can be calculated, they are usually taken together and summarised as a simple cooling function $\Lambda(T, Z)$, which is only a function of the temperature and

the metallicity Z. The cooling function directly quantifies the volumetric radiative cooling rate and is usually given in units of erg cm^3 s^{-1}. The cooling function gives directly the loss of energy of the gas due to optically thin radiative cooling at a volumetric rate of

$$\frac{\partial e}{\partial t} = n_e n_i \Lambda(T, Z), \tag{2.176}$$

where n_e is the number density of electrons and n_i is the total number density of all species of ions. The energy equation in conservative form including optically thin radiative cooling is then

$$\frac{\partial e}{\partial t} + \frac{\partial}{\partial x_i}\left(e v_i\right) = -\frac{\partial}{\partial x_i}\left(P v_i\right) + \rho F_i v_i + n_e n_i \Lambda(T, Z). \tag{2.177}$$

We note that the atomic cooling function drops rapidly at temperatures of $\sim 10^4$ K, preventing cooling to lower temperatures through the atomic processes we listed above. At low enough temperatures, the formation of molecules becomes however possible, which permits further cooling channels through collisional excitation of vibrational or rotational modes which de-excite under emission of photons. At even lower temperatures, e.g. in molecular clouds, which are the sites of star formation, cooling to the lowest temperatures is aided by interaction of gas molecules with much heavier dust grains. Note that optically thin cooling is only a valid assumption if the photons can escape the system without being re-absorbed. As soon as the mean free path of those photons becomes comparable to the mean inter-particle distance in the gas cloud, the optically thin assumption becomes invalid.

2.7 Time scales

Often in astrophysics, it is important to give back-of-the-envelope arguments in order to decide whether certain processes are relevant. An intuitive way to do this is by comparing the time scales on which certain processes proceed. By calculating which process occurs on a shorter time-scale than others, it is then possible to decide that this process must be dominant. We will see how this is done next.

The sound-crossing time

We have seen over and over that the most important feature for pressure effects to be able to stabilise a system is that sound waves can cross through a system before other motions do so. The time-scale on which sound propagates through a system can be estimated as the sound-crossing time through an object of size R as

$$t_{\text{sound}} \sim \frac{R}{c_s} \sim \frac{1}{c_s}\left(\frac{3M}{4\pi\bar{\rho}}\right)^{1/3}, \tag{2.178}$$

where in the last equality we have estimated the size from mass and mean density.

The free-fall time

For a spherically symmetric system with a mass profile $M(r)$, neglecting pressure forces, we can calculate the time a freely falling mass shell at a radius R needs to fall to the centre. If the mass shell of mass dm starts at a radius R_0 at rest, then its initial energy is given by $E_0 = -\frac{GM(<R_0)}{R_0}\, dm$, while at

a later time it will have a velocity U and be located at a position R. Since the mass interior to the shell rests constant, we can simply write $M(R(t)) =: M$ at all times. Energy conservation then requires

$$\frac{1}{2}U^2 = \frac{GM}{R} - \frac{GM}{R_0}. \tag{2.179}$$

We thus can write using $U = dR/dt$ that

$$dt = -\left[2GM\left(\frac{1}{R} - \frac{1}{R_0}\right)\right] dR, \tag{2.180}$$

and substituting $\xi = R/R_0$ and so also $d\xi = dR/R_0$ one can write this using that the enclosed mass remains constant as

$$dt = -\left(\frac{8\pi G\bar{\rho}}{3}\right)^{-1/2}\left(\frac{\xi}{1-\xi}\right)^{1/2} d\xi. \tag{2.181}$$

Now we simply have to integrate both sides, and ξ from 0 to 1 to find the free-fall time

$$t_{\rm ff} = \left(\frac{3\pi}{32G\bar{\rho}}\right)^{1/2}. \tag{2.182}$$

The cooling time

Another important time scale is the time scale on which an object will lose a significant amount of its internal energy through optically thin radiative cooling. We had that the internal energy gets reduced through cooling as

$$\frac{\partial e}{\partial t} = n^2\Lambda(T, Z), \tag{2.183}$$

while the internal energy itself is $e = \frac{3}{2}nkT$, so that the cooling time of the system can be estimated to be

$$t_{\rm cool} \simeq \frac{e}{\partial e/\partial t} = \frac{3}{2}\frac{kT}{n\Lambda}. \tag{2.184}$$

Naturally, in the presence of a heating source (e.g. a star or another energetic process that transfers energy to the gas) with a heating rate Γ, if $\Lambda > \Gamma$, then

$$t_{\rm cool} = \frac{3}{2}\frac{kT}{n(\Lambda - \Gamma)}. \tag{2.185}$$

Instability time scales

For all of the instabilities we have discussed before, we can also estimate a time scale in terms of the dispersion relation. For a system of scale L to undergo an instability governed by a dispersion relation expressed in terms of ω/k, we can estimate $\omega \sim 2\pi/t_{\rm instab.}$ and $k \sim 2\pi/L$ so that

$$t_{\rm instab.} \simeq L\left[\frac{\omega}{k}\right]^{-1}_{k=2\pi/L}, \tag{2.186}$$

where the suffix $k = \ldots$ means that we need to evaluate the dispersion relation for a wave number $k = 2\pi/L$.

2.8 Turbulence

As the last topic we shall discuss in the context of fluid mechanics, we will briefly touch upon the topic of turbulence.

2.8.1 Transition to turbulence

We have already seen the beginning of the transition from laminar flow to turbulent flow when the Reynolds number is varied in the Kárman vortex street experiment (Fig. 2.3) of the flow around an obstacle, where stronger and stronger vortices appear with increasing Reynolds number, which reflects the ratio of fluid velocity times a typical length scale of the problem to the kinematic viscosity. In Figure 2.15, we see two experiments that show turbulent flows: the plume of hot air rising from a burning candle that becomes turbulent at large distances from the candle, and the turbulent wake behind a supersonic bullet. In the case of the bullet we can immediately understand that we must have a very high Reynolds number since the bullet is moving supersonically. In the case of the bullet, we have a shear flow between the upward rising hot air, and the colder air around it. This shear flow makes the boundary between the two flows unstable (much like in the interface instabilities that we have discussed before) which leads to the development of turbulence which ultimately mixes hot and cold air. This turbulent mixing is only possible, if the Reynolds number is high enough, otherwise the instability will be suppressed.

2.8.2 Statistical description of turbulence

As we have seen from the various examples that we have already encountered, turbulence is characterised by its chaotic and disordered appearance, in which structure, initially present in the laminar part of the flow, is lost. At the same time, turbulent flows are not random but have a 'rich' structure without preferred a point or direction in it when turbulence has fully developed. We say that a turbulent flow which has this property is statistically homogeneous and isotropic. We shall now aim for a statistical description of such a turbulent velocity field. The properties of any homogeneous field (i.e. without a preferred point) can only depend on the distance between two points, i.e. relative distances: let $\mathbf{x}_A$ and $\mathbf{x}_B$ be two arbitrary points in space, then the vector $\mathbf{x}_B - \mathbf{x}_A$ is independent of arbitrary translations of our coordinate system, while $\mathbf{x}_A$ and $\mathbf{x}_B$ themselves are not. Similarly, the properties of any isotropic field (i.e. without preferred direction) can only depend on the magnitude of this relative vector, i.e. can depend only on $\|\mathbf{x}_B - \mathbf{x}_A\|$.

Let us next decompose the fluid velocity field $\mathbf{v}(\mathbf{x}, t)$ into a (smooth) mean field $\overline{\mathbf{v}}$ and a fluctuating part $\delta\mathbf{v}$, i.e.

$$\mathbf{v}(\mathbf{x}) = \overline{\mathbf{v}}(\mathbf{x}) + \delta\mathbf{v}(\mathbf{x}) \tag{2.187}$$

In practice we can imagine some averaging procedure, where we take a volume V that is much larger than the largest vortices in our turbulent flow and take $\overline{\mathbf{v}}$ to be the mean velocity in this volume. To characterise the fluctuations, we best go to Fourier space so that we have the pair

$$\delta\tilde{\mathbf{v}}(\mathbf{k}) = \frac{1}{V}\int \mathrm{d}^3x \delta\mathbf{v}\, \exp(-i\mathbf{k}\cdot\mathbf{x}) \quad \text{and} \quad \delta\mathbf{v}(\mathbf{x}) = (2\pi)^{-3}\int \mathrm{d}^3k\, \delta\tilde{\mathbf{v}}\, \exp(i\mathbf{k}\cdot\mathbf{x}). \tag{2.188}$$

The specific energy due to turbulence, analogously to the specific thermal energy that we encountered before, is thus

$$\epsilon_{\text{turb}} = \frac{1}{V}\int \mathrm{d}^3x\, \frac{1}{2}\overline{|\delta\mathbf{v}|^2} = \frac{1}{(2\pi)^3 V}\int \mathrm{d}^3 3k \frac{1}{2}\overline{|\delta\tilde{\mathbf{v}}|^2} =: \int_0^\infty \mathrm{d}k \epsilon_k, \tag{2.189}$$

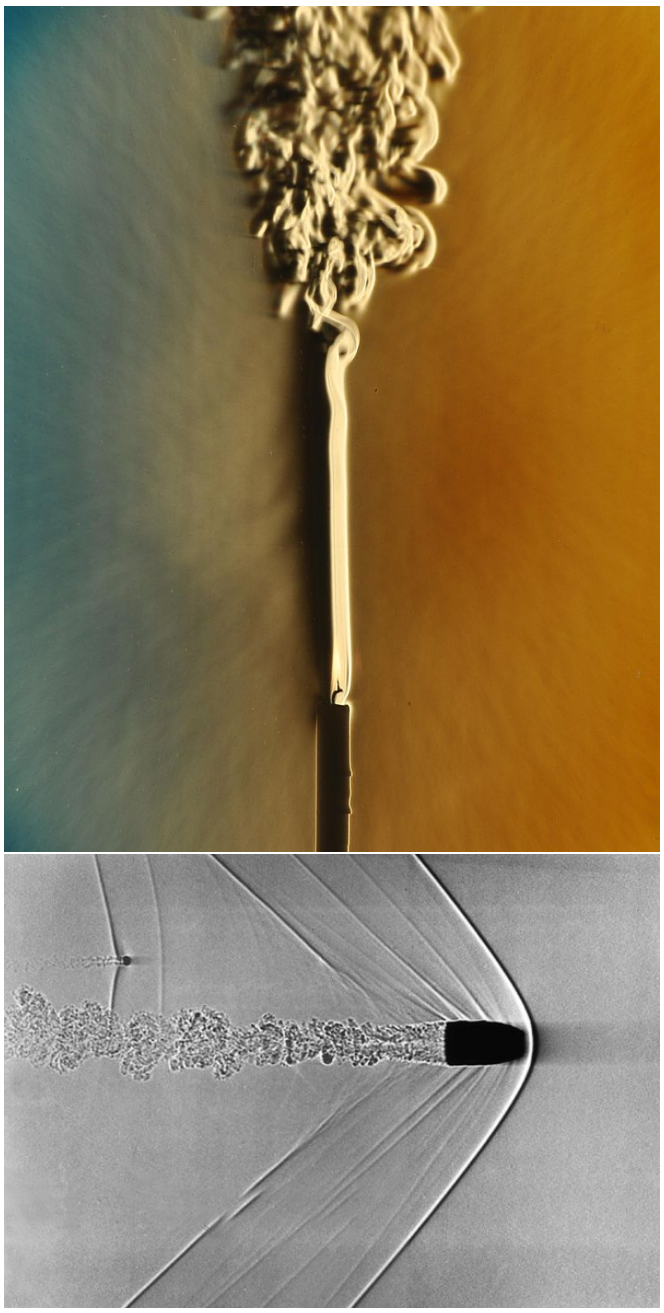

Figure 2.15: *Top:* Schlieren photograph of the hot air plume rising from a burning candle. The flow is first laminar before it quickly transitions to turbulence. [Image from Wikipedia, by G. Settles, CC BY-SA 3.0]. *Bottom:* Shadowgraph of a supersonic gun bullet showing the bow shock wave and the trailing turbulent wake. [Image by Andrew Davidhazy]

where we made use of Parseval's theorem, assumed spatial isotropy of the fluctuations (allowing us to assume that everything only depends on the modulus of $\mathbf{k}$ and not the vector part), and defined a specific energy per unit wave number, called the spectral energy per unit mass, as

$$\epsilon_k := \frac{k^2 \overline{|\delta\tilde{\mathbf{v}}|^2}}{4\pi^2 V}. \tag{2.190}$$

Let now ℓ be the scale of the largest eddies so that $k_{\min} = 2\pi/\ell$ is the wave number corresponding to them. On the other side of the spectrum, let us assume that the smallest eddies correspond to some $k_{\max}$ which is much larger than $k_{\min}$. We can estimate the turbulent turnover time to be the scale of the eddy divided by the velocity on that scale, i.e.

$$\tau_{\text{turnover}} \approx \frac{2\pi}{k\, v(k)} \tag{2.191}$$

If now assume that over the same time, each eddy of size ℓ splits into eddies of $\ell/2$ then this implies that turbulent energy is transferred between wave numbers k and $2k$ over the time τ. Let us denote the amount of energy q transferred from k to $2k$ per unit time and unit mass, then

$$q \approx \frac{\frac{1}{2}v^2}{\tau} \approx v^3 k \quad \Rightarrow \quad v(k) \sim \left(\frac{q}{k}\right)^{1/3} \tag{2.192}$$

The same energy transfer in terms of the specific spectral energy is

$$\int_k^{\Delta k} \mathrm{d}k\, \epsilon_k \approx k\epsilon_k \quad \text{so that} \quad \epsilon_k \approx v^2(k)/k \tag{2.193}$$

so that we finally arrive at the famous Kolmogorov spectrum for fully developed isotropic turbulence

$$\epsilon_k \sim q^{2/3} k^{-5/3} \quad \text{for} \quad k_{\min} \ll k \ll k_{\max}. \tag{2.194}$$

The largest scale $k_{\min}$ corresponds to the largest eddies, which typically correspond to the energy injection, or driving, scale of the turbulence, while $k_{\min}$ corresponds to the scale where the turbulence is dissipated into thermal energy (i.e. heat). Since this dissipation scale is related to the viscosity, the smallest eddies by definition correspond to a Reynolds number of order unity, i.e.

$$\mathcal{R}(k_{\max}) \sim \frac{v(k_{\max})k_{\max}^{-1}}{\nu} \sim 1 \quad \text{so that} \quad k_{\max} \sim q^{1/4}\nu^{-3/4}, \tag{2.195}$$

while the largest eddies have a turnover velocity $v_\ell \sim (q/k_{\min})^{1/3}$ so that

$$\mathcal{R}_\ell := \mathcal{R}(k_{\min}) \sim \frac{(q/k_{\min})^{1/3} k_{\min}^{-1}}{\nu} \quad \text{implying} \quad \frac{k_{\max}}{k_{\min}} \sim \left(\frac{v_\ell \ell}{\nu}\right) = \mathcal{R}_\ell^{3/4}. \tag{2.196}$$

Chapter 3

Plasmas and Magnetohydrodynamics

3.1 Charged particles in Astrophysics

3.1.1 Astrophysical Plasmas

In many cases in astrophysics, we are dealing with ionised atoms. In an ionised system, the constituent particles thus carry charge (the electrons a negative one and the ions a positive one). These charged particles will interact with each other through long-range electromagnetic interactions that can radically change the behaviour of the system. Whether we can treat an ionised gas as an ideal gas, or whether we have to treat it as a plasma thus depends on the relative importance of these long-range electromagnetic interactions.

Plasma orbit theory

In a neutral medium (or in an ionised medium where we can neglect electromagnetic fields), the motion of a particle of mass m is given by Newton's law

$$m\frac{d\mathbf{u}}{dt} = \mathbf{F}, \tag{3.1}$$

where $\mathbf{F}$ is the gravitational force. A charged particle of charge q will however be subject to an electric force $q\mathbf{E}$ and a Lorentz force $\frac{q}{c}\mathbf{u} \times \mathbf{B}$ and thus move according to

$$m\frac{d\mathbf{u}}{dt} = q\left(\mathbf{E} + \frac{\mathbf{u}}{c} \times \mathbf{B}\right) + \mathbf{F}. \tag{3.2}$$

We see that phenomenologically, the gravitational force and the acceleration due to the electric field are identical, but the effect of the magnetic field $\mathbf{B}$ dramatically alters the motion of a particle. To see this, let us assume the particle is moving with a velocity $\mathbf{u}_\perp$ perpendicular to $\mathbf{B}$ and we neglect $\mathbf{E}$ and $\mathbf{F}$. Then

$$m\frac{d\mathbf{u}_\perp}{dt} = \frac{q}{c}\mathbf{u}_\perp \times \mathbf{B}. \tag{3.3}$$

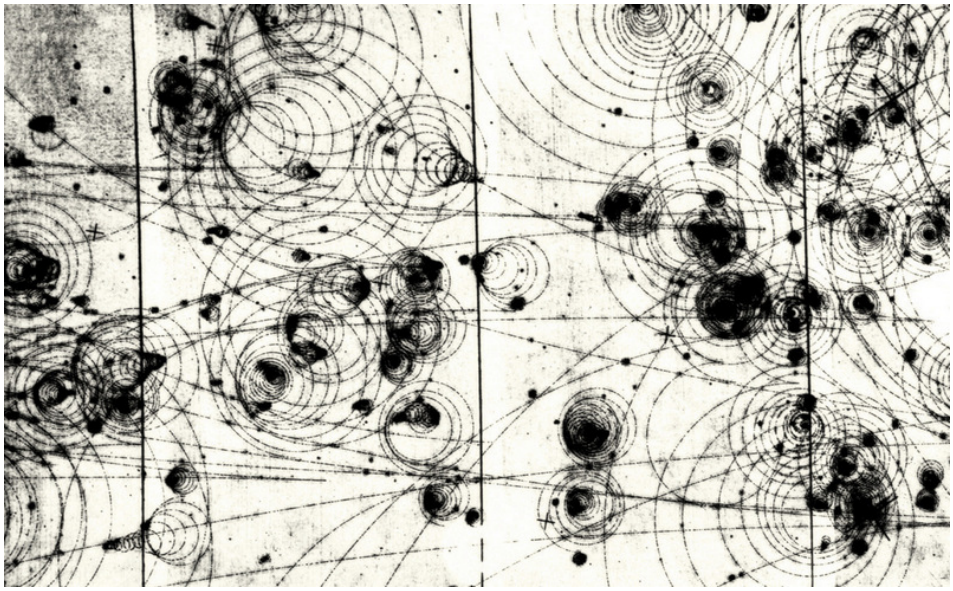

Figure 3.1: The tracks of charged particle in a so-called "bubble chamber" of a superheated liquid with a magnetic field applied. This photo was taken of a bubble chamber at SLAC in 1967. [Photo courtesy SLAC National Accelerator Laboratory]

For simplicity, let $\mathbf{B} = B\mathbf{e}_z$ be directed along the z-axis. Then for $\mathbf{u}_\perp = (u_x, u_y, 0)$, we find

$$\frac{d}{dt}\begin{pmatrix} u_x \\ u_y \end{pmatrix} = \frac{Bq}{mc}\begin{pmatrix} u_y \\ -u_x \end{pmatrix}. \tag{3.4}$$

We see immediately that this is solved for $u_x = U_0\cos(\omega_c t)$, $u_y = U_0\sin(\omega_c t)$ with the gyrofrequency

$$\omega_c = \frac{qB}{mc}. \tag{3.5}$$

The particle thus moves in a circle in the plane perpendicular to $\mathbf{B}$ with a radius

$$r_g = \frac{u_\perp}{\omega_c} = \frac{mc}{qB}u_\perp, \tag{3.6}$$

which is called the gyroradius, or also sometimes called the Larmor radius. Motion along the direction $\mathbf{u}_\parallel$ that is parallel to $\mathbf{B}$ will not be affected by the magnetic field. The complete motion of the particle will thus be helical around the direction of the magnetic field with the two components:

1. circular motion around a moving central point, called the guiding centre, and
2. translatory motion of the guiding centre.

Even for non-uniform magnetic fields, it is usually possible to write the motion in terms of these two components.

This gyro-motion of charged particles around magnetic field lines can be used to detect particles in a bubble chamber containing a superheated liquid (see Figure 3.1).

In the presence of either an electric field, a gravitational field, or both, the equation of motion is

$$m\frac{d\mathbf{u}}{dt} = \frac{q}{c}\mathbf{u}\times\mathbf{B} + \mathbf{F}, \tag{3.7}$$

where we have combined both gravity and electric force into the term $\mathbf{F}$. We can again split the velocity into two components $\mathbf{u}_\parallel$ and $\mathbf{u}_\perp$ parallel and perpendicular to the magnetic field. The parallel component will then again be unaffected by the magnetic field and simply obey

$$m\frac{d\mathbf{u}_\parallel}{dt} = \mathbf{F}_\parallel, \tag{3.8}$$

where $\mathbf{F}_\parallel$ is the part of $\mathbf{F}$ that is parallel to $\mathbf{B}$. The perpendicular velocity $\mathbf{u}_\perp$, we can break up into the motion of the guiding centre $\mathbf{u}_{\text{gc}}$ and the circular motion $\mathbf{u}_{\circlearrowleft}$

$$\mathbf{u}_\perp = \mathbf{u}_{\circlearrowleft} + \mathbf{u}_{\text{gc}} \tag{3.9}$$

The circular component is unaffected by $\mathbf{F}_\perp$ and just follows (as before)

$$\frac{d\mathbf{u}_{\circlearrowleft}}{dt} = \frac{q}{mc}\mathbf{u}_{\circlearrowleft}\times\mathbf{B}, \tag{3.10}$$

while the guiding centre motion now has to be uniform and thus satisfy

$$0 = \mathbf{F}_\perp + \frac{q}{c}\mathbf{u}_{\text{gc}}\times\mathbf{B} \tag{3.11}$$

in order for the equation of motion to be satisfied. Taking the cross-product with $\mathbf{B}$, we find

$$\mathbf{F}\times\mathbf{B} = \frac{q}{c}\mathbf{B}\times(\mathbf{u}_{\text{gc}}\times\mathbf{B}) = \frac{q}{c}B^2\mathbf{u}_{\text{gc}}, \tag{3.12}$$

so that

$$\mathbf{u}_{\text{gc}} = \frac{c}{q}\frac{\mathbf{F}_\perp\times\mathbf{B}}{B^2} \qquad \left[= c\frac{\mathbf{E}\times\mathbf{B}}{B^2}, \quad \text{if } \mathbf{F}_\perp = q\mathbf{E}\right]. \tag{3.13}$$

Gradient Drift

Let us now consider a magnetic field which is changing in strength. For simplicity let us set $\mathbf{B} = B(y)\mathbf{e}_z$, i.e. it is unidirectional in the z-direction, but varying in strength in the y-direction. The y-component of the Lorentz force is then

$$F_y = -\frac{q}{c}u_x B(y). \tag{3.14}$$

If we measure the y-coordinate relative to the guiding centre and assume that the variation of $B(y)$ is small over the trajectory of the particle, then to first order

$$B(y) = B_0 + y\frac{dB}{dy}. \tag{3.15}$$

This implies that the Lorentz force is

$$F_y = -\frac{q}{c}u_x\left[B_0 + y\frac{dB}{dy}\right], \tag{3.16}$$

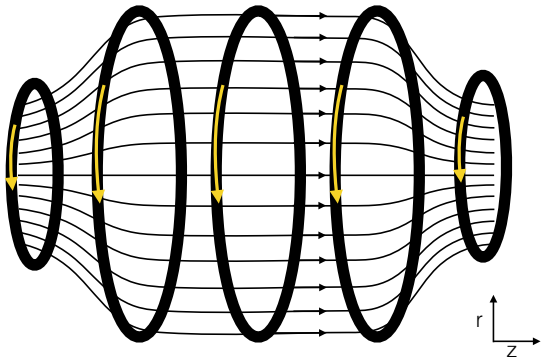

Figure 3.2: A basic magnetic mirror machine: the convergence of fields lines at the ends, and the associated increase in magnetic field strength leads to a reflection of charged particles and thus to a confinement of most particles to the interior. Such magnetic mirrors can be used to confine plasma in fusion reactors.

which we can average over the circular motion (for which $\overline{u}_x = 0$), but $\overline{u_x y}$ can be calculated to be

$$\overline{u_x y} = \frac{1}{2} u_\perp r_g, \tag{3.17}$$

where r_g is the gyroradius. Hence

$$\overline{\mathbf{F}} = \mp \frac{q}{2c} u_\perp r_g \boldsymbol{\nabla} B. \tag{3.18}$$

We can plug this averaged Lorentz force now into equation (3.13) for the guiding centre motion to find the expression for the gradient drift

$$\mathbf{u}_{\boldsymbol{\nabla} B} = \pm \frac{1}{2} u_\perp r_g \frac{\mathbf{B} \times \boldsymbol{\nabla} B}{B^2}. \tag{3.19}$$

It is important to note that the respective signs $\pm$ apply to negative and positive charges respectively, so that gradients in the transverse magnetic field lead to electrons and ions drifting in opposite directions, which gives rise to an electric current.

Magnetic Mirrors

Next, we consider a magnetic field with a gradient in field strength in the z-direction. When working with a magnetic field, we always have to make sure that the $\mathbf{B}$-field is divergence-free. Working in cylindrical coordinates, this constraint equation $\boldsymbol{\nabla} \cdot \mathbf{B} = 0$ becomes

$$\frac{1}{r} \frac{\partial}{\partial r} (r B_r) + \frac{\partial B_z}{\partial z} = 0. \tag{3.20}$$

We can integrate this equation to find (assuming B_z is constant with radius r)

$$r B_r = -\int_0^r r' \frac{\partial B_z}{\partial z} \, dr' =\simeq -\frac{1}{2} r^2 \frac{\partial B_z}{\partial z} \quad \Leftrightarrow \quad B_r = -\frac{1}{2} r \frac{\partial B_z}{\partial z}. \tag{3.21}$$

The Lorentz-force in cylindrical coordinates is given by

$$\begin{pmatrix} F_r \\ F_\phi \\ F_z \end{pmatrix} = \frac{q}{c} \begin{pmatrix} u_\phi B_z - u_z B_\phi \\ u_z B_r - u_r B_z \\ u_r B_\phi - u_\phi B_r \end{pmatrix}, \tag{3.22}$$

so that in our case $F_z = -\frac{q}{c} u_\phi B_r$ since we have set $B_\phi = 0$ and we can write $u_\phi = \mp u_\perp$. We thus get

$$F_z = \mp \frac{q}{2c} u_\perp r_g \frac{\partial B_z}{\partial z} = -\mu \frac{\partial B_z}{\partial z}, \tag{3.23}$$

where we have defined the magnetic moment

$$\mu = \pm \frac{q}{2c} u_\perp r_g = \frac{\frac{1}{2} m u_\perp^2}{B}. \tag{3.24}$$

Alternatively one can express the magnetic moment by eliminating $u_\perp$ instead of r_g as

$$\mu = \pm \frac{\omega_c}{2\pi} \frac{q}{c} \pi r_g^2. \tag{3.25}$$

The z-component of the particle motion is given by

$$m \frac{du_\parallel}{dt} = F_z = -\mu \frac{\partial B_z}{\partial z}, \tag{3.26}$$

and the rate of change of the longitudinal kinetic energy is given by

$$\frac{d}{dt} \left(\frac{1}{2} m u_\parallel^2 \right) = u_\parallel m \frac{du_\parallel}{dt} = -\mu \frac{dB}{dt}. \tag{3.27}$$

Since obviously the sum of the transverse and longitudinal kinetic energies cannot change, we must also have

$$\frac{d}{dt} \left(\frac{1}{2} m u_\parallel^2 + \frac{1}{2} m u_\perp^2 \right) = 0, \tag{3.28}$$

which after a short calculation leads to

$$\frac{d\mu}{dt} = 0, \tag{3.29}$$

which means that the magnetic moment μ is a conserved quantity. This leads to an interesting effect called a magnetic mirror: The transverse kinetic energy $\frac{1}{2} m u_\perp^2$ has to increase when the particle moves into a region of stronger magnetic field B. However, it can never exceed the total kinetic energy, so that there will be a limiting B into which the particle cannot penetrate. Instead it will be reflected back!

3.1.2 Particle Acceleration in Astrophysics

Local changes in magnetic field strength can not only reverse particle motion, but lead to much more dramatic effects of particle acceleration. In fact, they are responsible for the highest energy particles in the Universe: cosmic rays.

Particle acceleration in magnetic clouds: the second order Fermi mechanism

The effect of magnetic mirrors can also act to accelerate particles. For this, we assume that a magnetised cloud (in which the $\mathbf{B}$-field is much stronger than outside) acts like the region of convergent field lines of the magnetic mirror. The cloud can transfer energy to the particle if it has a relative velocity with respect to the particle. Let's assume the cloud is moving with a velocity V. Let us assume the particle is coming in with a velocity u directly towards the cloud. In the rest frame of the cloud, the particle thus

has a velocity $V + u$. In the rest frame of the cloud, the collision can be assumed to be elastic, so that the particle will be reflected with a velocity $-(V + u)$. Transforming back to the rest frame, we get for the incoming velocity u and for the outgoing $-(2V + u)$. The energy gain in the observer rest frame is thus

$$\Delta E_+ = \frac{1}{2}m(u + 2V)^2 - \frac{1}{2}mu^2 = 2mV(u + V). \tag{3.30}$$

If the collision is not head on but trailing (i.e. the cloud and the particle move in the same direction), then we have the energy transfer

$$\Delta E_- = -2mV(u - V). \tag{3.31}$$

If head-on collisions would be equally likely as trailing collisions, then we would have no net energy transfer. However, head-on collisions turn out to be more frequent (this is the same effect as that when driving fast on the highway, one passes more cars moving in the opposite direction than one has to overtake cars). The probability p_+ for head-on collisions is proportional to $u+V$, while that for trailing collisions p_- is proportional to $u - V$. Normalising so that $p_+ + p_- = 1$, we have $p_+ = (u + V)/2u$ and $p_- = (u - V)/2u$ and thus after averaging over many collisions

$$\overline{\Delta E} = p_+ \, \Delta E_+ + p_- \, \Delta E_- = 4mV^2. \tag{3.32}$$

It turns out that the relativistic calculation gives

$$\frac{\overline{\Delta E}}{E} = 4\left(\frac{V}{c}\right)^2, \tag{3.33}$$

which is equal to the non-relativistic result for $E = mc^2$, i.e. when the particle kinetic energy is small compared to the rest mass. This result thus implies that the energy of a particle averaged over many collisions will increase with time. Assuming that collisions occur with some rate proportional to $1/\alpha$, then we can write

$$\frac{dE}{dt} = \alpha E \quad \Rightarrow \quad E(t) = E_0 \exp(\alpha t). \tag{3.34}$$

This means that in order to be accelerated to an energy E from an initial energy E_0, the particle needs to spend a time $t = \frac{1}{\alpha}\log(E/E_0)$ in the region where it can be accelerated. If the mean time that the particle remains in the acceleration region is τ, then the probability that the particle spends a time between t and $t + dt$ there is given by the negative exponential distribution

$$P(t)\,dt = \frac{1}{\tau}\exp(-t/\tau)dt. \tag{3.35}$$

If we substitute E for t, we find

$$P(E)\,dE = \frac{1}{\tau}\exp\left[-\frac{1}{\alpha\tau}\log(E/E_0)\right]\frac{dE}{\alpha E}, \quad \Rightarrow P(E) \propto E^{-\left(1+\frac{1}{\alpha\tau}\right)}, \tag{3.36}$$

which means that we expect that particles accelerated in such a process follow a power law distribution in energy. We see however that the acceleration process will be very slow, since the energy gain is proportional to $(V/c)^2$ and the clouds are moving at velocities $V \ll c$. This problem is circumvented in the first order Fermi mechanism.

Particle acceleration at shocks: the first order Fermi mechanism

The relative inefficiency of the second order Fermi mechanism resulted from the fact that head-on collisions and trailing collisions cancel out the first order acceleration term. If we can find an astrophysical

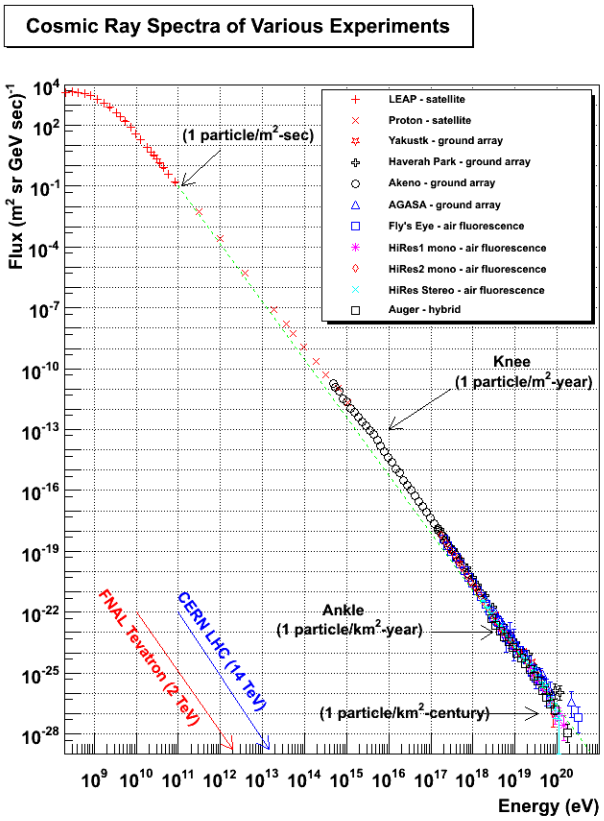

Figure 3.3: Energy spectrum of cosmic ray particles. Composed mainly of protons and light nuclei they are accelerated to energies far in excess of energies available in particle accelerators on earth. Graph taken from http://www.physics.utah.edu/~whanlon/spectrum.html.

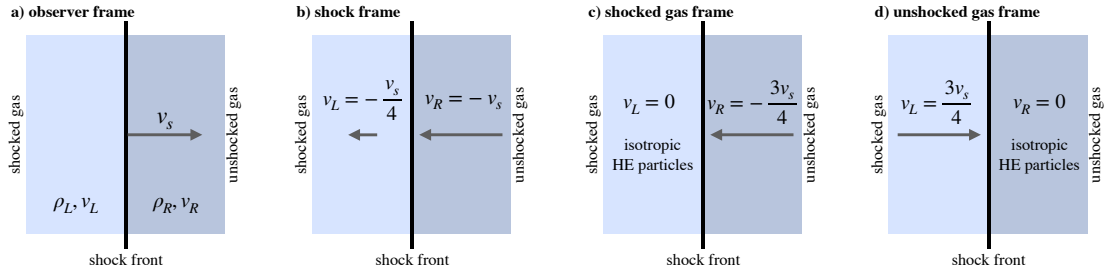

Figure 3.4: High energy particles in the vicinity of a shock wave as seen in different reference frames. From left to right: (a) The strong shock propagating through a medium. The Rankine-Hugoniot relations eq. (2.90)-(2.92) connect the left and the right state. (b) The gas velocity in the immediate vicinity of the shock front in the reference frame in which the shock front is at rest. The ratio of the upstream to downstream velocities is $\frac{v_R}{v_L} = \frac{\gamma+1}{\gamma-1} = 4$ for an ideal non-relativistic gas with $\gamma = 5/3$. (c) In the reference frame in which the upstream gas is stationary, the velocity distribution of the upstream high energy particles is isotropic and downstream particles are approaching with $v_R = -\frac{3v_s}{4}$. (d) In the reference frame in which the downstream gas is stationary, the velocity distribution of the downstream high energy particles is isotropic and upstream particles are approaching with $v_R = +\frac{3v_s}{4}$.

scenario in which only head-on collisions occur, then the acceleration would be dramatically stronger. It turns out that particles can be trapped in shock fronts which leads to a first order acceleration mechanism. When we discussed jump conditions at shocks we had that the continuity equation implies that at the shock front, which is moving with the shock velocity v_s, we have in the rest-frame of the shock ($v_s = 0$, cf. eq. 2.90)

$$\rho_L v_L = \rho_R v_R. \tag{3.37}$$

See Figure 3.4, for an illustration of the situation in the vicinity of the shock front. We also found that for a stationary strong shock (assuming a very large Mach number, $\mathcal{M} \to \infty$), the compression is $\rho_R/\rho_L = (\gamma+1)/(\gamma-1)$, which for an ideal monoatomic and non-relativistic gas with $\gamma = 5/3$ becomes $\rho_R/\rho_L = 4$. Under these conditions we thus have $v_R = v_L/4$. This means that in the rest-frame of the left state, the gas in the right state moves with $v_R = -\frac{3}{4}v_s$ (just by inserting into eq. 2.90), while in the rest-frame of the right state, the gas in the left state moves with $v_R = \frac{3}{4}v_s$. When the particle, moving itself at a velocity $+u$ in the left state, enters the right state, it can thus be reflected with a change of energy

$$\Delta E_{LR} = \frac{1}{2}m\left(u + \frac{3}{2}v_s\right)^2 - \frac{1}{2}mu^2 = \frac{3}{2}muv_s + \frac{9}{8}mv_s^2. \tag{3.38}$$

When it moves from the left state back to the right state, it will again see the same relative velocity, so that $\Delta E_{RL} = \Delta E_{LR}$ and the total relative energy gain in one round-trip is given by

$$\frac{\overline{\Delta E}}{E} = 3\frac{v_s}{u} + \frac{9}{4}\left(\frac{v_s}{u}\right)^2. \tag{3.39}$$

This shows us that indeed, we have found a first order mechanism. The relativistic calculation, with a correct averaging over scattering angles gives the result

$$\frac{\overline{\Delta E}}{E} = \frac{4}{3}\frac{v_s}{c}. \tag{3.40}$$

One can show that in this case

$$P(E)\,dE \propto E^{-2}\,dE. \tag{3.41}$$

A spectrum of cosmic ray particles measured by various experiments on Earth is shown in Figure 3.3.

3.2 Many particles in a plasma

3.2.1 The Vlasov-Maxwell equations

When we consider many particles in a plasma, we can apply the same reasoning as for uncharged particles. As when we derived the Boltzmann equation, we can express the phase space density of electrons and ions as $f_e(\mathbf{x}, \mathbf{p}, t)$ and $f_i(\mathbf{x}, \mathbf{p}, t)$, respectively. In the limit of no binary collisions, we then obtain the new Vlasov equation of the form

$$\frac{\partial f_k}{\partial t} + \frac{\mathbf{p}}{m_k} \cdot \boldsymbol{\nabla}_{\boldsymbol{x}} f_k + q_k \left(\mathbf{E} + \frac{\mathbf{p}}{m_k c} \times \mathbf{B} \right) \cdot \boldsymbol{\nabla}_{\boldsymbol{p}} f_k = 0 \qquad k \in \{i, e\}\,, \tag{3.42}$$

where the subscript k is e for electrons and i for ions, with the respective charges $q_i = +e$, $q_e = -e$ (if the ions are singly ionized) and masses m_k. Again, we can define the respective number densities by integrating over momentum space, i.e.

$$n_e(\mathbf{x}, t) = \int d^3p\, f_e(\mathbf{x}, \mathbf{p}, t), \quad \text{and} \quad n_i(\mathbf{x}, t) = \int d^3p\, f_i(\mathbf{x}, \mathbf{p}, t), \tag{3.43}$$

and take the first moment to obtain the respective velocity fields

$$\mathbf{v}_e(\mathbf{x}, t) = \frac{1}{m_e n_e} \int d^3p\, \mathbf{p}\, f_e(\mathbf{x}, \mathbf{p}, t), \quad \text{and} \quad \mathbf{v}_i(\mathbf{x}, t) = \frac{1}{m_i n_i} \int d^3p\, \mathbf{p}\, f_i(\mathbf{x}, \mathbf{p}, t). \tag{3.44}$$

If we neglect any external magnetic or electric field (otherwise they have to be added separately), the charge density $(n_i - n_e)e$ and the current density $(n_i \mathbf{v}_i - n_e \mathbf{v}_e)e$ will self-consistently generate the electric and magnetic fields by virtue of Maxwell's equations. This means that we have the additional set of equations

$$\boldsymbol{\nabla} \cdot \mathbf{E} = 4\pi(n_i - n_e)e, \tag{3.45}$$

$$\boldsymbol{\nabla} \times \mathbf{E} = -\frac{1}{c}\frac{\partial \mathbf{B}}{\partial t}, \tag{3.46}$$

$$\boldsymbol{\nabla} \cdot \mathbf{B} = 0, \tag{3.47}$$

$$\boldsymbol{\nabla} \times \mathbf{B} = \frac{4\pi}{c}(n_i \mathbf{v}_i - n_e \mathbf{v}_e)e + \frac{1}{c}\frac{\partial \mathbf{E}}{\partial t}. \tag{3.48}$$

This gives the full set of equations for the collisionless two-fluid plasma model, the Vlasov-Maxwell equations. It is not usually sufficient to simply apply the Vlasov-Maxwell system, except for dilute collisionless plasmas, due to the possible strong two-particle interactions in the plasma. For this reason, for most applications, just as in the hydrodynamic case, one will consider two-body collisions in a statistical sense. We will present the respective magnetohydrodynamic equations shortly.

3.2.2 Debye shielding

An interesting phenomenon occurs for the electric field in a plasma which is not present for gravity. In a Plasma, Poisson's equation for the electrostatic potential ϕ is

$$\nabla^2\phi = -4\pi(n_i - n_e)e. \tag{3.49}$$

If we introduce a local charge perturbation Q, then we should expect that in thermodynamic equilibrium, the electron and ion densities should be simply

$$n_e = \bar{n}\exp\left[\frac{e\phi}{kT}\right], \quad \text{and} \quad n_i = \bar{n}\exp\left[-\frac{e\phi}{kT}\right]. \tag{3.50}$$

If we substitute this into Poisson's equation, we find that

$$\nabla^2\phi = 4\pi\bar{n}e\left(\exp\left[\frac{e\phi}{kT}\right] - \exp\left[-\frac{e\phi}{kT}\right]\right). \tag{3.51}$$

In the case that $e\phi/kT \ll 1$, we can write this to first order as

$$\nabla^2\phi = \frac{1}{\lambda_D^2}\phi, \quad \text{where} \quad \lambda_D = \sqrt{\frac{kT}{8\pi\bar{n}e^2}} \tag{3.52}$$

is the Debye length. This means that the solution for the gravitational potential is not $\phi = Q/r$ but takes instead the form of a screened potential

$$\phi = \frac{Q}{r}\exp\left[-\frac{r}{\lambda_D}\right]. \tag{3.53}$$

This means that a charge perturbation from charge neutrality is only felt to a distance $\sim \lambda_D$. One can turn this into a dimensionless number by considering the mean number of particles onto which a charge perturbation would have an influence. The inverse of this is the plasma parameter

$$g = \frac{1}{n\lambda_D^3} = \sqrt{\frac{(8\pi)^3 e^6\bar{n}}{(kT)^3}}, \tag{3.54}$$

and it gives the relative importance of the energy scale of electrostatic interactions to the thermal energy. A small g implies thus that the plasma can be treated as a non-interacting perfect gas. This is why we can use the ideal gas law also in stars!

3.2.3 The two-fluid model

If we take moments of the Vlasov-Maxwell system and assume a local thermodynamic equilibrium, we will, just as in the hydrodynamic case, end up with a set of equations which describe the evolution of the moments of the distribution function. Since we have separate phase space distribution functions for electrons and ions, we will naturally end up with the equations for two fluids, one representing the electrons and one the ions. This is the two-fluid model. We will not repeat in depth the derivation of the moment equations as it is completely analogous to the hydrodynamic case. We end up with the following set of equations

$$\frac{\partial n_k}{\partial t} + \boldsymbol{\nabla}\cdot(n_k\mathbf{v}_k) = 0 \tag{3.55}$$

$$m_k n_k\left[\frac{\partial \mathbf{v}_k}{\partial t} + (\mathbf{v}_k\cdot\boldsymbol{\nabla})\mathbf{v}_k\right] = -\boldsymbol{\nabla}P_k + q_k n_k\left(\mathbf{E} + \frac{\mathbf{v}_k}{c}\times\mathbf{B}\right), \tag{3.56}$$

which represent the continuity and Euler equation which are fulfilled separately by electrons and ions. We note that naturally we also have a distinct pressure P_k for the two types of particles. Three cases of equations of state are most important. These are

$$P_k = 0 \qquad \text{for cold collisionless plasmas,} \tag{3.57}$$
$$P_k = k n_k T_k \qquad \text{for constant but distinct temperatures,} \tag{3.58}$$
$$P_k = K n_k^\gamma \qquad \text{for adiabatic processes.} \tag{3.59}$$

Naturally, to have a closed set of equations, one needs to supplement these equations with Maxwell's equations (3.45-3.48).

Electromagnetic oscillations in cold plasmas

We saw in Section 2.4.1 that in a hydrodynamic fluid, small perturbations lead to acoustic waves. This was due to the pressure force propagating the perturbation at the sound speed through the fluid. We will now show that a plasma can sustain oscillations even in the absence of a thermodynamic pressure, i.e. we set $P_k = 0$ and thus consider cold collisionless plasmas. Analogous to our discussion of acoustic waves, we can linearise the Euler equation of the electrons for velocity perturbations $\mathbf{v}_1$ around a mean electron density n_0. In addition, we will also have to perturb Maxwell's equations so that $\mathbf{E} = \mathbf{E}_0 + \mathbf{E}_1$, where $\mathbf{E_0} = 0$ and $\mathbf{B} = \mathbf{B}_0 + \mathbf{B}_1$, where $\mathbf{B_0} = 0$, i.e. we set the unperturbed fields to zero. We then have at first order for the Euler equation

$$m_e n_0 \frac{\partial \mathbf{v}_1}{\partial t} = -e n_0 \mathbf{E}_1. \tag{3.60}$$

The Lorentz force $\mathbf{v}_1 \times \mathbf{B}_1$ is a second order term and can thus be neglected at linear order in the perturbations. From Maxwell's equations we get in addition

$$\frac{1}{c}\frac{\partial \mathbf{E}_1}{\partial t} = \boldsymbol{\nabla} \times \mathbf{B}_1 + \frac{4\pi}{c} n_0 e \mathbf{v}_1 \tag{3.61}$$
$$\frac{1}{c}\frac{\partial \mathbf{B}_1}{\partial t} = -\boldsymbol{\nabla} \times \mathbf{E}_1. \tag{3.62}$$

We can now perform directly a Fourier transform in the time domain, so that we can replace all $\partial/\partial t$ with multiplications by $-i\omega$. We then get for the linearised Euler equation

$$\mathbf{v}_1 = \frac{e}{i\omega m_e}\mathbf{E}_1 \tag{3.63}$$

We can then directly insert this into the remaining equations to obtain the following relation between the perturbations to the magnetic and electric fields

$$\boldsymbol{\nabla} \times \mathbf{B}_1 = -\frac{i\omega}{c}\epsilon \mathbf{E}_1, \tag{3.64}$$

where ϵ is the dielectric constant of the plasma and is defined as

$$\epsilon := 1 - \frac{\omega_p^2}{\omega^2}, \quad \text{with} \quad \omega_p^2 := \frac{4\pi n_0 e^2}{m_e}. \tag{3.65}$$

The frequency ω_p is called the plasma frequency. We can now Fourier transform this equation back to obtain the well known form of one of Maxwell's equations in a dielectric medium

$$\frac{1}{c}\frac{\partial \mathbf{D}}{\partial t} = \boldsymbol{\nabla} \times \mathbf{B}, \quad \text{where} \quad \mathbf{D} = \epsilon \mathbf{E}. \tag{3.66}$$

We can also take a time derivative of the Euler equation, as we had done for the acoustic waves, to obtain (after Fourier transformation in time, and combining all three equations)

$$\frac{\omega^2}{c}\epsilon\mathbf{E}_1 = c\boldsymbol{\nabla}\times(\boldsymbol{\nabla}\times\mathbf{E}_1). \tag{3.67}$$

We can now perform a Fourier transform in space and we obtain

$$\mathbf{k}\times(\mathbf{k}\times\mathbf{E}_1) = -\frac{\omega^2}{c^2}\left(1-\frac{\omega_p^2}{\omega^2}\right)\mathbf{E}_1. \tag{3.68}$$

This is a wave equation which describes two distinct waves. If we consider a single mode of this wave, which we set along the z-axis, we can write the wave equation for this single mode as

$$\begin{pmatrix} \omega^2-\omega_p^2-k^2c^2 & 0 & 0 \\ 0 & \omega^2-\omega_p^2-k^2c^2 & 0 \\ 0 & 0 & \omega^2-\omega_p^2 \end{pmatrix}\begin{pmatrix} E_{1x} \\ E_{1y} \\ E_{1z} \end{pmatrix} = \begin{pmatrix} 0 \\ 0 \\ 0 \end{pmatrix}. \tag{3.69}$$

There are two fundamentally different waves:

1. **plasma oscillations**: One solution is $E_{1x} = E_{1y} = 0$, with $\omega^2 = \omega_p^2$. This corresponds to non-propagating longitudinal oscillations with a frequency equal to the plasma frequency. They becomes propagating waves if a non-zero electron pressure is included.
2. **electromagnetic waves:** The other solution is $E_{1z} = 0$, with $\omega^2 = \omega_p^2 + k^2c^2$. These are propagating transversal waves with a phase velocity $v_{\rm ph} = \omega/k = c/\sqrt{\epsilon}$ and group velocity $v_{\rm gr} = d\omega/dk = c\sqrt{\epsilon}$. If $\omega \gg \omega_p$, then we obtain the limit $\omega^2 = k^2c^2$ which is the dispersion relation for electromagnetic waves in vacuum. This means that only for low enough $\omega > \omega_p$, the plasma will affect the propagation of the electromagnetic wave. In the case $\omega < \omega_p$, $\sqrt{\epsilon}$ becomes imaginary which means that electromagnetic waves with $\omega < \omega_p$ cannot pass through the plasma and are instead reflected.

The Dispersion measure of radio emitters

As we have seen above, the phase velocity of electromagnetic waves propagating through a plasma depends on the plasma frequency. We had

$$v_{\rm gr} = \frac{d\omega}{dk} = c\sqrt{1-\frac{\omega_p^2}{\omega^2}}. \tag{3.70}$$

This means that a wave of frequency ω travels a distance $dl = v_{\rm gr}dt$ in a time interval dt. The time to travel a distance D is then

$$t = \int_0^D \frac{dl}{v_{\rm gr}} = \frac{1}{c}\int_0^D \left(1-\frac{\omega_p^2}{\omega^2}\right)^{-1} dl \simeq \frac{1}{c}\int_0^D \left(1+\frac{\omega_p^2}{2\omega^2}\right) dl, \tag{3.71}$$

where we have expanded the reciprocal term to linear order. Inserting the definition of the plasma frequency, we find

$$t = \frac{D}{c} + \frac{2\pi e^2}{m_e c\omega^2}\int_0^D n_e\, dl. \tag{3.72}$$

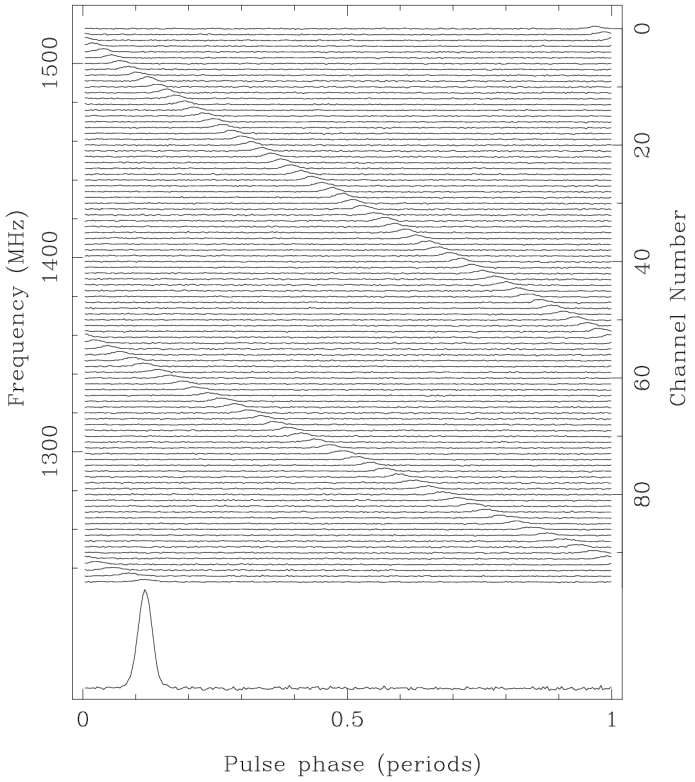

Figure 3.5: Pulsar dispersion: Observation of a pulsar in 96 radio channels between 1230 and 1520 MHz. The dispersion of the pulse is clearly visible in the data and can be used to determine the dispersion measure. [From: Handbook of Pulsar Astronomy, by Lorimer and Kramer]

This means that waves of different frequency will arrive at different times. If the source of the emitted radio waves is a pulsar, then we should expect the emission to be a short pulse at a wide range of radio wavelengths. From the different arrival times of the pulse in different frequencies, on can then calculate the dispersion measure

$$\int_0^D n_e \, dl = \bar{n}_e D. \tag{3.73}$$

If the distance to the pulsar is determined otherwise, one can thus measure the mean electron density in the interstellar medium, or vice versa, based on an estimate of the mean electron density in the ISM ($\bar{n}_e \sim 0.03\,\mathrm{cm}^{-3}$ in the solar neighbourhood), one can measure the distance of the pulsar. See Figure 3.5 for an example of pulsar dispersion.

3.3 Basic Magnetohydrodynamics

An important simplification occurs when we consider only length scales much larger than the Debye length and time scales much larger than the inverse of the plasma frequency. In that regime, it is allowed to assume that electron and ion densities and velocities follow each other. In this case, we can treat the entire plasma as a single fluid. This allows to combine the equations of the two-fluid system into the equations of ideal magnetohydrodynamics.

3.3.1 The Fundamental Equations

The fundamental, *ideal*, MHD equations are very similar to the equations of ideal hydrodynamics and take the form

$$\frac{\partial \rho}{\partial t} + \boldsymbol{\nabla} \cdot (\rho \mathbf{v}) = 0 \tag{3.74}$$

$$\frac{\partial v_i}{\partial t} + v_j \frac{\partial v_i}{\partial x_j} = F_i - \frac{1}{\rho} \frac{\partial}{\partial x_i} (P_{ij} + M_{ij}) \tag{3.75}$$

$$\frac{\partial \mathbf{B}}{\partial t} - \boldsymbol{\nabla} \cdot (\mathbf{v} \times \mathbf{B}) = 0, \tag{3.76}$$

where P_{ij} is the pressure tensor ($P_{ij} = P\delta_{ij}$ if we only have thermodynamic pressure, otherwise it also includes viscous terms), and

$$M_{ij} := \frac{B^2}{8\pi}\delta_{ij} - \frac{B_i B_j}{4\pi} \tag{3.77}$$

is the magnetic stress tensor. We thus gained one additional vector equation, the induction equation, which couples the evolution of the magnetic field to the fluid velocity field. The magnetic field acts back on the fluid velocity through the magnetic stress. We can understand its meaning if we look at M_{ij} for a magnetic field that is uniform in the z-direction, i.e. $\mathbf{B} = B\mathbf{e}_z$. Then

$$M_{ij} = \frac{B^2}{8\pi} \begin{pmatrix} 1 & 0 & 0 \\ 0 & 1 & 0 \\ 0 & 0 & 1 \end{pmatrix} - \frac{B^2}{4\pi} \begin{pmatrix} 0 & 0 & 0 \\ 0 & 0 & 0 \\ 0 & 0 & 1 \end{pmatrix}, \tag{3.78}$$

which shows that the magnetic field produces an isotropic pressure in the first term, and a negative pressure only in the z-direction. This negative anisotropic pressure corresponds to a tension of the

magnetic field. While the positive isotropic part opposes compression of magnetic fields, the anisotropic second term opposes stretching along magnetic field lines. The isotropic magnetic pressure is

$$P_{\mathrm{mag}} = \frac{B^2}{8\pi}, \tag{3.79}$$

and it can be directly compared to the thermodynamic pressure of a gas to determine whether magnetic fields are dynamically important in a fluid. This means one can define a dimensionless number, the plasma-β, which is defined as

$$\beta = \frac{P}{B^2/8\pi}. \tag{3.80}$$

In the corona of the sun, one has $\beta \sim 0.01$,

3.3.2 Hydromagnetic Waves

We remember that the hydrodynamic equations allowed wave solution with a sound speed $c_s^2 = \partial P/\partial\rho$. These waves will of course still exist also in the MHD case but they will split into two different waves. The tension of magnetic fields lines gives rise to an additional wave. In total, we have the following different waves:

Alfvén waves

These are waves that result from the restoring force due to the tension of the magnetic field lines. They are thus propagating parallel to the magnetic field and have a velocity

$$\mathbf{v}_A = \frac{1}{\sqrt{4\pi\rho_0}}\mathbf{B}_0, \tag{3.81}$$

where ρ_0 and $\mathbf{B}_0$ are the unperturbed mean density and magnetic field in which the waves propagate.

Slow and fast magnetosonic waves

These are the MHD equivalent of sound waves and they come as a slow and a fast wave. If θ is the angle between the wave vector $\mathbf{k}$ and the magnetic field $\mathbf{B}$, the magnetosonic wave velocities are

$$v_{ms}^2 = \frac{1}{2}(c_s^2 + v_A^2) \pm \frac{1}{2}\sqrt{(c_s^2 + v_A^2)^2 - 4c_s^2 v_A^2 \cos^2\theta}. \tag{3.82}$$

Magneto-hydrostatic configurations

Just as we considered hydrostatic configurations for non-magnetized fluids as the balance between the gravitational force and pressure gradients, we can consider fluid configurations in MHD, where the thermal pressure balances magnetic forces. The MHD Euler equation (3.75) in the absence of gravity can also be written as

$$\frac{\mathrm{D}\mathbf{v}}{\mathrm{D}t} = -\frac{1}{\rho}\boldsymbol{\nabla}P + \frac{1}{4\pi\rho}(\boldsymbol{\nabla}\times\mathbf{B})\times\mathbf{B}. \tag{3.83}$$

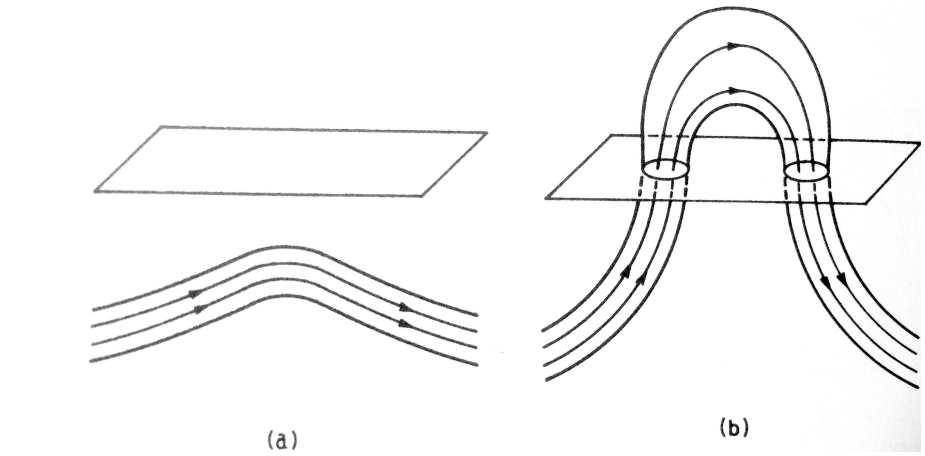

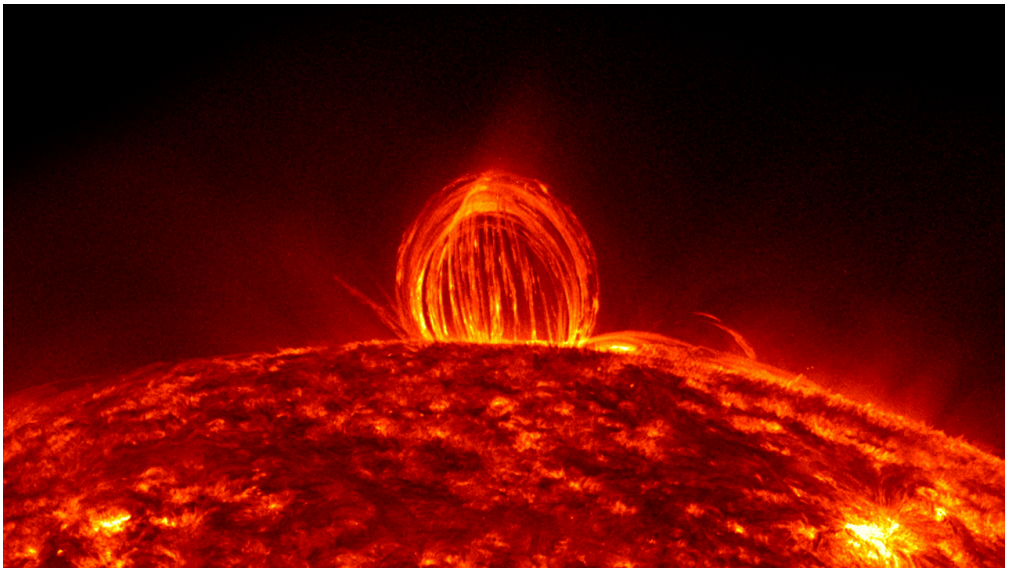

Figure 3.6: **Top:** Magnetic buoyancy of a flux tube originally parallel to the surface of the sun. (a) Some part of the flux tube becomes buoyantly unstable and begins to rise. (b) The tube buckles out of the surface, leaving two sunspots and a magnetic loop. [From: The Physics of Fluids and Plasmas by Choudhuri]. **Bottom:** A coronal loop on the sun. Plasma is flowing along the flux tube in an arc. [Photo by NASA].

This means that the condition for magnetohydrostatic equilibrium in the absence of gravity is

$$(\boldsymbol{\nabla} \times \mathbf{B}) \times \mathbf{B} = 4\pi \boldsymbol{\nabla} P. \tag{3.84}$$

A magnetic field that satisfies this equation, is called a *pressure balanced field*. If the plasma is a low-β plasma, i.e. one in which the gas pressure is negligible compared to magnetic pressure, then magnetic field lines will arrange themselves in order to yield a static configuration in which

$$(\boldsymbol{\nabla} \times \mathbf{B}) \times \mathbf{B} = 0. \tag{3.85}$$

A field which obeys this equation is called a *force-free* field. We can also note that this equation implies that $\mathbf{B}$ is parallel to $\boldsymbol{\nabla} \times \mathbf{B}$, i.e. for a force-free field on has

$$\boldsymbol{\nabla} \times \mathbf{B} = \mu \mathbf{B}, \qquad \mu \in \mathbb{R}. \tag{3.86}$$

3.3.3 Magnetic Buoyancy

Based on the MHD equations, it is an easy exercise to argue that sun-spots should come in pairs, connected by magnetic field lines. For this, one can assume a magnetic flux tube parallel to the sun's surface, i.e. a tube of parallel magnetic field lines. If we assume the flux tube is in pressure balance with its environment, we have

$$P_e = P_i + \frac{B^2}{8\pi}, \tag{3.87}$$

where P_e is the exterior thermodynamic pressure, P_i the interior one, and B the magnetic field strength inside the tube. This already implies that $P_i < P_e$. If we additionally assume that the temperature in the exterior equals the temperature inside the flux tube, then

$$\frac{k}{m}\rho_e T = \frac{k}{m}\rho_i T + \frac{B^2}{8\pi}, \tag{3.88}$$

which can be rewritten as

$$\frac{\rho_e - \rho_i}{\rho_e} = \frac{B^2}{8\pi P_e} > 0. \tag{3.89}$$

We see immediately that in this case, the interior of the flux tube must be lighter and can thus buoyantly rise. If the condition is not everywhere fulfilled, then we expect some parts of the flux tube to become unstable before others (details are of course complicated). The general picture of such a configuration that emerges is however that shown in Figure 3.6.

3.3.4 Vorticity

We can again consider the vorticity equation, that we have already encountered for non-magnetized fluids in eq. (2.25). In MHD flow, it takes the form

$$\frac{\partial \omega}{\partial t} + \boldsymbol{\nabla} \times (\boldsymbol{\omega} \times \mathbf{v}) = \frac{\boldsymbol{\nabla}\rho \times \boldsymbol{\nabla} P}{\rho^2} + \frac{\boldsymbol{\nabla} \times ((\boldsymbol{\nabla} \times \mathbf{B}) \times \mathbf{B})}{4\pi\rho}, \tag{3.90}$$

and we have on the right-hand-side in addition to the usual baroclinic term a new term that indicates that vorticity can be generated from the magnetic field. As it turns out, this is e.g. the case when magnetic field lines untwist and create vorticity in the process (cf. Figure 3.7a).

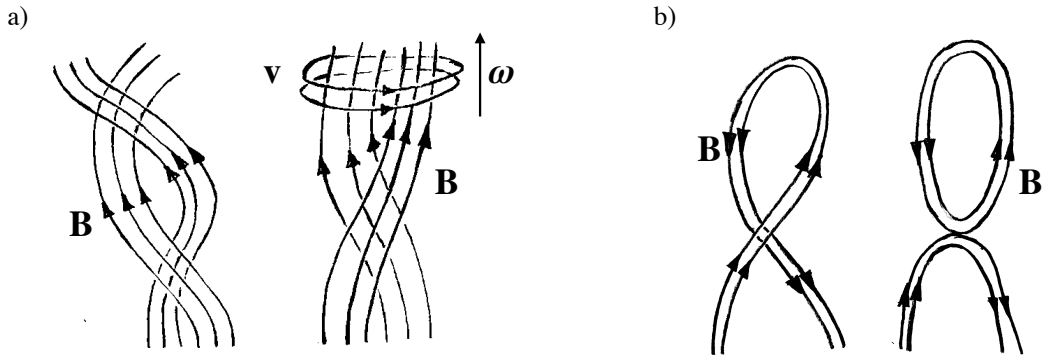

Figure 3.7: **(a)** Untangling of twisted field lines requires vortical motion, so that in the process of untwisting vorticity is generated in the flow. **(b)** Topological changes in the magnetic field by magnetic reconnection, which however is only possible in non-ideal MHD.

3.3.5 Magnetic topology, non-ideal MHD and reconnection

Two magnetic field configurations are said to be topologically identical, if they can be differentiably transformed into one another, without having to cut and re-glue field lines. If a magnetofluid is ideal, i.e. it has no resistivity, then its magnetic topology is conserved. On the other hand, for a strong magnetic field in equilibrium, the field must obey eq. (3.86). It might well be that this configuration is forbidden by topological considerations (the equation is only a local, not a global topological statement). It would then mean that no force-free configuration can exist and that the magnetized fluid would move ad infinitum. This is of course no physical. As it turns out, in a realistic, non-ideal MHD fluid, one has diffusive terms just as in non-ideal fluids. In this case, the induction equation takes the form

$$\frac{\partial \mathbf{B}}{\partial t} = \boldsymbol{\nabla} \times (\mathbf{v} \times \mathbf{B}) + \lambda \nabla^2 \mathbf{B}, \qquad \lambda = \frac{c^2}{4\pi\sigma}, \tag{3.91}$$

where λ is called the magnetic diffusivity and σ is the electrical conductivity. Ideal MHD corresponds to the limit of infinite conductivity, i.e. $\sigma \to \infty$. In the presence of such a non-ideal term, in regions where the magnetic field gradient is large, reconnection can occur that changes the topology of magnetic field lines in order to reduce their curvature (cf. Figure 3.7b). When reconnection happens, the magnetic stress energy changes rather drastically. This mechanism is thought to be responsible for coronal mass ejections on the Sun.

Chapter 4

First steps in Computational Fluid Dynamics

4.1 Discretising the fluid equations – Eulerian and Lagrangian schemes

In the astrophysical community, predominantly two rather different approaches are used to simulate the dynamics of fluids on computers. In the first, the Eulerian schemes, the equations are discretised on a regular grid structure that remains fixed in physical space (but can be locally refined e.g.) and the evolution of the fundamental fluid quantities, i.e. either the primitive variables $(\rho, \mathbf{v}, e)$ or the conservative quantities $(\rho, \rho\mathbf{v}, \rho\mathbf{v^2} + e)$ are evolved at the grid point locations. In the second class of schemes, the Lagrangian schemes, the equations are discretised in terms of characteristic points that move with the fluid. Typically, the main advantage of Lagrangian schemes is that they are self-adaptive, i.e. the points where the solution is known move into regions of high density, therefore preserving information about the flow. The usual price to pay in Lagrangian schemes is that it is much harder to correctly treat mixing of different fluid phases correctly. On the other hand, numerical errors are usually much better controlled in Eulerian schemes, but sophisticated schemes have to be employed (adaptive mesh refinement) in order to introduce new grid points in regions of convergent flow, in order to not wash out details of the flow and preserve information. Here, we will just attempt to give a flavour of both approaches using PYTHON notebooks. For simplicity, we resort here to a set of two equations, the continuity and Euler equation, closed with a barotropic equation of state. This set of equations is by definition isentropic, but allows us to illustrate the fundamental features.

4.1.1 The fluid equations in an Eulerian frame

We just summarise here once again the relevant simplified fluid equations in an Eulerian frame (cf. Section 2.1.2), which are in primitive form in one spatial dimension given by

$$\frac{\partial \rho}{\partial t} + \frac{\partial}{\partial x}(\rho v) = 0 \tag{4.1}$$

$$\frac{\partial v}{\partial t} + v\frac{\partial v}{\partial x} = -\frac{1}{\rho}\frac{\partial P}{\partial x}, \tag{4.2}$$

while the equivalent equations in conservative form are

$$\frac{\partial \rho}{\partial t} + \frac{\partial}{\partial x}(\rho v) = 0 \tag{4.3}$$

$$\frac{\partial (\rho v)}{\partial t} + \frac{\partial}{\partial x}\left(\rho v^2\right) = -\frac{\partial P}{\partial x}. \tag{4.4}$$

4.1.2 The fluid equations in a Lagrangian frame

We recall the Lagrangian derivative of some quantity $q(\mathbf{x}(t))$ along a characteristic $x(t)$, for which $\dot{\mathbf{x}} = \mathbf{v}(\mathbf{x}(t))$ (i.e. it is moving along with the flow), is given by

$$\frac{\mathrm{D}q}{\mathrm{D}t} = \frac{\partial q}{\partial t} + \mathbf{v} \cdot \nabla q. \tag{4.5}$$

This means that we can write the continuity and Euler equation in the form

$$\frac{\mathrm{D}\rho}{\mathrm{D}t} = -\rho \nabla \cdot \mathbf{v}, \tag{4.6}$$

$$\frac{\mathrm{D}\mathbf{v}}{\mathrm{D}t} = -\frac{1}{\rho}\nabla P. \tag{4.7}$$

And the fluid parcel of course follows the characteristic $\dot{\mathbf{x}} = \mathbf{v}$ by definition. We see that in principle the fluid equations take a very simple form in terms of the characteristic curves $(\mathbf{x}_i, \mathbf{v}_i)$,

$$\dot{\mathbf{x}}_i = \mathbf{v}_i, \tag{4.8}$$

$$\dot{\mathbf{v}}_i = -c_s^2 \frac{\nabla \rho}{\rho}\bigg|_{x_i}. \tag{4.9}$$

If we have a way to estimate the density ρ and its gradient $\nabla\rho$ from the characteristics, we can solve these equations. We will see how to do this later. Note that in the second equation, we have exploited that $c_s^2 = \partial P / \partial \rho$.

4.2 A simple finite difference Eulerian method

4.2.1 Finite difference discretisation

One way to discretise the Eulerian equations above is by means of finite differences, i.e. we approximate the temporal and spatial derivatives of a quantity q by

$$\frac{\partial q}{\partial t} \simeq \frac{q(x, t+\Delta t) - q(x,t)}{\Delta t} \quad \text{and} \quad \frac{\partial q}{\partial x}\bigg|_x \simeq \frac{q(x+\Delta x, t) - q(x-\Delta x, t)}{2\Delta x}, \tag{4.10}$$

which can be easily shown to be accurate at first order in Δt and to second order in Δx (i.e. coincide with the respective Taylor expansions up to that order). For simplicity we will assume that we know the quantities $q(x)$ at uniformly spaced discrete locations $i\Delta x$, $i \in \mathbb{N}$, so that we can simply write $q_i = q(i\Delta x)$. We will do likewise in time and write $q^n = q(t_0 + n\Delta t)$ so that $q^0 = q(t_0)$.

Putting everything together, we can thus write down a finite difference version of the conservative form of the equations as

$$\rho_i^{n+1} = \rho_i^n - \frac{\Delta t}{2\Delta x}\left[(\rho v)_{i+1}^n - (\rho v)_{i-1}^n\right], \tag{4.11}$$

$$(\rho v)_i^{n+1} = (\rho v)_i^n - \frac{\Delta t}{2\Delta x}\left[(\rho v^2 + P)_{i+1}^n - (\rho v^2 + P)_{i-1}^n\right], \tag{4.12}$$

with a polytropic equation of state $P = K\,\rho^\gamma$ to close the system.

In order to avoid dealing with boundary conditions, we will use a periodic grid of length N, i.e. for an index i the relation $i + N = i$ holds. Let's code this up in PYTHON, try using a JUPYTER notebook so that you can directly visualise the results. Dealing with periodic boundaries is particularly simple if we use the NUMPY function ROLL, which can shift the cells by a specified amount and automatically wraps around the boundaries.

```
import numpy as np
import matplotlib.pyplot as plt
%matplotlib notebook

# compute the right-hand side of the FD equations
def RHS( rho, rhou, K, gamma ):
    pressure = K * rho**gamma
    rhou2 = rhou**2 / rho
    drho = -0.5 * (np.roll(rhou,-1)-np.roll(rhou,+1))
    drhou = -0.5 * (np.roll(rhou2+pressure,-1)-np.roll(rhou2+pressure,+1))

    return (drho,drhou)

# perform a single time step
def step( rho, rhou, dt, dx, K, gamma ):
    (drho,drhou) = RHS(rho,rhou,K,gamma)
    rho = rho + dt/dx * drho
    rhou = rhou + dt/dx * drhou

    return (rho,rhou)
```

4.2.2 Test problem: a convergent flow developing a reflected shock wave

Now, all we need is a main routine that sets the initial conditions, parameters and calls the time-stepping function STEP. As our first initial conditions, we will assume a periodic domain $0 \leq x \leq 1$, on which we have an initially uniform density $\rho(x, t_0) = 1$ and we put a sinusoidal velocity perturbation $v(x) = \sin(2\pi x, t_0)$.

```
# initialise homogeneous particle distribution
Lbox = 1.0
Ngrid = 256
gamma = 5.0/3.0
K = 0.3
totmass = 1.0
```

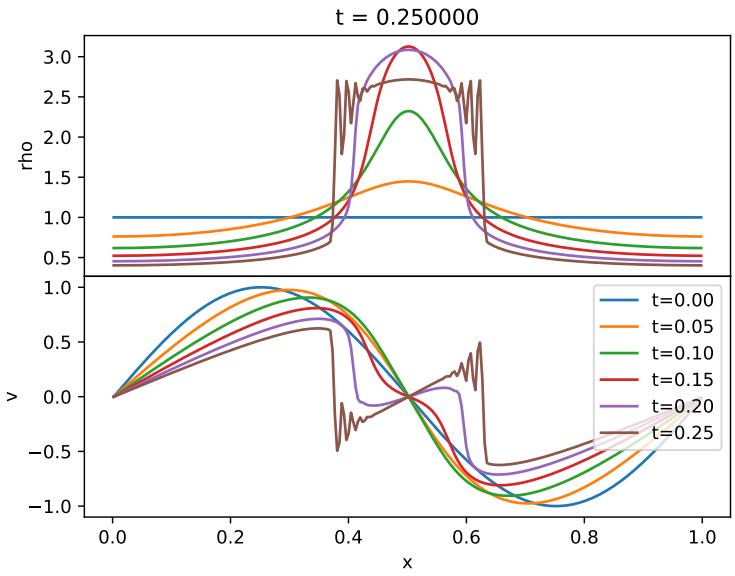

Figure 4.1: Numerical evolution using finite differences of an initially homogeneous density under a sinusoidal velocity perturbation evolving into an outward propagating shock. The shock develops but the 2nd order finite difference discretisation leads to oscillatory features.

```
dx = Lbox / Ngrid

x = np.arange(Ngrid) * dx
rho = np.ones_like(x) * totmass / Lbox
u = np.sin(2.0*np.pi * x)
rhou = rho * u

dt = 0.001
t = 0
tend = 0.25
while t<tend:
    (rho,rhou) = step( rho, rhou, dt, dx, K, gamma )
    t = t+dt
```

The results of this little numerical experiment are shown in Figure 4.1. We see nicely how the flow that is convergent towards $x = 0.5$ increases the density at that location until the pressure force has grown large enough to push back the material. This outward travelling material quickly develops into two shocks, which are however not well reproduced by the finite difference scheme since a strongly oscillatory feature develops along with the shock. There are two problems with our simple scheme. First, the shock is a discontinuity, and so we should not be using a second order spatial approximation, since it will almost certainly over- or undershoot the true solution in a bad way.

The second problem is that our finite difference discretisation does not respect the causal structure of the problem. When calculating the updated solution at a location x_i, neighbouring locations in both

directions, i.e. $i+1$ and $i-1$, are used. However, the pre-shock material should not be allowed to have information about the shock before it actually arrives. It can be shown in a simple stability analysis that the simple finite difference scheme is unstable for this reason. Incorporating the causal structure properly into such schemes can be achieved by the usage of so-called Riemann solvers, which are explicitly built to reproduce correctly the causal wave structure of discontinuous solutions. We will look into this later. First, we will exploit a physical mechanism to prevent oscillations at discontinuities, since the terms that are causing the instability can be shown to contain terms of the form $\nabla^2 v$ and $\nabla^2 \rho$, the first clearly being of the form of viscosity and the second of diffusion, albeit with a coefficient with the wrong sign so that oscillations grow and are not damped out.

4.2.3 Artificial viscosity

In order to both get a more intuitive understanding of the role of viscosity, as well as to exploit it as a mechanism to damp oscillations at high spatial frequency and produce a stable scheme, we make use of what is called artificial viscosity. Since the leading unstable terms causing the oscillations are of the same form as a negative viscosity, we should be able to eliminate them with a large enough *positive* viscosity.

We remember that the momentum equation with non-zero bulk viscosity ζ takes the form

$$\frac{\partial(\rho v)}{\partial t} + \frac{\partial}{\partial x}\left(\rho v^2\right) = -\frac{\partial P}{\partial x} + \zeta \frac{\partial^2 v}{\partial x^2}. \tag{4.13}$$

While in a physical medium the value of ζ is of course given by the material properties, we will treat it here as a parameter that we are free to adjust. In order to include it along with our finite-difference solver, we just have to understand how to express it as a finite difference. We remember that at second spatial order, the second derivative is given by

$$\left.\frac{\partial^2 v}{\partial x^2}\right|_i \simeq \frac{v_{i+1} - 2v_i + v_{i-1}}{\Delta x^2}. \tag{4.14}$$

All we need to do is thus to modify the right-hand-side function with the new term:

```
def RHS( rho, rhou, K, gamma, zeta ):
    pressure = K * rho**gamma
    rhou2 = rhou**2 / rho
    u = rhou / rho

    drho = -0.5 * (np.roll(rhou,-1)-np.roll(rhou,+1))
    drhou = -0.5 * (np.roll(rhou2+pressure,-1)-np.roll(rhou2+pressure,+1))

    drhou = drhou + zeta * (np.roll(u,1) - 2.0*u + np.roll(u,-1))/dx**2

    return (drho,drhou)
```

The results for $\zeta = 10^{-5}$ in code units can be seen in Figure 4.2. The artificial viscosity has indeed completely removed the oscillatory features. Of course this comes at the price of smeared-out shocks, which haven been significantly broadened. This is exactly the effect of bulk viscosity. With a proper Riemann-solver based method, we would be able to obtain a non-oscillatory solution with very sharp shocks – the reason why such methods are generally preferred. *The main problem of finite difference*

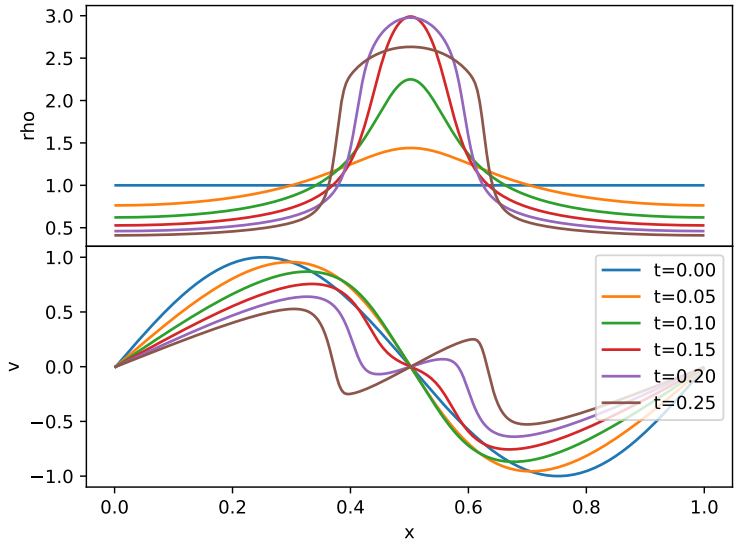

Figure 4.2: Same problem and numerical integration scheme (finite difference) as in Figure 4.1 but with added artificial viscosity. This produces a stable scheme, but the solution is smoothed out.

schemes is however that they are not guaranteed to be conservative! So mass, momentum and energy will not remain constant in the system. This problem can be completely circumvented in finite volume methods which we discuss next.

4.2.4 Godunov's method: Finite Volume and Riemann solvers

Above, we tried to discretise the conservative form of the hydrodynamic equations:

$$\frac{\partial \rho}{\partial t} = -\frac{\partial}{\partial x}(\rho v) \tag{4.15}$$

$$\frac{\partial (\rho v)}{\partial t} = -\frac{\partial}{\partial x}\left(\rho v^2 + P\right) \tag{4.16}$$

and ran into problems with our finite difference approach because the flow can develop discontinuities, at which we cannot easily evaluate derivatives. One solution was to smooth out discontinuities with artificial viscosity, but another solution can be found by focusing directly on weak solutions of the equations. If we integrate these equations over a small volume (really a line segment between $x_{i-1/2}$ and $x_{i+1/2}$, as we are in 1D), we have

$$\frac{\partial}{\partial t}\int_{x_{i-1/2}}^{x_{i+1/2}} \rho \mathrm{d}x = -\int_{x_{i-1/2}}^{x_{i+1/2}} \frac{\partial}{\partial x}(\rho v)\,\mathrm{d}x = (\rho v)|_{x_{i-1/2}} - (\rho v)|_{x_{i+1/2}}$$

$$\frac{\partial}{\partial t}\int_{x_{i-1/2}}^{x_{i+1/2}} (\rho v)\,\mathrm{d}x = -\int_{x_{i-1/2}}^{x_{i+1/2}} \frac{\partial}{\partial x}\left(\rho v^2 + P\right)\mathrm{d}x = (\rho v^2 + P)\big|_{x_{i-1/2}} - (\rho v^2 + P)\big|_{x_{i+1/2}}.$$

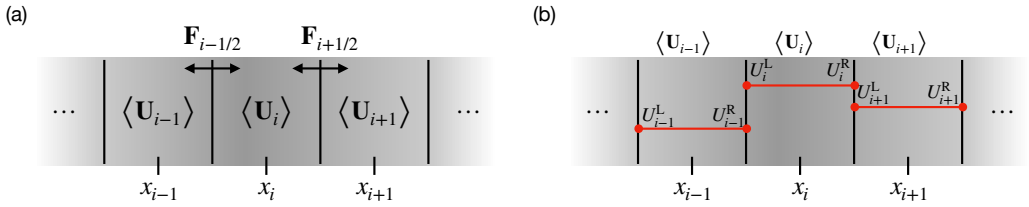

Figure 4.3: The finite volume method. (a) After integrating over the fluid equations, one can represent the conserved variables $\mathbf{U}$ in terms of an average over a cell volume $\langle \mathbf{U} \rangle_i$ whose value can only change by computing the fluxes $\mathbf{F}_{i\pm1/2}$ between adjacent cells. (b) The flux between cells can be obtained by considering the discontinuous Riemann problem at each cell interface. In its simplest flavour, we can reconstruct the left and right interface values $\mathbf{U}^{\mathrm{L}}$ and $\mathbf{U}^{\mathrm{R}}$ by assuming that the conserved variables are constant inside of each cell.

Obviously, if we define a "cell average"

$$\langle q \rangle_i := \frac{1}{\Delta x} \int_{x_{i-1/2}}^{x_{i+1/2}} q \, \mathrm{d}x \tag{4.17}$$

to be the volume average of a quantity q (where $\Delta x = x_{i+1/2} - x_{i-1/2}$), this is simply

$$\frac{\partial \langle \mathbf{U}_i \rangle}{\partial t} = -\frac{1}{\Delta x} \left(\mathbf{F}_{i+1/2} - \mathbf{F}_{i-1/2} \right) \tag{4.18}$$

where $\mathbf{U} = (\rho, \rho v)$ and $\mathbf{F} = (\rho v, \rho v^2 + P)$ are the conserved quantities and the flux function respectively. A visual depiction of this finite volume approach can be found in Fig. 4.3. *This means that the average value of the conserved quantity in a cell changes according to the net influx minus outflux into the cell.* The problem can thus be reduced to two steps: (1) reconstructing the left and right states at the interface between cells, and (2) computing the flux across the boundary. Since we are dealing with discontinuous solutions, a reasonable assumption is that $\mathbf{U}$ is constant inside of each cell. Then we have a discontinuity between $\mathbf{U}^{\mathrm{L}}$ and $\mathbf{U}^{\mathrm{R}}$ at each cell interface. Such a problem is a Riemann problem and can be solved either exactly, or approximately using so-called approximate Riemann solvers. A simple choice is the Haarten-Lax-Van Leer (HLL) approximate Riemann solver, which states that for input states $\mathbf{U}^{\mathrm{L}}$ and $\mathbf{U}^{\mathrm{R}}$ and left and right fluxes $\mathbf{F}^{\mathrm{L}} = \mathbf{F}(\mathbf{U}^{\mathrm{L}})$ and $\mathbf{F}^{\mathrm{R}} = \mathbf{F}(\mathbf{U}^{\mathrm{R}})$, the correctly averaged flux is given by

$$\mathbf{F}(\mathbf{U}^{\mathrm{L}}, \mathbf{U}^{\mathrm{R}}) = \frac{1}{2} \left(\mathbf{F}^{\mathrm{L}} + \mathbf{F}^{\mathrm{R}} \right) - \frac{S^*}{2} \left(\mathbf{U}^{\mathrm{R}} - \mathbf{U}^{\mathrm{L}} \right), \tag{4.19}$$

where

$$S^* = \max \left(|v^L| + c^L, \, |v^R| + c^R \right) \tag{4.20}$$

is the maximum signal speed, c^L and c^R the left and right sound speeds, respectively. We can thus use eq. (4.18) to obtain a full expression for an update

$$\langle \mathbf{U}_i \rangle (t + \Delta t) = \langle \mathbf{U}_i \rangle (t) - \frac{\Delta t}{\Delta x} \left[\mathbf{F}(\mathbf{U}_{i+1}^{\mathrm{L}}, \mathbf{U}_i^{\mathrm{R}}) - \mathbf{F}(\mathbf{U}_i^{\mathrm{L}}, \mathbf{U}_{i-1}^{\mathrm{R}}) \right]. \tag{4.21}$$

We can implement this easily in our previous scheme by just replacing the function RHS to

```python
# compute the right-hand side of the FD equations
def RHS( rho, rhou, K, gamma ):

    rhou2 = rhou**2 / rho
    u = rhou/rho

    pressure = K * rho**gamma
    cs = np.sqrt(gamma * pressure/rho)
    a = np.abs(u)+cs

    # Uleft
    rhoL = rho
    rhouL = rhou

    # Uright
    rhoR = np.roll(rho,-1)
    rhouR = np.roll(rhou,-1)

    # Fleft
    FrhoL = rhou
    FrhouL = rhou2 + pressure

    FrhoR = np.roll(rhou,-1)
    FrhouR = np.roll(rhou2+pressure,-1)

    # Sstar
    Sstar = np.maximum(a,np.roll(a,-1))

    # compute flux
    FHLLrho = 0.5*(FrhoL+FrhoR) - 0.5 * Sstar *(rhoR-rhoL)
    FHLLrhou = 0.5*(FrhouL+FrhouR) - 0.5 * Sstar *(rhouR-rhouL)

    # compute flux difference
    drho = -(FHLLrho - np.roll(FHLLrho,+1))
    drhou = -(FHLLrhou - np.roll(FHLLrhou,+1))

    return (drho,drhou)
```

This scheme can be shown to be stable if the CFL-condition (Courant-Friedrichs-Lewy) is fulfilled:

$$\Delta t < \frac{\Delta x}{2 \max\left(|v| + c\right)}. \tag{4.22}$$

The solution for our test problem is shown in Figure 4.4, where we see that the result is qualitatively similar to the finite difference solution with artificial viscosity. The shock is not perfectly sharp, but the solution has no oscillations and the scheme is stable as long as the CFL condition is fulfilled.

Typical improvements to this method can be made by (1) increasing the order of the reconstruction step to either piecewise linear or piecewise parabolic reconstructions of the interface states (away from discontinuities), (2) increasing the order of the time integration. Multi-dimensional solvers can be constructed easily by directional operator splitting. Here one solves sequentially one-dimensional problems.

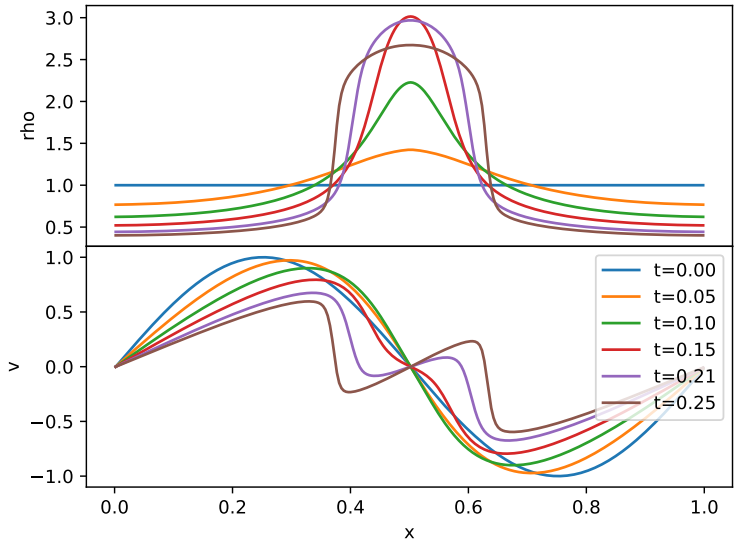

Figure 4.4: Numerical evolution using Godunov's method with an HLL approximate Riemann solver. The shock develops without oscillations and the scheme is stable. It is moderately diffusive itself (the shock is less sharp than in the finite difference method).

In 3D, one would solve first along the x-direction, then along y, then z, followed by a step in the reverse order: first z, then y, then x. Also unsplit methods exist, but they are somewhat more involved in the multi-dimensional flux calculation. These methods are very robust and are among the workhorses in computational astrophysics from planet formation to cosmology.

4.3 Smoothed-particle Hydrodynamics (SPH)

In our little excursion into the numerical world, we will next turn to a Lagrangian method, the so-called smoothed-particle hydrodynamics, or SPH, method. As we have seen above, the Lagrangian equations of motion for characteristics are particularly simple, but their use is hampered by the fact that we need an estimate of the density. This is what SPH is all about. The idea is to use the local density of characteristics (or fluid parcels) as an estimate of the density by means of so-called kernel density estimation.

4.3.1 Kernel density estimation

Kernel density estimation is a widely used method in statistics to obtain a non-parametric estimate of a probability density function of a random variable. The basic idea is that for a sample $(x_1, x_2, \ldots, x_n)$ that is fairly drawn from an unknown density f, one can use the kernel density estimator

$$\hat{f}_h(x) = \frac{1}{n}\sum_{i=1}^{n} K_h(x - x_i) = \frac{1}{nh}\sum_{i=1}^{n} K\left(\frac{x - x_i}{h}\right), \tag{4.23}$$

where $K(\cdot)$ is the kernel function and $h > 0$ is a smoothing parameter, which one wants to choose as small as possible while still averaging over enough points to obtain a low variance estimate. Assuming we know the density ρ_i at every point x_i, then the general kernel estimate of a variable A, that is known at those points, is given by

$$A(x) = \sum_{i=1}^{n} m_i \frac{A_i}{\rho_i} K\left(\frac{x - x_i}{h}\right), \tag{4.24}$$

where the term ρ_i^{-1} appears to avoid weighting the estimate by the density of points. For $A_i = \rho_i$, this trivially reduces to

$$\rho(x) = \sum_{i=1}^{n} m_i K\left(\frac{x - x_i}{h}\right). \tag{4.25}$$

The gradient of a density weighted kernel estimate, assuming that h is spatially constant can also be easily calculated to be

$$\nabla A(x) = \sum_{i=1}^{n} m_i \frac{A_i}{\rho_i} \nabla K\left(\frac{x - x_i}{h}\right), \tag{4.26}$$

which means that one only has to replace the kernel K with the gradient of the kernel ∇K. A natural choice for a kernel would be e.g. a Gaussian kernel, but more commonly a function with finite support is used so that points at distances larger than the support of the kernel can be neglected in the sum, making the calculation more efficient. The traditionally used kernel in SPH is the B-spline kernel (Monaghan 1992) of the form

$$K(q) = \begin{cases} \sigma_h \left[1 - \frac{3}{2}q^2\left(1 - \frac{q}{2}\right)\right], & \text{for } 0 \leq q \leq 1 \\ \sigma_h \frac{3}{4}\left(2 - q\right)^3, & \text{for } 1 < q \leq 2 \\ 0, & \text{for } q > 2 \end{cases} \tag{4.27}$$

with a normalisation constant which has in d spatial dimensions the value

$$\sigma_h = \begin{cases} \frac{2}{3h}, & \text{for } d = 1 \\ \frac{10}{7\pi h^2}, & \text{for } d = 2 \\ \frac{1}{\pi h^3}, & \text{for } d = 3 \end{cases}. \tag{4.28}$$

The gradient of the kernel can be readily calculated as

$$\nabla K = \begin{cases} \sigma_h \left[3q\left(\frac{q}{2} - 1\right) + \frac{3}{4}q^2\right], & \text{for } 0 \leq q \leq 1 \\ -\sigma_h \frac{9}{4}\left(2 - q\right)^2, & \text{for } 1 < q \leq 2 \\ 0, & \text{for } q > 2 \end{cases}. \tag{4.29}$$

The shape of the B-spline kernel and its gradient are shown in Figure 4.5.

4.3.2 Pressure force in SPH

Using these kernels, we can now finally write down the pressure force term that appears in the Lagrangian Euler equation. There is some ambiguity how exactly the pressure gradient should be formulated and in fact a lot of recent debate about new developments in SPH has gone in this direction. Here, we show two different kernel based discretisations. The first is due to Katz & Hernquist 1989 and has the form

$$\frac{\mathrm{D}v_i}{\mathrm{D}t} = -\sum_j m_j \left(2\frac{\sqrt{P_i P_j}}{\rho_i \rho_j}\right) \nabla_i K\left(\frac{x_j - x_i}{h}\right), \tag{4.30}$$

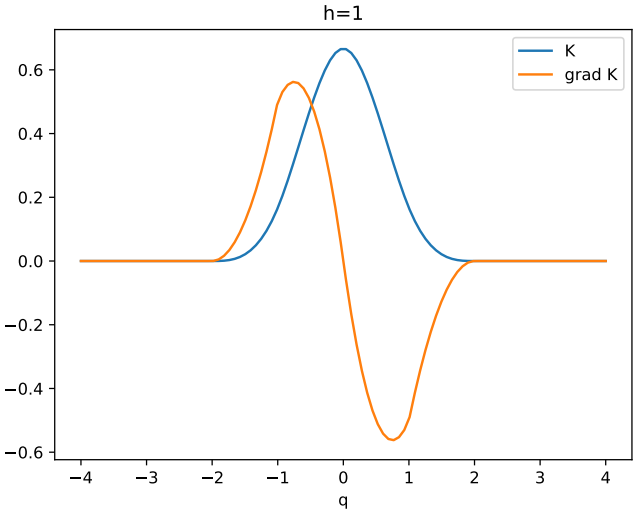

Figure 4.5: The B-spline density estimation kernel and its gradient which are commonly employed in the estimation of density and density weighted quantities in SPH.

where ∇_i indicates that the derivative is taken with respect to x_i and not x_j, and the sum is taken over all points x_j in the support of the kernel, i.e. with a distance smaller than $2h$. An alternative formulation is due to Morris 1996 and has the form

$$\frac{\mathrm{D}v_i}{\mathrm{D}t} = \sum_j m_j \left(\frac{P_i - P_j}{\rho_i \rho_j}\right) \nabla_i K \left(\frac{x_j - x_i}{h}\right). \tag{4.31}$$

A 1D SPH method

A full scheme is obtained by using the velocity/momentum updates as above, and the density can be computed by kernel estimation at any desired time. In principle, one could also evolve the density at the particle locations:

$$\frac{\mathrm{D}\rho_i}{\mathrm{D}t} = \sum_j m_j \left(v_i - v_j\right) \nabla_i K \left(\frac{x_j - x_i}{h}\right), \tag{4.32}$$

but the mass is trivially conserved in Lagrangian schemes by just keeping the mass of the SPH particles fixed. With all the equations at hand, we can now turn all that we have so far into a small Python program that evaluates the pressure force based on the locations of the characteristics x_i. First the code for the kernels in 1D:

```
def W_1D(q,h):
    q = np.abs(q)/h

    i1 = np.where(np.logical_and(q>=0,q<=1))
    i2 = np.where(np.logical_and(q>1,q<=2))
    i3 = np.where(q>2)

```

```
    sigma = 2.0/(3.0*h)
    ret = np.zeros_like(q)
    ret[i1] = sigma*(1-1.5*q[i1]**2*(1-q[i1]/2))
    ret[i2] = sigma*0.25*(2-q[i2])**3
    ret[i3] = 0.0

    return ret
```

```
def grad_W_1D(q,h):
    s = np.sign(q)
    q = np.abs(q)/h

    i1 = np.where(np.logical_and(q>=0,q<=1))
    i2 = np.where(np.logical_and(q>1,q<=2))
    i3 = np.where(q>2)

    sigma = 2.0/(3.0*h)
    ret = np.zeros_like(q)
    ret[i1] = sigma*(3*(q[i1]/2-1.0)*q[i1]+0.75*q[i1])
    ret[i2] = -3*sigma*0.25*(2-q[i2])**2
    ret[i3] = 0.0

    return s*ret
```

In order to compute the pressure force, we will for simplicity just loop over all particles and zero the contribution due to the particle itself. We also have to take into account periodic boundaries when evaluating the kernel: let's assume our domain has an extent L. For two points x_i and x_j, under periodic boundary conditions, the distance vector d is $d = x_i - x_j$ if $-L/2 < x_i - x_j \leq L/2$. If however $x_i - x_j > L/2$, then $d = x_i - x_j - L$, and if $x_i - x_j < -L/2$, then $d = x_i - x_j + L$. Putting this together we can calculate the pressure force in a periodic domain using a kernel estimate as

```
def compute_pressure_force( x, rhop, L, pmass, h, K, gamma ):
    pressure = K * rhop ** gamma

    ipart = 0
    pressure_force = np.zeros_like(x)
    # loop again over all particles
    for xp in x:
        # compute distance obeying periodic boundaries
        d = x - xp
        ii1 = np.where( d > 0.5*L )
        ii2 = np.where( d < -0.5*L)
        d[ii1] = d[ii1] - L
        d[ii2] = d[ii2] + L

        # Morris (1996) SPH
        force_i = -(pressure[ipart] - pressure)/(rhop[ipart]*rhop) \
                        * grad_W_1D( d, h ) / h

```

```
        # zero self-force
        force_i[ipart] = 0.0
        pressure_force[ipart] = np.sum(force_i)

        ipart = ipart + 1

    return pmass * pressure_force
```

We also need to evaluate the density, if we are interested in it, which we can write as follows:

```
def compute_density( x, L, pmass, h ):
    rho = np.zeros_like( x )
    ipart = 0
    for xp in x:
        d = x - xp
        ii1 = np.where( d > 0.5*L )
        ii2 = np.where( d < -0.5*L)
        d[ii1] = d[ii1] - L
        d[ii2] = d[ii2] + L
        rho_i = pmass * W_1D( d, h )
        rho[ipart] = np.sum(rho_i)
        ipart = ipart + 1
    return rho
```

4.3.3 Test problem: a convergent flow developing a reflected shock wave

Once again we consider the test problem from above, an initially uniform density and a sinusoidal velocity perturbation. Instead of the first order time integration method we used for the finite difference scheme, we will here use a leap-frog integration scheme which is second order accurate in time: we first update the density and particle positions by a half time-step $\Delta t/2$, then we perform a full time-step for the velocities, followed by a final half time-step for positions and densities using the new velocities. The code fragment that sets up the initial conditions and performs the time integration should then look like this:

```
Lbox = 1.0
Npart = 256
h = 0.01
totmass = 1.0
gamma = 5.0/3.0
K = 0.3
pmass = totmass / Npart
dx = Lbox / Npart
tend = 0.25

x = np.arange(Npart) * dx
rho = np.ones_like(x) * totmass / Lbox
v = np.sin(2.0*np.pi * x)

dt = 0.01
```

```
t = 0
while t<tend:
    # drift
    x = x + 0.5*dt * v

    # kick
    rho = compute_density( x, Lbox, pmass, h )
    acc = compute_pressure_force( x, rho, Lbox, pmass, h, K, gamma )
    v = v + dt * acc

    #drift
    x = x + 0.5*dt * v

    t = t + dt
```

The final solution can be seen in Figure 4.6. We recover a solution that is very similar to our first try with the finite difference scheme, a shock develops but again produces oscillations. Once again these could be reduced by adding artificial viscosity. The main advantage of Lagrangian methods such as SPH is that they are very simple to implement and solve advection problems trivially. They do have problems with correct entropy production however, since they do not correctly represent mixing in fluids in their simpler formulations. For these reasons, this old school SPH approach is no longer used and instead "moving mesh" methods have become more fashionable. In these methods, one still considers Lagrangian fluid elements, but allows for fluxes between them, similar to the finite volume method.

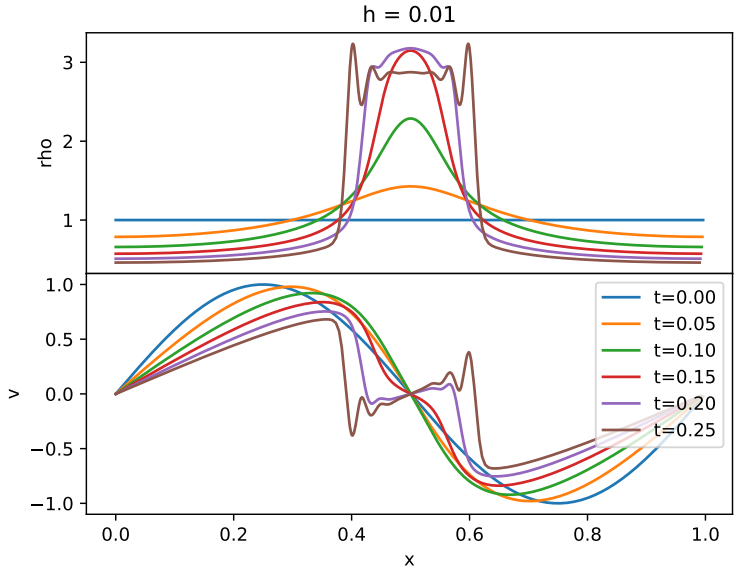

Figure 4.6: Numerical evolution using the SPH method of an initially homogeneous density under a sinusoidal velocity perturbation evolving into an outward propagating shock. As in the finitie difference scheme without artificial viscosity, the solution has oscillatory features. Once again, they can be suppressed using artificial viscosity.

Appendix A

Mathematics Formulary

A.1 Differential operators in curvilinear coordinates

A.1.1 Cartesian coordinates

The orthogonal base vectors (of unit length) are $\mathbf{e}_x, \mathbf{e}_y, \mathbf{e}_z$ and we have for a scalar field $f(\mathbf{x}) : \mathbb{R}^3 \to \mathbb{R}$ and a vector field $\mathbf{A}(\mathbf{x}) : \mathbb{R}^3 \to \mathbb{R}^3$ respectively

$$\boldsymbol{\nabla} f = \mathbf{e}_x \frac{\partial f}{\partial x} + \mathbf{e}_y \frac{\partial f}{\partial y} + \mathbf{e}_z \frac{\partial f}{\partial z} \tag{A.1}$$

$$\boldsymbol{\nabla} \cdot \mathbf{A} = \frac{\partial A_x}{\partial x} + \frac{\partial A_y}{\partial y} + \frac{\partial A_z}{\partial z} \tag{A.2}$$

$$\boldsymbol{\nabla} \times \mathbf{A} = \mathbf{e}_x \left(\frac{\partial A_z}{\partial y} - \frac{\partial A_y}{\partial z} \right) + \mathbf{e}_y \left(\frac{\partial A_x}{\partial z} - \frac{\partial A_z}{\partial x} \right) + \mathbf{e}_z \left(\frac{\partial A_y}{\partial x} - \frac{\partial A_x}{\partial y} \right) \tag{A.3}$$

$$\nabla^2 f = \frac{\partial^2 f}{\partial x^2} + \frac{\partial^2 f}{\partial y^2} + \frac{\partial^2 f}{\partial z^2}. \tag{A.4}$$

A.1.2 Cylindrical coordinates

The orthogonal base vectors (of unit length) are now $\mathbf{e}_r, \mathbf{e}_\phi, \mathbf{e}_z$, where $\phi \in [0, 2\pi[$ is the azimuthal angle. The conversion between Cartesian and cylindrical coordinates is

$$r = \sqrt{x^2 + y^2}, \quad \phi = \tan^{-1}\left(\frac{y}{x}\right), \quad z = z, \tag{A.5}$$

and the inverse conversion is

$$x = r\cos\phi, \quad y = r\sin\phi, \quad z = z. \tag{A.6}$$

The cylindrical surface area element is

$$\mathrm{d}\boldsymbol{\Omega} = \mathbf{e}_r \, r \, \mathrm{d}\phi \, \mathrm{d}z \tag{A.7}$$

and the volume element is

$$\mathrm{d}V = r\,\mathrm{d}r\,\mathrm{d}\phi\,\mathrm{d}z \tag{A.8}$$

The differential operators are

$$\begin{aligned}
\boldsymbol{\nabla} f &= \mathbf{e}_r \frac{\partial f}{\partial r} + \mathbf{e}_\phi \frac{1}{r}\frac{\partial f}{\partial \phi} + \mathbf{e}_z \frac{\partial f}{\partial z} && \text{(A.9)}\\
\boldsymbol{\nabla}\cdot A &= \frac{1}{r}\frac{\partial\left(rA_r\right)}{\partial r} + \frac{1}{r}\frac{\partial A_\phi}{\partial \phi} + \frac{\partial A_z}{\partial z} && \text{(A.10)}\\
\boldsymbol{\nabla}\times\mathbf{A} &= \mathbf{e}_r\left(\frac{1}{r}\frac{\partial A_z}{\partial \phi} - \frac{\partial A_\phi}{\partial z}\right) + \mathbf{e}_\phi\left(\frac{\partial A_r}{\partial z} - \frac{\partial A_z}{\partial r}\right) + \mathbf{e}_z\frac{1}{r}\left(\frac{\partial\left(rA_\phi\right)}{\partial r} - \frac{\partial A_r}{\partial \phi}\right) && \text{(A.11)}\\
\nabla^2 f &= \frac{1}{r}\frac{\partial}{\partial r}\left(r\frac{\partial f}{\partial r}\right) + \frac{1}{r^2}\frac{\partial^2 f}{\partial \phi^2} + \frac{\partial^2 f}{\partial z^2}. && \text{(A.12)}
\end{aligned}$$

A.1.3 Spherical coordinates

The orthogonal base vectors (of unit length) are now $\mathbf{e}_r, \mathbf{e}_\theta, \mathbf{e}_\phi$, where θ is the azimuthal angle $\phi \in [0, 2\pi[$, and ϕ is the polar angle $\theta \in [0, \pi]$. We have the following conversion between Cartesian coordinates and spherical coordinates

$$r = \sqrt{x^2 + y^2 + z^2}, \quad \phi = \tan^{-1}\left(\frac{y}{x}\right), \quad \theta = \cos^{-1}\left(\frac{z}{r}\right) \tag{A.13}$$

and for the inverse conversion

$$x = r\cos\phi\,\sin\theta, \quad y = r\sin\phi\,\sin\theta, \quad z = r\cos\theta. \tag{A.14}$$

The spherical surface area element is

$$\mathrm{d}\boldsymbol{\Omega} = \mathbf{e}_r\, r^2 \sin\theta\,\mathrm{d}\theta\,\mathrm{d}\phi \tag{A.15}$$

and the volume element is

$$\mathrm{d}V = r^2\sin\theta\,\mathrm{d}\phi\,\mathrm{d}\theta\,\mathrm{d}r. \tag{A.16}$$

and for the differential operators we have

$$\begin{aligned}
\boldsymbol{\nabla} f &= \mathbf{e}_r \frac{\partial f}{\partial r} + \mathbf{e}_\theta \frac{1}{r}\frac{\partial f}{\partial \theta} + \mathbf{e}_\phi \frac{1}{r\sin\theta}\frac{\partial f}{\partial \phi} && \text{(A.17)}\\
\boldsymbol{\nabla}\cdot A &= \frac{1}{r^2}\frac{\partial\left(r^2 A_r\right)}{\partial r} + \frac{1}{r\sin\theta}\frac{\partial\left(\sin\theta\, A_\theta\right)}{\partial \theta} + \frac{1}{r\sin\theta}\frac{\partial A_\phi}{\partial \phi} && \text{(A.18)}\\
\boldsymbol{\nabla}\times\mathbf{A} &= \mathbf{e}_r\frac{1}{r\sin\theta}\left(\frac{\partial\left(\sin\theta\, A_\phi\right)}{\partial \theta} - \frac{\partial A_\theta}{\partial \phi}\right) + \mathbf{e}_\theta\left(\frac{1}{r\sin\theta}\frac{\partial A_r}{\partial \phi} - \frac{1}{r}\frac{\partial\left(rA_\phi\right)}{\partial r}\right)\\
&+ \mathbf{e}_\phi\frac{1}{r}\left(\frac{\partial\left(rA_\theta\right)}{\partial r} - \frac{\partial A_r}{\partial \theta}\right) && \text{(A.19)}\\
\nabla^2 f &= \frac{1}{r^2}\frac{\partial}{\partial r}\left(r^2\frac{\partial f}{\partial r}\right) + \frac{1}{r^2\sin\theta}\frac{\partial}{\partial \theta}\left(\sin\theta\frac{\partial f}{\partial \theta}\right) + \frac{1}{r^2\sin^2\theta}\frac{\partial^2 f}{\partial \phi^2}. && \text{(A.20)}
\end{aligned}$$

A.2 Integral Theorems

Gauss' theorem states that, for the integral of the divergence of a vector field $\mathbf{A}$ over a bounded volume V in n-dimensional space, the following relation holds

$$\int_V \boldsymbol{\nabla} \cdot \mathbf{A} \, \mathrm{d}V = \int_{\partial V} \mathbf{A} \cdot \mathrm{d}\boldsymbol{\Omega}, \tag{A.21}$$

where ∂V is the surface of V, and $\mathrm{d}\boldsymbol{\Omega}$ is the infinitesimal, oriented surface element, and $\mathrm{d}V = \mathrm{d}^n x$ is the volume element. For a scalar field f this implies that

$$\int_V \boldsymbol{\nabla} f \, \mathrm{d}V = \int_{\partial V} f \mathrm{d}\boldsymbol{\Omega}, \tag{A.22}$$

while for the curl of a vector field one has

$$\int_V \boldsymbol{\nabla} \times \mathbf{A} \, \mathrm{d}V = -\int_{\partial V} \mathbf{A} \times \mathrm{d}\boldsymbol{\Omega}. \tag{A.23}$$

Stokes's theorem on the other hand implies that for integrals over an area S (if in 3D) one has that

$$\int_S (\boldsymbol{\nabla} \times \mathbf{A}) \cdot \mathrm{d}\boldsymbol{\Omega} = \oint_{\partial S} \mathbf{A} \cdot \mathrm{d}\boldsymbol{\ell}, \tag{A.24}$$

where ∂S is the boundary of S (think closed space curve around the area if in 3D), and $\mathrm{d}\boldsymbol{\ell}$ is the oriented line element along the space curve.

A.3 The Fourier Transform

The Fourier transform $\tilde{f}(k)$ of a function $f(x)$ and the inverse transform are usually defined as

$$\tilde{f}(k) = \mathcal{F}[f] = \int_{-\infty}^{\infty} \mathrm{d}x \, f(x) \, \exp(-ikx) \quad \text{and} \quad f(x) = \mathcal{F}^{-1}[\tilde{f}] = \frac{1}{2\pi} \int_{-\infty}^{\infty} \mathrm{d}k \, \tilde{f}(k) \, \exp(ikx), \tag{A.25}$$

but where the factor of 2π is to be put unfortunately is a matter of definition. The Fourier transform is linear, i.e. for two functions f, g, and arbitrary complex constants $a, b \in \mathbb{C}$

$$\mathcal{F}[af + bg] = a\mathcal{F}[f] + b\mathcal{F}[g]. \tag{A.26}$$

Furthermore, the convolution theorem holds, i.e. convolution in real space becomes multiplication in Fourier space, and vice versa,

$$\mathcal{F}[f \star g] = \mathcal{F}[f] \, \mathcal{F}[g]. \tag{A.27}$$

And we have also Parseval's (or, more correctly, Plancherel's) theorem which states that the total "energy" in both spaces is identical

$$\int_{-\infty}^{\infty} \mathrm{d}x \, |f(x)|^2 = \frac{1}{2\pi} \int_{-\infty}^{\infty} \mathrm{d}k \, \left|\tilde{f}(k)\right|^2. \tag{A.28}$$

In addition, differentiation in real space becomes an algebraic operation in Fourier space (and vice versa), specifically

$$\frac{d^n f}{dx^n} = \frac{d^n}{dx^n} \mathcal{F}^{-1}[\tilde{f}] = \mathcal{F}^{-1}\left[(ik)^n \, \tilde{f}\right]. \tag{A.29}$$

This property allows us to turn ordinary differential equations into algebraic equations, and partial differential equations into ordinary differential equations: e.g. under Fourier transform, the Poisson equation behaves as follows

$$\nabla^2 \phi = \rho \quad \Leftrightarrow \quad -\|\mathbf{k}\|^2 \tilde{\phi} = \tilde{\rho} \tag{A.30}$$

and the wave equation under combined Fourier transformation in space $x \to k$ and time $t \to \omega$ as follows

$$\frac{\partial^2 \phi}{\partial t^2} = c^2 \nabla^2 \phi \quad \Leftrightarrow \quad \omega^2 = c^2 \|\mathbf{k}\|^2 , \tag{A.31}$$

where c is the constant wave speed. Both equations are purely algebraic after transformation. If c is allowed to be spatially varying, i.e. $c = c(x)$, then naturally eq. (A.31) cannot be the solution.

Derivatives in Fourier space with respect to k are of course possible too, i.e.

$$\tilde{f}'(k) := \frac{d}{dk} \mathcal{F}[f] = \mathcal{F}[-ix\, f] \tag{A.32}$$

They have the property that if we evaluate the derivative at $k \to 0$, we have

$$\tilde{f}'(0) = -i \int_{-\infty}^{\infty} \mathrm{d}x\, x\, f(x), \tag{A.33}$$

which is just the mean of f multiplied by $-i$. By iteration, one sees that the following relation between the raw moments μ_n of f and the n-th derivative in Fourier space holds:

$$\mu_n = \int_{-\infty}^{\infty} \mathrm{d}x\, x^n\, f(x) = (-i)^{-n}\, \tilde{f}^{(n)}(0). \tag{A.34}$$

The amplitude of the DC-mode $k = 0$ is $\hat{f}(k = 0)$ and in this lingo thus simply the zeroth moment, i.e. mean, of f.

Index

Bibliography

[1] A. R. Choudhuri. *The physics of fluids and plasmas : an introduction for astrophysicists*. Cambridge Univ. Press, Cambridge, UK, November 1998.

[2] L. D. Landau and E. M. Lifshitz. *Fluid mechanics*. Pergamon Press, Oxford, UK, 1959.

[3] D. Mihalas and B. W. Mihalas. *Foundations of radiation hydrodynamics*. Oxford Univ. Press, New York, NY, 1984.

[4] J. E. Pringle and A. King. *Astrophysical Flows*. Cambridge Univ. Press, Cambridge, UK, May 2014.

[5] K. S. Thorne and R. D. Blandford. *Modern Classical Physics: Optics, Fluids, Plasmas, Elasticity, Relativity, and Statistical Physics*. Princeton Univ. Press, Princeton, NJ, USA, 2017.